Integrated Hydrological Modeling for Water Resources Management of Heeia Coastal Wetland in Hawaii

PhD's Dissertation

Kariem A. Ghazal
University of Hawaii at Manoa
Department of Natural Resources
and Environmental Management

2017

Integrated Hydrological Modeling for Water Resources Management of Heeia Coastal Wetland in Hawaii

A dissertation submitted in partial fulfillment
of the requirements for the degree of
DOCTOR OF PHILOSOPHY

In

Natural Resources and Environmental Management

By
Kariem A. Ghazal

Dissertation Committee
Aly I. El-Kadi
Henrietta Dulai
Samir El-Swaify
Carl Evensen
Yin-Phan Tsang
University of Hawaii at Manoa
April 2017

Acknowledgments

These years of PhD's classes and research work is the output of many people who contributed either directly or indirectly. First of all, I would like to thank the almighty God for helping and giving me the strength to finish this study. I would like to make my work a sacrifice to the almighty God. I hope the almighty God accept my thanks and praise.

I am utmost indebted to my supervisor, Dr. Aly El-Kadi, for giving me the opportunity to work this research with him, for his step by step guidance and unreserved scientific support throughout the course of this research, and for correcting the dissertation. Thank you for all your help.

I would like to thank all the members of my committee for helping me with various aspects of this dissertation. Special thanks to Dr. Henrietta Dulai for reviewing this dissertation and giving constructive comments that allowed me further improvement throughout my study and research days. The input of Drs. Samir El-Swaify, Carl Evensen, and Yin-Phan Tsang is very much appreciated.

It is a beautiful gratitude and a nice response to thank very much my brother, friend, and problems solver Dr. Olkeba Tolessa Leta for sharing his ideas, for making pleasure working environment to work together for the Heeia project and his social, moral support during our stay in Hawaii.

I wish to thank all of those people who provided me information relevant to my project especially in Natural Resources and Environmental Department, Geology and Geophysics Department, and Water Resources Research Center.

My thanks to the Iraqi Cultural Attaché in Washington, DC, which is the sponsor of my scholarship. Special thanks and appreciation to the Prof.Tahani Al Sandook for her dedicated care to the Iraqi Scholars. Many thanks to the University of Hawaii Sea Grant College Program, which is the sponsor of parts of this research and the Kakoo Oiwi community for their help during my research.

Finally but not least, I would like to thank and pay tribute to my wife and kids for their moral and financial generous support throughout my study and our stay in Hawaii. I know that it was not so easy to tolerate those years stay in Hawaii due to my devotion to my study, even not being available for them during weekend, holidays, and coming back late from office. I really thank you for your love, patience, sacrifice, understanding and endurance during those moments. You were waiting this day than I did, thank you, we made it very fruitful together. My family brought me unlimited happiness, enjoyments

and pleasure to our life in Honolulu. They made me even to forget the stress and burden of work when I come to home with their smiled welcome.

I dedicate this dissertation to the spirits of my parents and my brothers, still living among us, despite their passing. I wish the almighty God made this work expiation for their sins.

Certification

We certify that we have read this dissertation and that, in our opinion, it is satisfactory in scope and quality as a dissertation for the degree of Doctor of Philosophy in Natural Resources and Environmental Management.

Dissertation Committee

Aly I. El-Kadi, (Chairman)

Henrietta Dulai

Samir El-Swaify

Carl Evensen

Yin-Phan Tsang

Abstract

The integrated hydrological models are an important tools that can be used to assess the water resources availability and sustainability for food security and ecological health of the coastal regions. In addition, such models are useful in assessing the current and future water budget under different conditions of climate and land use changes. This study addresses the Heeia Wetlands Restoration whereby different scenarios were developed to assess the effects of land cover change (LU), climate change (CL), and sea level rise (SLR) on the water balance components (WBCs), fresh water submarine groundwater discharge (FSGD), seawater intrusion, dissolved silicate (DSi) fluxes, and heat transport within the Heeia Coastal Wetland. The watershed (SWAT) model, the groundwater flow (MODFLOW) model, and the density dependent groundwater flow (SEAWAT) model were utilized in this integrated approach. The SWAT model was used to assess the impact of CL and LU on the WBCs.

The LU mainly focused on the conversion of a fallow wetland covered by california grass (invasive plant) to taro field (native plant). The groundwater recharge of the SWAT model output was used as input for both the steady state and transient-MODFLOW model to study the interaction between surface water and groundwater and its effect on the FSGD within the Watershed. The SEAWAT model was used to study the seawater intrusion, DSi fluxes and cold groundwater transport under several CL, LU, and SLR scenarios. The results indicated that the baseflow was the main components of the Heeia streamflow, especially during dry season. The annual recharge, surface runoff, lateral flow and ET comprised about 34%, 6%, 15%, and 45% of the annual rainfall, respectively. The WBCs were more impacted in the late of 2080s compared to the 2050s period.

To understand the comprehensive relationships between coastal hydrological processes and ecosystems, the FSGD was estimated under different scenarios of LU, CL, and SLR. The current daily average of the Heeia coastal FSGD was about 0.43 $m^3/d/m$, but expected to decrease by about 10% by the end of 21st century due to the combined effects of various changes. The FSGD comprised 18%, 11%, and 3% of the annual baseflow, recharge, and rainfall, respectively. Moreover, the FSGD fluxes would decline more during the dry season compared to the wet season. The FSGD fluxes were about 1.5 to 3.5 times than the fresh water delivered to the Kaneohe Bay via total Heeia streamflow. The outputs of SEAWAT model indicated that the seawater intrusion was not significantly influenced by SLR, CL, and LU. The average DSi fluxes was about 48 mole per day that increased by 15% during the wet

season, but decreased by16% during the dry season. The DSi fluxes were a function of the FSGD. The CL more negatively affected the DSi fluxes compared to the SLR. The respective average heat energy reduction within wetland under california grassland and taro cultivation would be 0.81and 1.12 (Kj/m^3) for inflow of cold groundwater, and 4.69 and 3.13 (Kj/m^3) for outflow of groundwater. The cold groundwater discharge at the shoreline was significantly mitigated the seawater temperature due to the high thermal gradient between the FSGD and seawater.

Despite data scarcity, the integrated hydrological modeling approach has provided a comprehensive assessment of the water resources that can help in the management of the Heeia Coastal Wetland under various land cover and climate conditions.

Table of Contents

List of Tables

List of Figures

List of Abbreviation

AET	Actual evapotranspiration
Alpha_Bf	Base flow recession alpha factor
Canmx	Maximum canopy water storage
C-CAP	Coastal change analysis program
CCMA	Center for coastal monitoring and assessment
CL	Climate change
CLLU	Combined effect of climate and wetland restoration changes
CLLU1.1SLR	Combined effect of climate change, wetland restoration, and sea level rise by 1.1 m
d	day
DEM	Digital elevation model
DOC	Department of commerce
DSi	Dissolved silicate
EPA	Environmental protection agency
ET	Evapotranspiration
FNWR	Forest national weather research
FSGD	Fresh submarine groundwater discharge
g/l	gram per liter
GMS	Groundwater modeling system
HCDA	Hawaiian community development authority
hec	hectare (10000 m^2)
HIMB	Hawaii institute of marine biology
hr	hour

HRU	Hydrologic response unit
IPCC	Intergovernmental panel on climate change
j	joule
Kh	Horizontal hydraulic conductivity
kg	kilogram
km^2	square kilometers
Kv	Vertical hydraulic conductivity
LU	Land cover change
m	meter
m^2	square meters
m^3	cubic meters
mg/l	milli gram per liter
min	minute
mm	milli meter
mon	month
NCDC	National Climatic Data Center
NOAA	National oceanic and atmospheric administration
NRCS	Natural resources conservation service
NSE	Nash-Sutcliffe Efficiency
PET	Potential evapotranspiration
r^2	Coefficient of determination
RCP	Representative Concentration Pathway
s	second

SA	Sensitivity analysis
SCS-CN	Soil conservation service curve number
SGD	Submarine groundwater discharge (includes freshwater and recirculated seawater)
SSURGO	Soil survey geographic database
SUFI-2	Sequential Uncertainty Fitting-version two
SWAT	Soil and water assessment tool
SWAT-CUP	SWAT calibration and uncertainty program
TDS	Total dissolved salt
TNC	The nature conservancy
USDA	United state department of agriculture
USFWS	United State fish and wildlife service
USGS	United States geological survey
w	watt
WBCs	water balance components
WETSPRO	water engineering time series processing tool
WRCC	Western region climate center
y	year

Chapter1 Introduction

1.1 Background

In the Hawaiian Islands, the integrated management of the surface and ground water resources has become the first priority of sustainable development plans in the coastal wetlands and watersheds (EMI, 2010, KBAC, 2007).The Coastal Wetlands and Watersheds represent the essential natural resources of Hawaiian economy and overall ecological health. The prominent features of these regions are considered as attractive habitats for native species and the major sources of ecosystem services. For instance, the Hawaiian Islands contain over 30 percent of the endangered species in the United States of America (Allen, 2000). Unfortunately, the coastal communities especially in the Hawaiian Islands, have faced a set of problems, including SLR, flooding, spread of invasive species, habitat destruction, coastal zone degradation, and water quality impairment (Oki, 1997, Rotzoll and Fletcher, 2013, Yost, *et al.*, 2009). These are likely to increase in the future due to global climate change, land use change, and increased population growth (Brasher, 2003, Pulwarty, *et al.*, 2010). The economic growth and prosperity of the State of Hawaii depend on the local water resources, especially groundwater that is very vulnerable to the sources of contamination as influenced by the nature of the resource and the local hydrogeological features (Mink and Lau, 1993, Nichols, *et al.*, 1997). Such a value is evident by the fact that 99 percent of the drinking water is from groundwater and 85 percent of the pumped groundwater is used for municipal, industrial, agricultural, and military uses (Gingerich and Oki, 2000, U.S. Army, 2004). This valuable resource is sensitive to climate and land use changes because of their direct effects on recharge and the interaction on surface water that interacts with groundwater. Hence it imperative that lead the population to adapt and prepare their lives for predicted changes in climate and land use through land use planning, alternative energy sources, and environmental regulations (Barnett, 2001). Assessing the groundwater flow system and its interaction with surface water is critical for devising plans to manage water resources in the coastal regions of the Hawaiian Islands (Ranjan, *et al.*, 2006, Rasmussen, *et al.*, 2013).

The hydrology of the coastal wetlands in windward sides of the Hawaiian Islands are very complicated due to the hydrogeological features of the Islands' Watersheds representing the drainage basins of the freshwater, which feeds the wetlands through the streams and baseflow (Bruland, 2008). The wetlands have unique characteristics compared against those in other regions of the continental United States,

including high amounts of rainfall (sometimes over 5000 mm/y), steep stream gradients, and unique subsurface features. The topographic variation and hydrogeological settings of these regions create wetlands with ample water for farming and aquaculture (Mitsch and Gosselink, 2007). Specifically to the study area, the wetland represents a reservoir of freshwater, which is gained through surface runoff, lateral flow, and groundwater discharge (Kakoo Oiwi, 2011).

The Wetlands enhance groundwater recharge through absorbing water during wet season and releasing it through dry season. They capture excess water during heavy rains and slowly release it during drought periods, such as active function to control flooding and sustainable wetting for vegetation cover (Stone, 1989). Unfortunately, most of these coastal wetlands, especially on the Island of Oahu, had been drained and devoted to urbanized services (Environmental Law Institute, 2008). In these areas after the 1950s, the unique assemblages of flora and fauna of coastal wetlands were lost due to wetland degradation and lost wetland functionalities by overgrowing of invasive species, like california grass and mangrove, which in turn negatively affect the unique habitats of birds, aquatic life, and loss of coral reefs near the coastal shoreline (Bantilan-Smith, et al., 2009).

In the last two decades, coastal wetlands have gained more attention since they have significant impacts on water resources, water quality improvement, and flood control through decreasing peak flow, reducing the runoff of sediments and nutrients, as well as acting as storage reservoir and natural filter against pollution (Kazezyılmaz-Alhan, et al., 2007). Therefore, information about hydrologic characteristics of wetland is very important for effective ecosystem restoration. Moreover, the functional importance of coastal wetland ecosystems and the changes in federal policies (Mitsch and Gosselink, 2007) to protect wetland, encourage some non-profit organizations to restore some degraded wetlands as one of the prominent strategies to maximize the ecosystem services (Chen, *et al.*, 2013).

In that direction, with a financial and moral support from environmental conservation agencies, the non-profit organization Kakoo Oiwi has committed to restore the Heeia Wetland, which is located at the windward sector of Oahu Island. The main effort involves converting the california grassland into taro cultivation in order to maximize the ecosystem services and enhance the agricultural production to sustain the culture and economy of the Heeia community (Kakoo Oiwi, 2010). As studies indicate, wetland restoration efforts are effective means for maximizing the ecosystem services (Chen, et al., 2013). By investing in such an effort, the community of Heeia Coastal Wetland would serve as role

model for similar communities who are living in low land areas of Oahu or other islands. Such an endeavor is significant considering that this and similar areas are susceptible to seawater intrusion, flooding, invasive plants, degradation of coastal habitats, and decreased land productivity due to climate and land use changes (Rotzoll and Fletcher, 2013).

The main issues of concern regarding the restoration activities of the Heeia Wetland are related to the likely impacts on water availability, climate and land use changes, as well as setting the appropriate locations of restorations (Kakoo Oiwi, 2011). The conversion of california grassland to taro field would impact the hydrological and biogeochemical processes of the riparian wetland (Fang, *et al.*, 2013, Ncube, 2008). Furthermore, hydrologic components are expected to significantly and cumulatively influenced by climate and land use changes, including runoff, groundwater discharge, and streamflow (Lin, *et al.*, 2007). This study was conducted in collaboration with Kakoo Oiwi's community thus to assess the water availability under wetland restoration and the impacts on the WBCs taking into account the current and the future climate and land use changes scenarios. Furthermore, the study will evaluate the change in the upland stream portion and the related effects on the hydrologic processes of the coastal wetland. This area is expected to be influenced by the spatial and temporal variability of the hydrologic processes in high elevation of the Watershed where, unfortunately, hydrologic data is scarce (Cortes, *et al.*, 2011). In addition, the study will investigate the consequences of restoration on the coastal ecosystems regarding FSGD, DSi, and heat transport. The study results regarding WBCs estimates are expected to strengthen water management decision-making by improving the validity of visions and strategies of the wetland restoration. Such efforts will stress the important role of the integrated hydrological models for making decision regarding water management plans under the impacts of climate and land use changes.

1.2 Statement of the problem

The hydrogeological setting of the Heeia Watershed is supplying ample water for farming and aquaculture. For this reason, historically, the Ahupuaa of Heeia was considered as very valuable and productive in terms of both marine and terrestrial food resources. But unfortunately, with the rapid demographic and land use changes during the 1950s, the taro patches were converted to fallow land and overgrown with invasive species, which are choking the main stream and have destructed the habitats of native species. Therefore, the Heeia Wetland restoration becomes inevitable plan to restore the cultural,

environmental, and agricultural significance of this place as model for another lowland in other Hawaiian Islands (Kakoo Oiwi, 2011).

On September 2011, the Kakoo Oiwi community, and based on authorization from the landowner of the Heeia property (Hawaiian Community Development Authority, HCDA), started to restore a few acres of the Wetland and Heeia stream by converting the california grass to organic taro. The mangrove forest was also removed and the area was converted to pond as a native wetland habitat for bird and other aquatic species. This restoration project was supported by many scientific and environmental agencies, including The Nature Conservancy (TNC), the United State Fish and Wildlife Service (USFWS) Hawaii Fish Habitat Partnership, the U.S. Department of Agriculture, Natural Resources Conservation Service (NRCS), the National Oceanic and Atmospheric Administration (NOAA), and the Environmental Protection Agency (EPA). The sponsors also included the University of Hawaii Sea Grant College Program, which is the sponsor of this research. The project benefited from cooperation with Kakoo Oiwi community (Kakoo Oiwi, 2010, Kakoo Oiwi, 2011).

Water resources management decisions have a vital role in implementing and sustaining the restoration project for the Heeia Wetland area. Both surface and groundwater comprise the source of freshwater that feed the Heeia Coastal Wetland and the important Heeia fishpond. Water quality and quantity are the main factors affecting the indigenous wetland taro farming and coastal health ecosystems through the flow of a cooler freshwater with DSi, which sustains a healthy environment for abiotic and biotic elements of the coastal ecosystem. Developing managing strategy for the study site requires the use of hydrological models utilizing historical data on spatial and temporal scales to assess hydrological components and different pathways of freshwater within the Watershed. The models are also needed to assess the impacts of climate and land cover changes on WBCs with respect to current land cover and to the proposed restoration efforts. Identifying the priority areas for restoration requires estimating the water availability in different zones with different scenarios for current and future interactions between surface and groundwater for both wet and dry seasons. The interaction between surface and groundwater in the downstream area of the Watershed is influenced by the hydrogeological conditions of upstream side in the Watershed that has a variable hydrogeological land scape.

1.3 Objectives

The general goal of this study focused on the water resources assessment under different scenarios of climate and land cover changes within the Heeia Coastal Wetland. The integrated hydrological modeling approach was used as tool to assess the water resources under different conditions. To achieve this goal, the research will address the following objectives:

1. Investigating the potential impacts of wetland restoration on the hydrology of Heeia Coastal Wetland and Watershed.
2. Assessing applicability of a specific watershed model to evaluate the impacts of land cover change and climate projections on the hydrology of Wetland and the whole Heeia Watershed.
3. Developing a groundwater flow model for steady state and transient analyses conditions as a tool for integrated management of groundwater in the Heeia Wetland.
4. Studying the interaction between surface and groundwater by using the watershed and the groundwater models.
5. Estimating the amounts of surface and groundwater that enter and exit the wetland and the expected relative changes in the future under different scenarios of CL and SLR.
6. Evaluating the impact of different LU scenarios of the Heeia Wetland on surface and groundwater resources.
7. Estimating the current and future FSGD across the coastline of the Heeia Watershed in response to CL and LU scenarios.
8. Assessing the distribution of DSi through aquifer and across the ocean-land interface, which is driven by dispersion and advection forces flow by using the density dependent groundwater flow model.
9. Evaluating the cold groundwater flow from mountain regions through the Heeia aquifers and across the ocean-land interface under different scenarios of CL and SLR by using the density dependent model.
10. Providing recommendations that will be used by the Heeia community and decision makers to support their adaptive management of the Heeia Wetland Restoration.

1.4 Research methodology

The main steps of the research methodology to achieve the above objectives of this dissertation research is illustrated in the flowchart, which includes the roadmap of setting the research agenda to achieve the research targets (Figure 1):

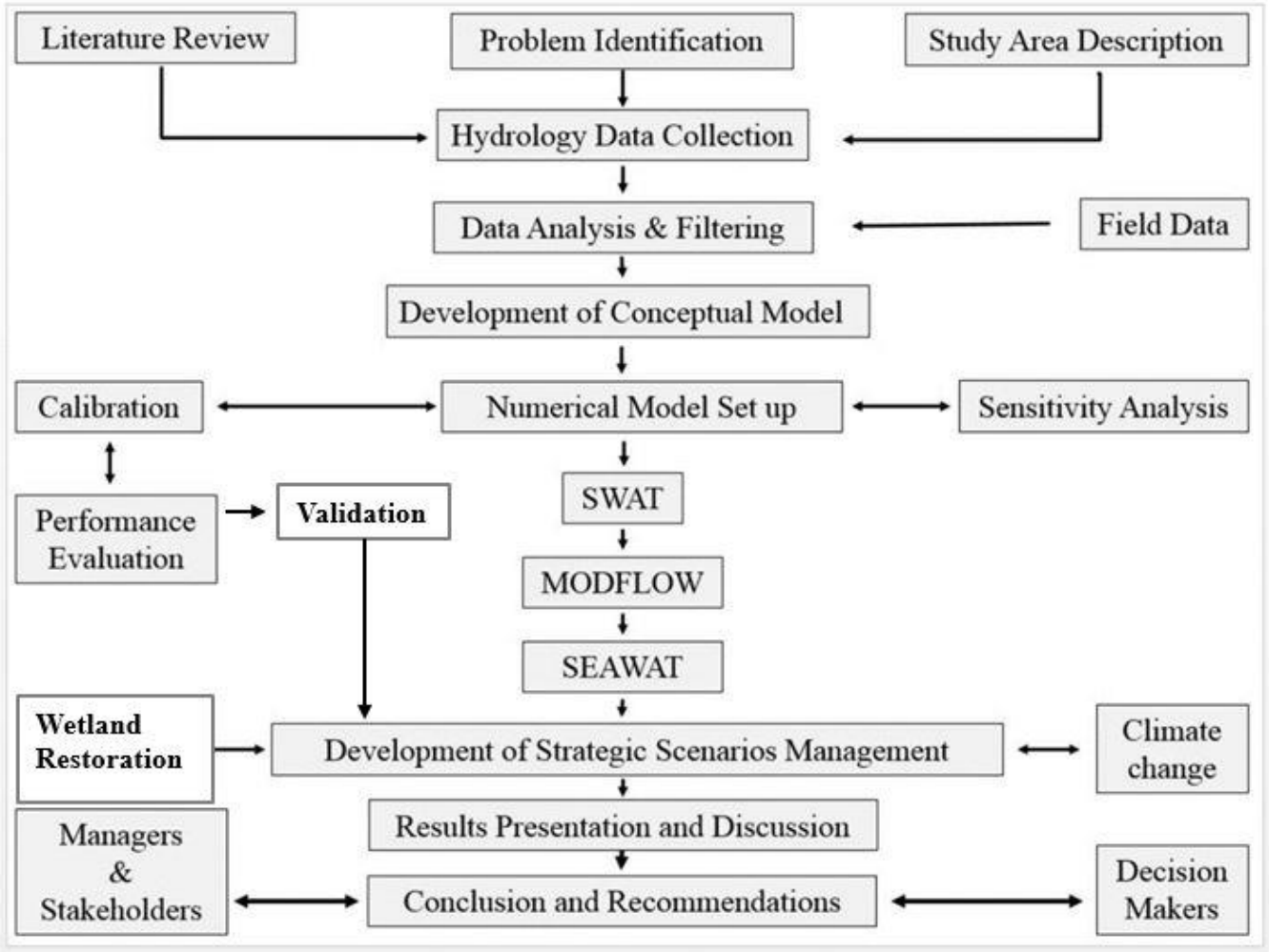

Figure 1: Flow chart for the research methodology.

1.5 Structure of the dissertation

Following the above introductory Chapter 1, the dissertation consists of additional six chapters whose contents can be summarized as follows:

- Chapter two covers an overview of the study region and a description of its characterizations regard to geography, topography, climatic components, and the history of human activities within the Heeia Wetland. Information will include the hydrogeological properties of the whole Heeia Watershed and the available data, which will be used for the integrated hydrological modeling for water resources management in the Heeia Wetland.
- Chapter three, describes the baseline applicability of a watershed model for the Heeia Watershed, covering model set-up and input data, parameter sensitivity analysis, calibration, validation, performance, and output data analysis.
- Chapter four, is addressed to use the watershed model to evaluate the predicted hydrological changes of Heeia Wetland Restoration under different scenarios of LU and CL.
- Chapter five, develops a groundwater model for the area in terms of conceptualization, simulation for both steady state and transient conditions under time-varying stresses. Following, calibration and validation the model is used to estimate the impacts of climate and land use changes on the groundwater sustainability. Furthermore, the model is used to estimate the FSGD for different scenarios of CL, LU, and SLR.
- Chapter six presents the setup of the density-dependent model, which is used for simulating seawater intrusion, DSI fluxes, and heat transport. The results of the calibrated model are used to investigate the cold groundwater flow and the distribution of the DSi from the mountain regions through the Heeia aquifers and across the ocean-land interface. The model is also used to study the effect of management scenarios on the seawater intrusion.
- Chapter seven, provides recommendations regarding the hydrology of the Heeia Wetland Restoration efforts.

Chapter2 The study area

2.1 Location and physical geography

The Heeia Watershed is one of the Koolau Poko Watersheds, which is located on the windward side of northeast coast of Oahu Island between 157.7925 and 157.8397 west, and 21.3941 and 21.4545 north (Figure 2). The watershed is located in the central part of the Koolau Poko District that is bounded to the north by the Kahaluu Watershed and to the south by the Kaneohe Watershed. The watershed is bounded by the Heeia fishpond and Kaneohe Bay to the east and the crests of Koolau Mountains to the west. The 2000 Census estimated that a population of 13,595 populations reside within the Heeia Watershed (KBAC, 2007). Heeia means "washed way", which is the famous name of Ahupuaa, Watershed, Stream, and Fishpond (Devaney, 1976). The Heeia region holds much cultural and historical importance for the people of Heeia community.

Historically, the Heeia Watershed was considered as one of the highest productive coastal areas in the Island of Oahu due to taro and rice cultivation. In addition, the region is considered as an important economic resource due to the existence of the largest fishpond on Oahu at the Heeia Stream estuary. The Heeia Watershed is a precipitous, rugged, and narrow valley that transforms into a flat swamp region, which represents about half of the coastal plain (Izuka, *et al.*, 1993). The Haiku and Iolekaa streams are the major perennial streams that converge together approximately at 240 meters downstream of Kahekili Highway and finally fan out to wetland, mangrove swamp areas and then to the Heeia fishpond. The main Heeia stream and its tributaries drain an area of 11.5 square kilometers with total stream length of about 12 kilometers. The average continuous main streamflow is 6851cubic meters per day with an average gradient of 11%. The median flow of Haiku and Iolekaa streams are 3915, 1223 cubic meters per day, respectively (Wilson, 2004). The Heeia stream feeds most of the largest federally designated wetlands and fishpond by freshwater (Figure 2). The wetland provides a natural habitat for endemic endangered species, like native Hawaiian water-birds, migratory waterfowl and shorebirds (Kealoha, 2009). In addition, the wetland serves as a water purifier for Kaneohe Bay by trapping sediment, pollutants and modulating the freshwater discharge in the Bay.

There are three main sources of potable water in the watershed: Haiku tunnel, Haiku well, and Iolekaa well (Figure 2), with average monthly productions of 51113, 38346, 5403 cubic meters per month,

respectively, for the period from 2000 to 2014 (Figure 3) (Board of Water Supply, 2012). The data show a drastic decline in production for the Haiku tunnel starting in 2008 due to increase the permits of the publicity and privately owned wells (Wilson, 2008). In addition, the data show an increase in pumping for the Iolekaa well starting in 2013.

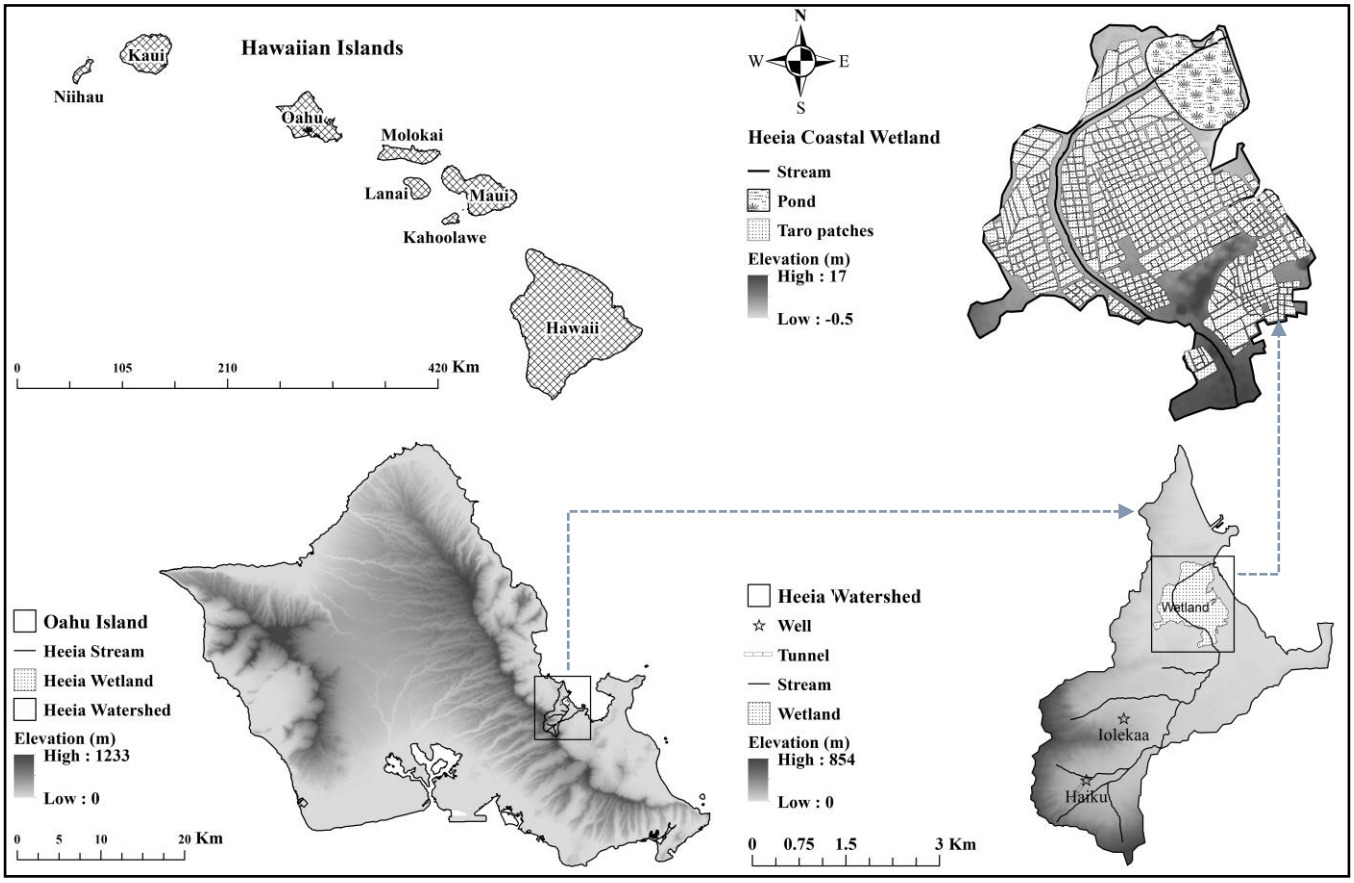

Figure 2: Geographic and topographic maps of the Heeia Coastal Wetland.

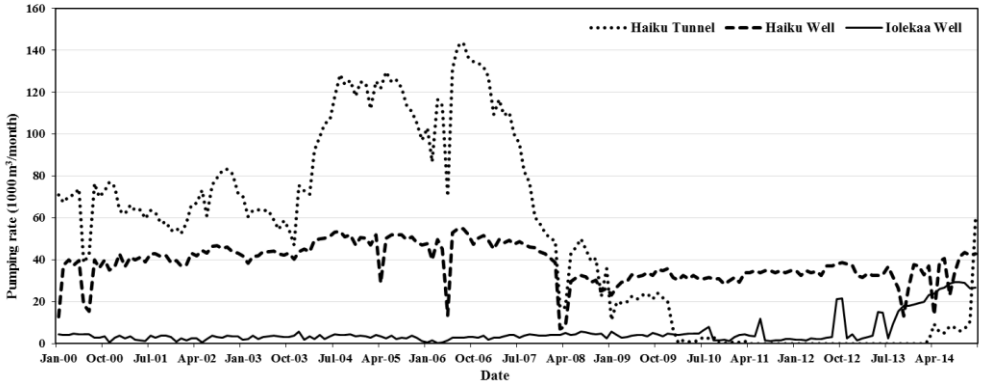

Figure 3: The monthly pumping rate of potable water sources in the Heeia Watershed.

2.2 Climate

The climate in the Heeia Watershed is considered as semitropical, which lies in the northeast trade-wind belt. The prevailing winds blow from east to west contrasting with the winds in mainland, which blow from west to east (Bankoff, 2006). About 70% of the time, trade-winds blow from northeast and east direction with average daily speed of 16 to 31 kilometers per hour in the Heeia Watershed (Jokiel, *et al.*, 2004, NOAA, 2016), while the average monthly speed is approximately 5 kilometers per hour in the Heeia Coastal Wetland (Figure 5). The strongest trade-winds speed occurs during winter storms, while the trade-winds are more consistent during summer months.

The rainfall is plentiful and greater from November through April in the windward sector of the Oahu Island. The reason of abundant rainfall is due to the orthographic effect of prevailing trade-wind directions, which are perpendicular to the Koolau mountain chain. This effect occurs when the moist air rises up the mountain cliff and suddenly contacts the colder air mass then its moisture will be condensed and falls as rain (Carlquist, 1980, NOAA, 2016). Consequently, the annual rainfall of the Heeia Watershed varies from 1000 to 3000 mm per year (Giambelluca, *et al.*, 2011) as shown in (Figure 4). The maximum daily rainfall, usually takes place in winter season (November to April) during the storms, which counteract the strong trade-wind flow. In contrast, the dry season extends from May to October (Timm, *et al.*, 2015).

The air temperature ranges between 20 °C to 28 °C through the year. Temperature is highest during August to September and lowest in January to February (Carlquist, 1980, Jokiel, *et al.*, 2004). Due to ocean effect, the coastal regions have narrow temperature ranges (Figure 5). In addition, the yearly average of water loss through evaporation and transpiration is about 1100 mm for the Heeia Watershed (Carlquist, 1980, Takasaki, *et al.*, 1969).

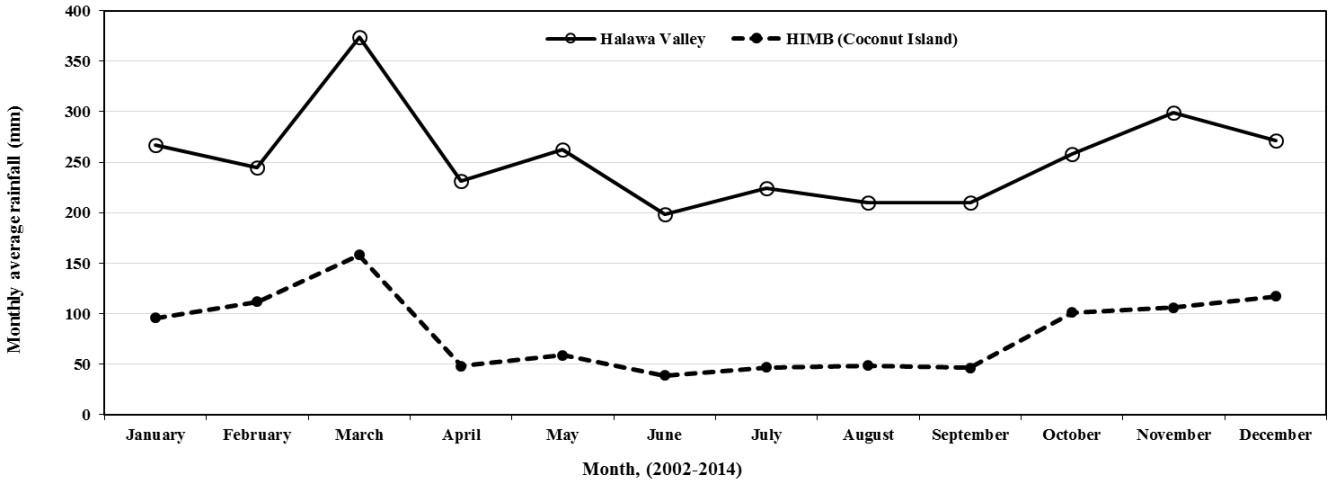

Figure 4: The monthly average rainfall data of stations in the vicinity of the Heeia Watershed from 2002 to 2014.

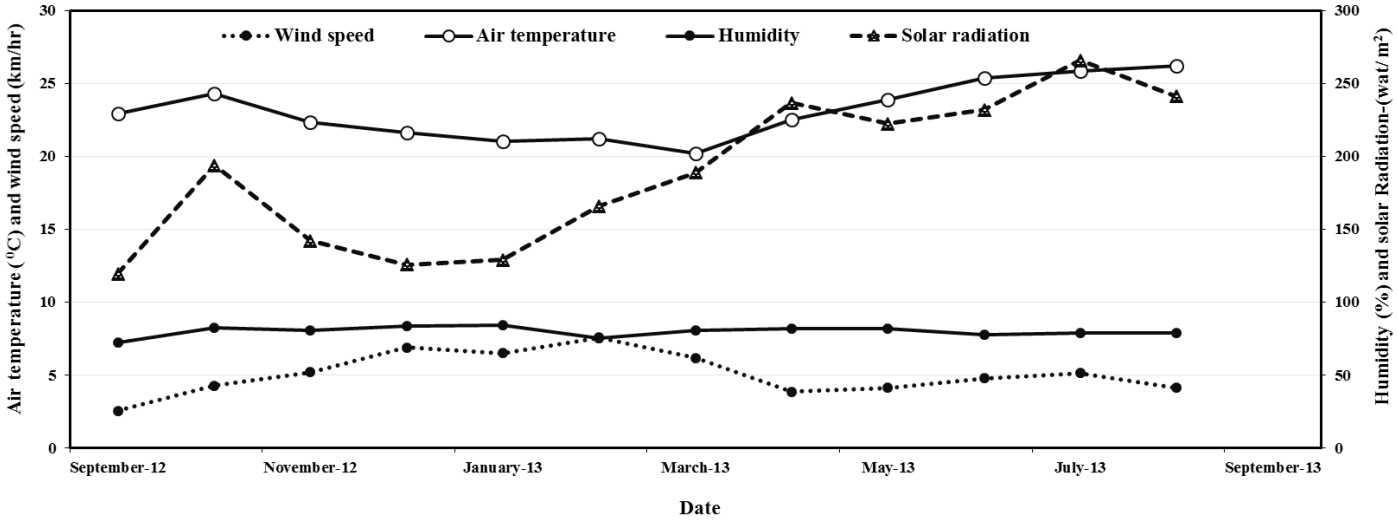

Figure 5: Monitoring of weather parameters through an automatic weather station (WatchDog 2900ET).

2.3 Hydrogeological features

The Heeia Coastal Wetland represents the drainage basin of the main stream of Heeia Watershed. Therefore, it is considered the reservoir of freshwater, which is flowing from the springs in the mountains as surface water, lateral flow, and subsurface seepage through groundwater discharge (baseflow). These hydrologic features enable the indigenous society to meet their needs from land and sea in prized coastal region (Hunter and Evans, 1995). The elevation of the Heeia Watershed ranges from 0 to 854 meter above mean sea level with an average slope of 40%, while the elevation of Heeia Wetland ranges from (-0.5 to 17) meters above mean sea level with an average slope of 5% (Kakoo

Oiwi, 2011). The land use of the Wetland is dominated by emergent wetland (77%), forested wetland (8%), shrub wetland (5%), evergreen (4%), and other land use (6%) (Figure 6). The proposed taro land use will cover cultivated land, shrub wetland, and emergent wetland, while the proposed pond area will cover part of the forest wetland. Currently, most of the wetland area are blanketed by the invasive california grass (Urochla mutica), while the forest wetland is covered by mangrove trees (https://coast.noaa.gov/ccapatlas/).

The majority of soils in the Heeia Wetland include Hanalei silty clay (HnA) in the southern part and Marsh (MZ) in the northern part (Figure 7) with an average slope of 5% according to Natural Resources Conservation Service (NRCS). The typical soil profile in Hanalei silty clay is composed of poorly drained silty clay and silty clay loam texture down to 0.91 meters below surface, moderate available water capacity, and with frequent flooding. The Marsh soil is composed of mucky peat from 0 to 1.5 meter in depth with very poorly drained, very high available water capacity, frequent flooding, and ponding (Kakoo Oiwi, 2011). The coastal plains, which form the base of Koolau Mountains and spread out into the Heeia fishpond and Kaneohe Bay, are flat and some of them are covered by water ponds (Hastert and Planners, 2007). The average saturated hydraulic conductivities of Hanalei silty clay and Marsh soil are 0.605 and 2.42 meter per day, respectively (Arnold, *et al.*, 2012).

The geologic features of the study area are characterized by the presence of thousands of thin lava flows that has the greatest hydrological importance. These lava flows are very porous due to an abundance of clinker sections, voids between flow surfaces, shrinkage joints and fractures, lava tubes, and gas vents. The porous rock layers are highly permeable and serve as excellent aquifers. The aquifer accumulates the fresh water in a large lens, which is maintained through direct recharge by rainfall and indirect recharge by seepage from high water level of dike-impounded groundwater (Armstrong and Bier, 1973, Stearns and Vaksvik, 1935). A generalized geologic section (Figure 8) indicates that the geologic materials of the Heeia Watershed are composed of Koolau Basalt (45.8 %), Honolulu Volcanics (3.1 %), Older alluvium (37.4 %), Alluvium (13.2 %), and Beach deposit (0.5 %) (Izuka, *et al.*, 1993, Stearns and Vaksvik, 1935). The Koolau basalt, which is characterized by very high hydraulic conductivity of up to 1500 m d-1, largely covers the mountain region of the watershed. The latter may have significant effects on the hydrological processes (e.g., groundwater recharge), with the Koolau ridge of the watershed receiving the highest recharge. In addition, the bed rock layer includes marginal

and complex dikes zones. The groundwater in the marginal dikes zone of high-level aquifers flows through cracks or overflows via eroded dikes supplying abundant water to the basal aquifer, which is a freshwater lens floating on the top of seawater. This setting historically provided ample water for farming and aquaculture (Takasaki, *et al.*, 1969). Between half and three fourths of recharge in high level aquifer, can be taken as sustainable yield, which represents the forced withdrawal rate of groundwater indefinitely without compromising the future quality of pumping rate (Board of Water Supply, 2012, Wilson, 2008). The sustainable yield of Heeia aquifer that saves yield of water extraction per unit time, was 12656 cubic meter per day as part of Koolau Poko aquifers (Board of Water Supply, 2012, Wilson, 2008). The groundwater flow directions is influenced by the dike orientation at Koolau Mountains, which represents the upland part of the Heeia Watershed. The recharge generally is greatest for the upper elevation of the Koolau Mountains with annual recharge rates exceeding 3.81 meter (Shade and Nichols, 1996). The shallow and deep aquifers in the dike-intruded lava flows, receive recharge of 0.00492 meter per day from the 2.54 square-kilometer drainage area of Haiku Valley. The Haiku stream receives about 2936 cubic meter per day as baseflow, which represents 75% of median streamflow at Haiku station (Izuka, *et al.*, 1993). The Heeia aquifer is classified as high-level fresh water none contact with seawater, unconfined aquifer in dike compartments, drinking uses, fresh water and low salinity in low land, irreplaceable, and high vulnerable to contamination according to aquifer classification of Oahu Island (Code 30603212, 11111, Figure 9) (Mink and Lau, 1993).

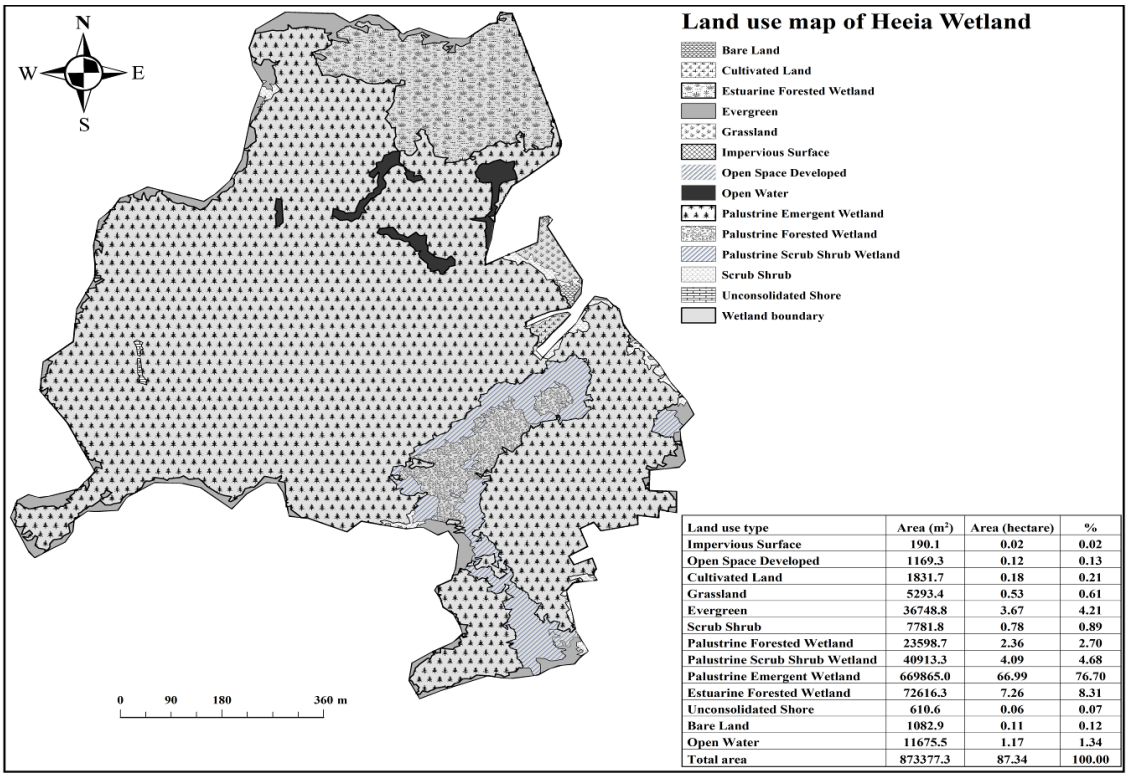

Land use type	Area (m^2)	Area (hectare)	%
Impervious Surface	190.1	0.02	0.02
Open Space Developed	1169.3	0.12	0.13
Cultivated Land	1831.7	0.18	0.21
Grassland	5293.4	0.53	0.61
Evergreen	36748.8	3.67	4.21
Scrub Shrub	7781.8	0.78	0.89
Palustrine Forested Wetland	23598.7	2.36	2.70
Palustrine Scrub Shrub Wetland	40913.3	4.09	4.68
Palustrine Emergent Wetland	669865.0	66.99	76.70
Estuarine Forested Wetland	72616.3	7.26	8.31
Unconsolidated Shore	610.6	0.06	0.07
Bare Land	1082.9	0.11	0.12
Open Water	11675.5	1.17	1.34
Total area	873377.3	87.34	100.00

Figure 6: The current land use types of the Heeia Wetland.

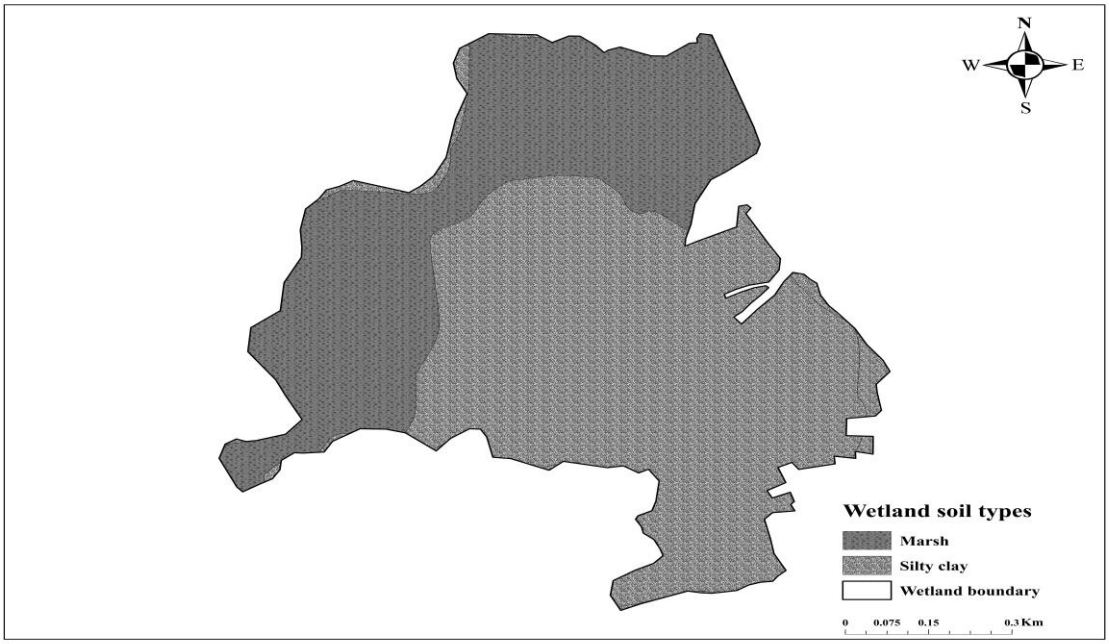

Figure 7: Soils map of the Heeia Wetland.

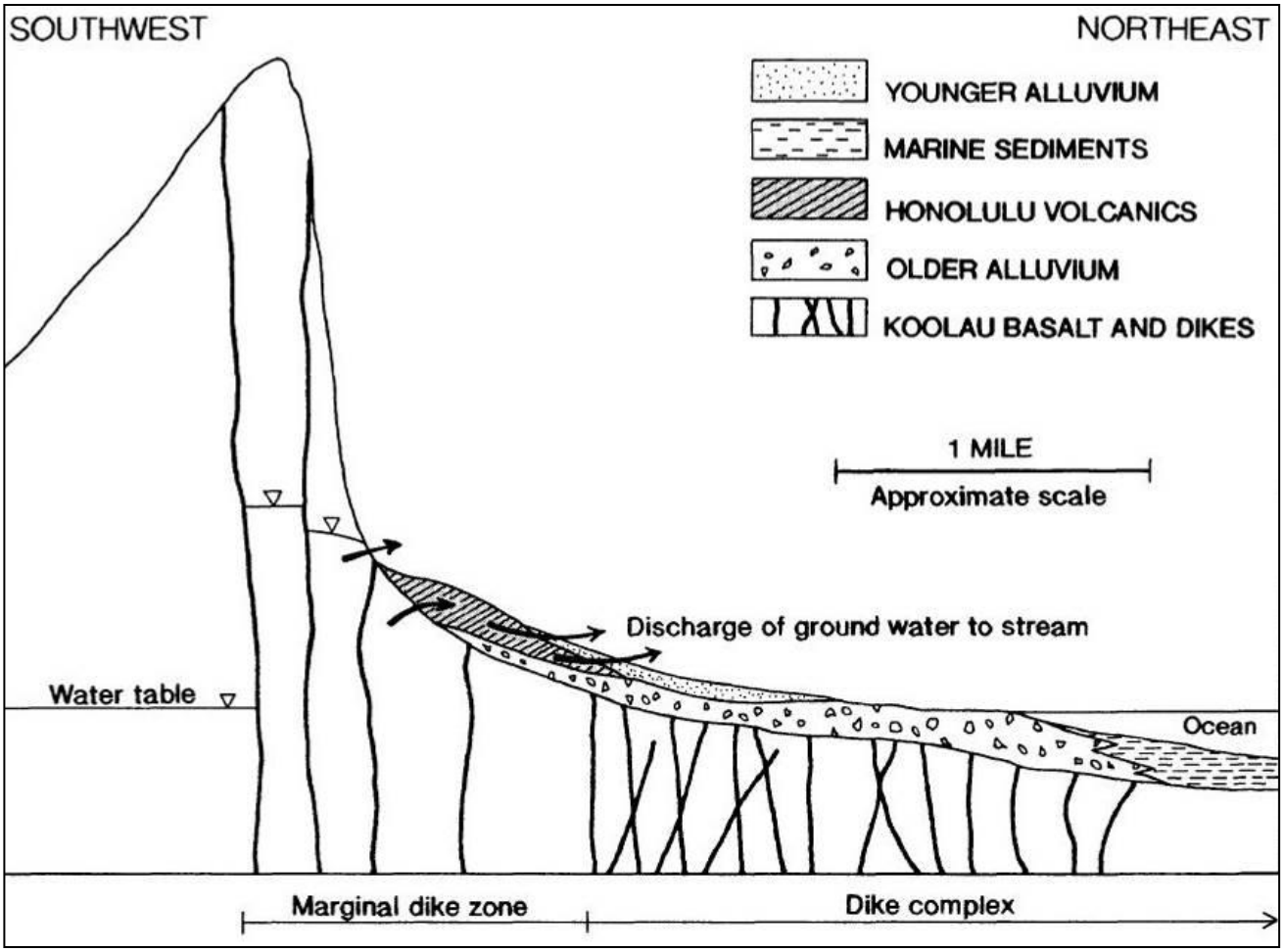

Figure 8: Geological section of the Heeia Watershed (Izuka, et al., 1993).

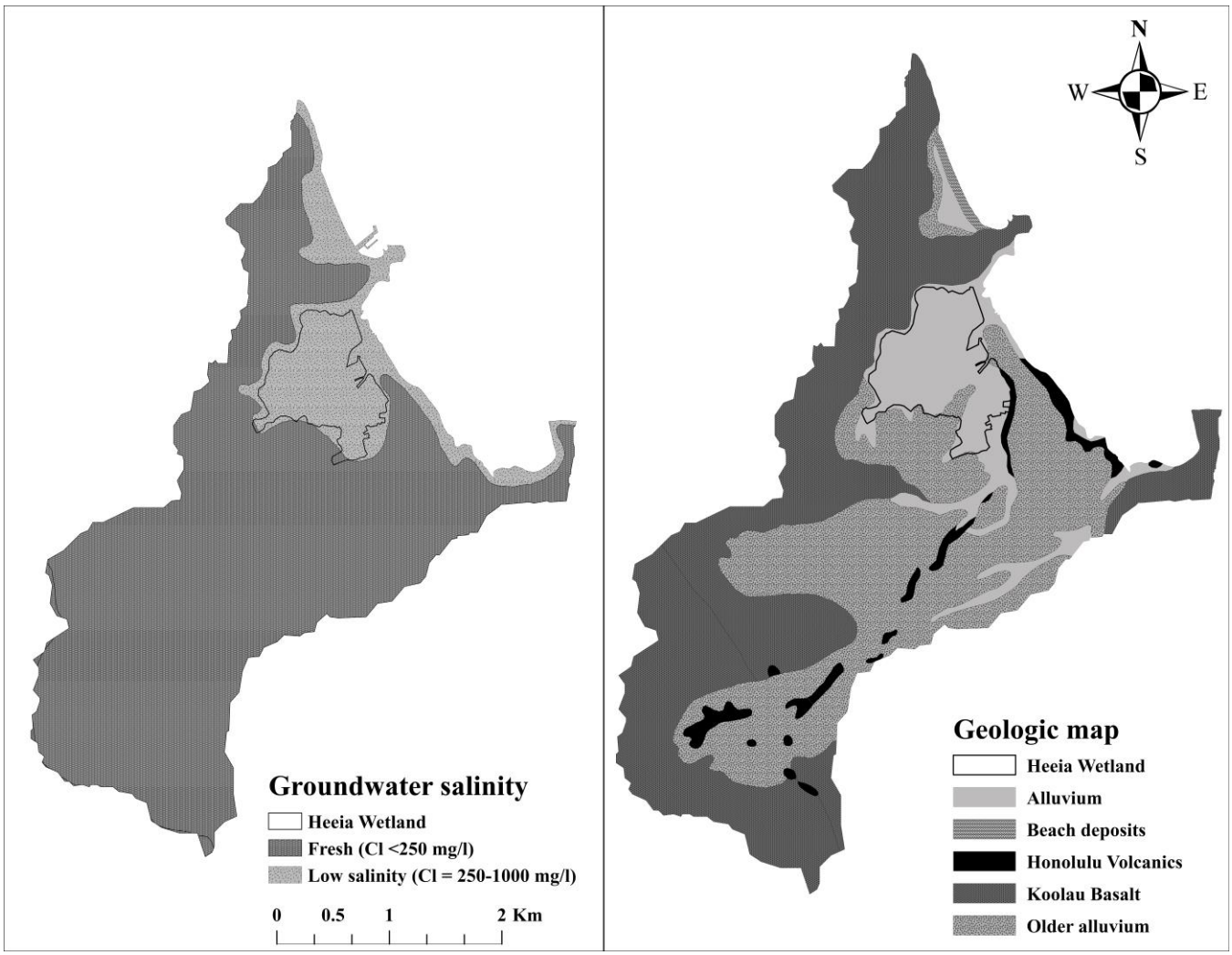

Figure 9: The aquifers salinity and geologic maps of the Heeia Watershed.

2.4 Available Data and Approaches

The research started by collecting available hydrogeological and related data from historical records, reports, maps from available sources, and making contacts with local specialists of the study area. The integrated models will be constructed based on the following data:

1. Digital elevation maps:

a. A 10x10 m Digital Elevation Models (DEM) obtained from Department of Commerce (DOC), National Oceanic and Atmospheric Administration (NOAA), Center for Coastal Monitoring and Assessment (CCMA), and represents the upstream of the Heeia Watershed.

b. A 3x3 m Coastal Lidar map obtained from NOAA Office for Coastal Management, and represents the coastal wetland area of the downstream of the Heeia Watershed.

c. A 4x4 m the Heeia Bathymetry map provided by Pacific Islands Benthic Habitat Mapping Center, represents the Heeia shore.

2. Historical daily streamflow data of 1950 to 2014 were downloaded from the Haiku station (USGS gauging station: 16275000).

3. Baseflow was estimated from the historical daily streamflow data at the Haiku station (USGS gauging station: 16275000), by using the Water Engineering Time Series Processing tool (WETSPRO) (Willems, 2004). Field streamflow discharge measurements completed during this study at the stream entry point to the Heeia Wetland, which was completed by using current meter method (Khan, *et al.*, 1997). These data were correlated with the Haiku's streamflow by using an overlapping data collection period to obtain continuous time series data at the Wetland.

4. Groundwater levels were recorded within the Heeia Wetland at different points completed during this study by using Schlumberger and Solinst levelogger sensors as well as conductivity and temperature recorders (Black, *et al.*, 2008, Grant, *et al.*, 2013). These data will be used for groundwater model calibration and validation.

5. The aquifer parameters and geological structure are estimated and extrapolated from the wells information within the study area, which were obtained from previous studies in the same region (Izuka, *et al.*, 1993, Takasaki, *et al.*, 1969, Taniguchi, 1982, VTN Pacific, 1983, Whittier, *et al.*, 2006).

6. Historical monthly well and tunnel productions obtained from the Honolulu Board of water supply (Board of Water Supply, 2012).
7. Historical sea level, air temperature, and ocean water temperature data were obtained from the Department of Commerce (DOC), National Oceanic and Atmospheric Administration (NOAA), National Climatic Data Center (NCDC). The daily rainfall, solar radiation, wind speed, and maximum / minimum temperature data for the coastal zone were obtained from the Hawaii Institute of Marine Biology (HIMB) at Coconut Island for the period of 2000 to 2014. Moreover, the daily rainfall data for the upland zone were downloaded from the USGS station at the North Halawa Valley. Another source of daily rainfall and maximum/minimum temperature were obtained from the National Climatic and Data Center (NCDC) of NOAA at Kaneohe 838.1 station (http://www.ncdc.noaa.gov/cdo-web/datasets). Available daily relative humidity data were derived from the Western Region Climate Center (WRCC) at the Oahu Schofield East and Oahu Forest National Weather Research (NWR) (http://www.raws.dri.edu/wraws/hiF.html).

   During this research, limited climatic data were obtained for two years (2012-2013) from a weather station, which was installed in the Heeia Wetland (WatchDog 2000 Series-Spectrum Technologies, Inc.). Rainfall Atlas of Hawaii (250x250 m, http://rainfall.geography.hawaii.edu/) was used as reference of some climatic spatial patterns, which was used for data rescaling.
8. A 2.4x2.4m land use map data was downloaded from the NOAA Coastal Change Analysis Program (C-CAP) http://coast.noaa.gov/ccapftp/.
9. A geologic map was obtained from the U.S. Geological Survey (USGS) (Sherrod, *et al.*, 2007).
10. A 1:24,000 scale soil map was obtained from the Soil Survey Geographic (SSURGO) database as provided by the U.S. Department of Agriculture, Natural Resources Conservation Service (USDA-NRCS).
11. Crop database: as the taro land use is not included in the crop database of SWAT, the specific plant parameters were obtained from the actual field measurement and literature values (Arnold, *et al.*, 2012, Gingerich, *et al.*, 2007, Mat, *et al.*, 2006, Onwueme, 1999, Penn, 1997, Pratiwi, *et al.*, 2014, Shih and Snyder, 1984).

Considering hydro-meteorological data's scarcity in the Heeia Watershed, various approaches were used to resolve this problem. The techniques include interpolation, scaling, and estimation based on the observed data and contour maps of the surrounding Watersheds. For instance, fifteen virtual stations were created within the Heeia Watershed that were distributed according to the spatial variability of rainfall. The climatic data (e.g., rainfall) were generated for each station on the basis of the closest rain gauge station and on the isohyets of the Rainfall Atlas of Hawaii (Giambelluca, *et al.*, 2011). For the other variables (temperature, wind speed, solar radiation, and relative humidity), a correlation analysis was performed among the data from the Heeia and those stations, which are located outside the Watershed. The purpose of the correlation analysis was to fill missing data in the Heeia records. Those stations had reasonable correlations ($r^2 \geq 0.5$) for daily values, which were used to fill in the missing data.

For model parameter optimization, daily streamflow data recorded at the Haiku station (USGS gauging station: 16275000) and wetland flow sampling station were used. As streamflow data were not available at the coastal plain and at the estuary, total daily streamflows at the coastal plain were estimated based on the discharge measurements at the stream entry point to the Heeia Wetland and the observed streamflow data at the Haiku station. Streamflow at the wetland station was measured using a Pygmy flow meter for stream stages ranging from 1 to 1.4 m, over the year corresponding to 0.2 to 1 $m^3 s^{-1}$ in the period from May to December 2013. During each measurement, multiple discharge readings were taken across the stream to cover every 0.25 m of the stream for which a cross section was also measured. A Solinst pressure depth sensor was installed to monitor water level every 30 minutes for the same period. It should be mentioned that the USGS 16275000 station used a non-submersible pressure transducer with a bubbler system to accurately measure water level at every 15 minutes during the low and medium flows and every 5 minutes during the high flow periods. The recorded water level was converted to streamflow by the USGS processing software (Ronald L. Rickman, personal communication, 2015). A scaling factor was derived between the gauged streamflow at the Haiku and the corresponding measured values at the Wetland for the overlapping period. It should be recognized however that the scaling factor is biased because the measurements only covered baseflow conditions and do not reflect variability of this relationship due to changes in surface runoff and recharge with rainfall, including land use and topography. However, due to the lack of appropriate data, the study opted to use the developed scaling factor at

least to evaluate the simulated time evolution of daily streamflow at the downstream location. Based on the analysis, the stream discharge at the wetland entry was approximately 2.5 times the Haiku streamflow value. In addition, the output of calibrated groundwater flow modeling provided similar scaling factor. Consequently, a scaling factor of 2.5 was used to estimate daily streamflow data at downstream. Hereafter, the downstream streamflow estimate location is termed “Wetland Station”.

Chapter3 Assessment of coastal wetland restoration impacts on the water balance components of Heeia Watershed in Hawaii

3.1 Introduction

In the Hawaiian Islands, the coastal wetlands represent the critical interface between the terrestrial and ocean zones, which have gained vital importance in terms of economic and environmental aspects. Coastal wetlands naturally purify the water from sediments and contaminants, transform nutrients, slowdown the flow of freshwater from the mountains to the ocean, provide suitable habitats for flora and fauna assemblages, mitigate air temperature, decrease greenhouse emission through carbon sequestration processes, and consider very attractive and productive regions for tourists and residents (Mitsch and Gosselink, 2007). These regions play important role in Hawaii against flooding, pollution, and the negative impacts of climate and land cover changes as well as work as sponge (absorbing water during wet season and releasing it through dry season)(Bantilan-Smith, *et al.*, 2009, Bruland, 2008). The dynamic functionalities of coastal wetlands forced various organizations including scientific research centers to be more active in restoring and managing the natural resources of the coastal wetland. In addition, the recent financial and moral supports of federal policies regarding preserved wetlands, such as "no net loss of wetlands in United States", encourage many non-profit organizations to restore the degraded wetlands (Mitsch and Gosselink, 2007).

The Heeia Coastal Wetland is a typical example of the degraded wetlands in Hawaii, where wetland restoration has been planned (Henry, 2006). Before 1950s, it was considered the most productive ecosystem for both marine and terrestrial food resources in the Oahu Island (KBAC, 2007). After 1950s, the Heeia Wetland was overrun by the invasive california grass (*Urochla mutica*) and lost most of its great ecological functionalities. The passive restoration approach (i.e., restoration based on nature's work) cannot significantly restore the degraded wetland, unless physical human interventions is directly employed in restoration to control various processes (Kusler, 1990). Consequently, human intervention for the coastal wetland restoration has a paramount importance for the Heeia Coastal Wetland. The recently proposed Heeia Wetland Restoration plan includes the conversion of about 69 hectares of wetland covered by california grass into organic wetland taro (*Colocasia esculenta*) and eight hectares

of wetland mangrove forest to wetland sedges papyrus, which will serve as a convenience habitat for the native bird and nursery site for juvenile fish (Kakoo Oiwi, 2011).

While the wetland restoration activities can improve the ecological functioning of a coastal wetland, it may have considerable effect on the hydrologic cycle components of the site. For example, the wetland evaporates water more than other land types, decreases air temperature through evaporation process, carbon sequestration process, sustains stream temperature (through shading, storing, and releasing cool water during dry season), and regulates the stream flows through working as a sponge (absorbing water during wet season and releasing it during dry season), (Bullock and Acreman, 2003). Such studies to assess the effect of restoration on the hydrologic cycle component are needed to aid the Heeia Coastal Wetland Restoration process. In addition, there is a need to assess the impacts of climate and land use changes on the wetland functions (Pandey, *et al.*, 2016, Pervez and Henebry, 2015, Rashford, *et al.*, 2016). Such impacts are poorly understood for coastal wetlands and their impacts on the WBCs in Hawaii (Bruland, 2008, Henry, 2006).

The anthropogenic interventions, climate patterns and variability interactions with the biologic ecosystem are the effective drivers for land cover changes, which in turn modify the WBCs like streamflow, evapotranspiration, and groundwater recharge (Guardiola-Claramonte, 2009). Many studies mentioned that anthropogenic land cover changes cause increase in runoff generation, lateral flow, and streamflow under high connectivity between surface and groundwater (Alden, 1983, Bruijnzeel, 1988, Bruijnzeel, 2004, Guardiola-Claramonte, 2009, Hornbeck, *et al.*, l970). Tropical environments show high sensitivity to land use disturbance. The land cover changes disturb the surface soil and decreased soil infiltration, which in turn causes high runoff and increased streamflow (Bruijnzeel, 2002b). Therefore, the land cover changes need a restoration of appropriate vegetation communities that are suitable for the regional natural hydrologic conditions.

This study assessed the WBCs of Heeia Coastal Wetland under current and future land cover change conditions. The future land cover change was formulated based on the Heeia Coastal Wetland Restoration plan (Kakoo Oiwi, 2011). In addition, the study investigated the land cover change impacts on the spatial and temporal variability of the hydrologic processes within the coastal wetland and its relationship with the hydrologic processes in the high elevated land of Heeia Watershed(Cortes, *et al.*, 2011). Such studies need a tool to assess the WBCs of Heeia Wetland. The Soil and Water Assessment

Tool (SWAT) model is a useful tool to assess the WBCs under current and future land use conditions (Green, *et al.*, 2006).

The SWAT model is appropriate for the study area because it is a dynamic processed model in terms of its ability to change the input data of land use and climate projections over time to predict the future impacts of wetland restoration on the WBCs (Arnold, *et al.*, 1998). Furthermore, it is computationally efficient to operate under different scales and applicable to simulate the effects of management changes for long periods. The model has a great potential to simulate and evaluate the land use change effect on the WBCs (Kiros, *et al.*, 2015).

The objectives of this study include evaluation of the capability and effectiveness of the SWAT model to assess the impact of different land cover change scenarios on the WBCs of the whole Watershed and the Coastal Wetland scale. In addition, this study can be used as a baseline to quantify the potential impacts of the future climate projections impacts on the Heeia Wetland Restoration plan.

3.2 Methodology

The watershed (SWAT) model was used as tool to assess the land cover change impacts on the WBCs of Heeia Coastal Wetland and the whole Watershed. The main challenges in this study included the lack of long-term historical climate data, small scale with lack of landscape parameter information, no flow gauging station at downstream, absence of taro crop and management database in SWAT model, and scarcity of hydrologic studies of Heeia Watershed. The study approach started by defined the problem, collected the historical climate data from the weather stations close to the study area, installed weather station within the Heeia Coastal Wetland, and added new field of taro crop into the SWAT model database based on the field measurements and the literatures review.

3.2.1 SWAT model description

The SWAT model is a deterministic, semi-distributed, physically based, and continuous Watershed simulator operating on different time steps (Arnold, *et al.*, 1998, Gassman, *et al.*, 2007). The SWAT model has ability to model ungauged or poorly gauged watersheds as it is a physically-based model. The model is user-friendly and easy to perform sensitivity, calibration, and uncertainty analysis. The SWAT linked tools are freely available on-line that enable the users to model the quantity and quality of surface

water of watersheds worldwide (Kiros, *et al.*, 2015, Ndomba, *et al.*, 2008). The limitations of the SWAT model are non-spatial variability within its hydrologic response unit (HRU) (Glavan and Pintar, 2012).

The SWAT model has been widely applied for studies dealing with watershed hydrology, soil erosion, sediment transport, water quality variables, climate and land use changes, and watershed management impacts (Gassman, *et al.*, 2007). The SWAT uses water balance equations, which includes precipitation, surface runoff, actual evapotranspiration, interflow, percolation, return flow, and deep groundwater losses components (Neitsch, *et al.*, 2011). The model uses a modified Soil Conservation Service Curve Number (SCS-CN) method (Cronshey, 1986), which determines the surface runoff based on the area's hydrologic group, land use, and antecedent moisture content for each HRU. In this study, the SCS-CN method for surface runoff simulations, the Penman-Monteith method (Giambelluca, *et al.*, 2014) for potential evapotranspiration estimation, and the variable storage routing method (King, *et al.*, 1999, Williams, 1969) for daily streamflow routing were used for the Heeia Watershed simulation.

The SWAT model performance is significantly influenced by the quality of input data. Specifically in the case of this study, the main challenge is the absence of the hydrological and metrological data within the Watershed except the USGS Haiku streamflow station. Therefore, the absence of observed input data, need to adopt different techniques in generating, estimating, and editing various missing model parameters, like climate components, crop database, and management file to match the land use in Watershed and Wetland Restoration (Nyeko, 2015).

3.2.2 Model setup

The study area of SWAT model was built up by using ArcSWAT2012 (revision 627) based on the available geospatial data, which included DEM, land use, soil map, and the hydro-metrological data (Figure 10). The model ran at a daily time-step from 1/1/2000 to 12/31/2014. The SWAT model simulation time was split into three periods, which encompassed a warming-up period (2000-2001) to initialize the state variables of the system; a calibration period (2002-2008), and a validation period (2009-2014). The modeled Heeia Watershed was divided into 22 subbasins and 984 hydrologic response units (HRUs) based on the similar combinations of land use, soil type, and slope. The subbasins were delineated based on both DEM and user defined threshold value (minimum area) to be considered as a subbasin. The lower threshold value was used in order to capture the spatial (topographic) variability of the Watershed as stream flow routing process was performed at subbasin scale. Zero threshold value

was used for HRUs definition, which was particularly important for land use change or management studies. To further capture the topographic variability of the Watershed, five slope classes of 0-10%, 10-25%, 25-40%, 40-70% and >70% were defined, based on the slope classes of Heeia Watershed (Kakoo Oiwi, 2011).

3.2.3 SWAT model sensitivity, calibration, validation, and uncertainty analysis

Prior to the calibration, a sensitivity analysis (SA) was performed using the Latin Hypercube-One-factor-At-a-Time (LH-OAT) technique as implemented in SWAT-CUP (Abbaspour, *et al.*, 2007). Then, the SWAT model was calibrated using the parameters to which the model showed high sensitivity. For model calibration process, which implemented the Sequential Uncertainty Fitting (SUFI2) algorithm of SWAT-CUP (Abbaspour, *et al.*, 2007), a manual calibration was performed to fine tune the calibrated parameters, particularly to obtain a reasonable agreement for various WBCs (Van Liew, *et al.*, 2005). Such an approach substantially reduced the time-consuming manual calibration and also allows making quantitative and qualitative comparisons (Arnold, *et al.*, 2012). The daily streamflow data of USGS Haiku station and Wetland station, were used for calibration and validation.

The SWAT-CUP 2012 (version 5.1.6) was used for uncertainty analysis of the Heeia stream flow prediction by using the SWAT model. This tool was developed to interface with the SWAT model and includes different uncertainty analysis techniques. One of the optimized technique namely Sequential Uncertainty Fitting Algorithm (SUFI-2) was used for uncertainty analysis, which has ability to account all sources of uncertainties like parameters, driving variables (e.g., rainfall), model structure, and measured data (Abbaspour, 2014). The (SUFI-2) technique has a high ability to provide reasonable predicted results such as uncertainty bands and model performance of stream flow (Khoi and Thom, 2015). The strength of calibration and uncertainty analysis was evaluated by two statistical values; *P*-factor and *R*-factor. *P*-factor indicates to the percentage of measured data bracketed by 95% prediction uncertainty band (95PPU), while *R*-factor was the average thickness of the 95PPU band divided by the standard deviation of the measured data. The values of *P*-factor and *R*-factor range between (0 – 1) and (0 – ∞), respectively. If the *P*-factor equal 1 and *R*-factor close to zero, mean the simulated results are exactly matching with the observed values (Abbaspour, 2014).Model performance evaluation

Since single statistical metrics only evaluates a specific part of the model performance (Moriasi, *et al.*, 2007), the performance of the SWAT model for daily streamflow simulation is evaluated based on

the statistical evaluation criteria, such as, the Nash-Sutcliffe efficiency (NSE) (Nash and Sutcliffe, 1970), the percent bias (PBIAS), the ratio of the root mean square error (RMSE) to the standard deviation of measured data (RSR), the root mean square error (RMSE) (Sorooshian, *et al.*, 1993), the Mean Bias Error (MBE) (Allen, *et al.*, 1996), and the correlation coefficient (r) (Legates and McCabe, 1999). Each of these goodness-of-fit statistics is defined as follows:

$$NSE = 1 - \frac{\sum_{i=1}^{N}\left(q_{s,i} - q_{o,i}\right)^2}{\sum_{i=1}^{N}\left(q_{o,i} - \bar{q}_o\right)^2} \quad \text{Equation 1}$$

$$PBIAS = \frac{\sum_{i=1}^{N}\left(q_{s,i} - q_{o,i}\right)}{\sum_{i=1}^{N} q_{o,i}} * 100 \quad \text{Equation 2}$$

$$RSR = \frac{RMSE}{\sigma_o} = \frac{\sqrt{\sum_{i=1}^{N}\left(q_{s,i} - q_{o,i}\right)^2}}{\sqrt{\sum_{i=1}^{N}\left(q_{o,i} - q_{o,mean}\right)^2}} \quad \text{Equation 3}$$

$$MBE = \frac{1}{N}\sum_{i=1}^{N}\left(q_{s,i} - q_{o,i}\right) \quad \text{Equation 4}$$

$$r = \frac{N\sum_{i=1}^{N} q_{s,i}q_{o,s} - \sum_{i=1}^{N} q_{s,i}\sum_{i=1}^{N} q_{o,i}}{\sqrt{N\sum_{i=1}^{N} q_{o,i}^2 - \left(\sum_{i=1}^{N} q_{o,i}\right)^2}\sqrt{N\sum_{i=1}^{N} q_{s,i}^2 - \left(\sum_{i=1}^{N} q_{s,i}\right)^2}} \quad \text{Equation 5}$$

Where, $q_{s,i}$ is the simulated streamflow at time step i [m^3/s], $q_{o,i}$ is the observed streamflow at the time step i [m^3/s], and $\bar{q}_o$ is the mean of the observed stream flow over the entire period [m^3/s], N is the total number of data, and σ_o is the standard deviation of the observation [m^3/s].

3.2.4 Land cover change scenario

The Coastal Wetland Restoration plan (Figure 2) includes conversion of the california grass (Urochla mutica) to organic wetland taro (*Colocasia esculenta*) and the existing wetland mangrove forest to a

pond as native habitat for aquatic species (Kakoo Oiwi, 2010). Based on the land use map data, the perennial california grassland mainly exists in the Coastal Wetland (Figure 6). It covers approximately 7% of the modeled area (8.5km^2). In addition, eight hectares of wetland mangrove forest (1% of the modeled area) is located around the Heeia stream estuary. The Estuarine Forested Wetland in the land use map of 2011 was treated as water code in the SWAT database during land cover change conversion, while the california grassland was converted to taro cultivation. As taro land use was not available in the current SWAT land uses database, a taro was added to the SWAT database. The taro properties that required in the SWAT model were, summarized in (Table 3). These parameters were created based on the literature values and field measurements (Figure 12). Also, some variable values of herbaceous land use from the SWAT database were used for wetland taro because taro was classified as herbaceous perennial tropical crop (Miyasaka, *et al.*, 2003). The taro crop is chosen in the restoration plan because it is an important staple food and spiritual plant in Hawaiian cultural heritage. Moreover, until 1940s, the Heeia Wetland was actively cultivated with taro (Allen, *et al.*, 1995).

3.2.5 Wetland taro management

The traditional system of producing flooded taro or wetland taro in Hawaii requires long hours of standing and working in mud and water. The open channel is the way to get water to the taro patches. The flooded taro patches are created along the channels (auwai in the Hawaiian language) with parallel drainage system to enhance water circulation through the flooded taro patches (Kalo lo'i in the Hawaiian language). Therefore, a good controlling scheme for water resources management provides a favorable conditions for taro growth. The irrigation system is designed having the inflow and out flow pipes installed at diagonally opposite corners of the taro patches (Figure 11). The farmers built a dam of soil and stone across the stream to create enough head for diverting water to taro patches (Gingerich, *et al.*, 2007, Uchida, *et al.*, 2008). This method creates a gradual slope of water flow that helps to control flooding and erosion. These special managements of taro production are taken into my consideration during the setting up of the SWAT model.

In order to allow the inflow and outflow of water from the taro patches, pothole was added to the taro's management files of the SWAT model to simulate the Heeia Wetland as depressional water body. This enables to control the water ditches of taro field (Xie and Cui, 2011). A pothole is a type of waterbody

that obtain water from subbasin's reach and release water through overflow via tile drainage. The water balance for a pothole (Neitsch, *et al.*, 2011) is defined as:

$$V = V_{stored} + V_{flowin} - V_{flowout} + V_{pcp} - V_{evap} - V_{seep} \quad \text{Equation 6}$$

Where V is the volume of stored water in the pothole at the end of the day (m^3), V_{stored} is the volume of initial stored water in the pothole at the beginning of the day (m^3), V_{flowin} is the volume of entered water to the pothole during the day (m^3), $V_{flowout}$ is the volume of water flowing out of the water body during the day (m^3), V_{pcp} is the volume of precipitation falling on the pothole during the day (m^3), V_{evap} is the volume of water lost from pothole by evaporation during the day (m^3), and V_{seep} is the volume of water lost from the pothole by seepage. The sources of water entering the pothole are from the subbasin's streamflow diversion to irrigate a given HRUs within the subbasin. Therefore, the inflow of water from reach and HRUs to the pothole is calculated as:

$$V_{flowin} = irr + \sum_{hru=1}^{n}[fr_{pot,hru} \cdot 10 \cdot (Q_{surf,hru} + Q_{gw,hru} + Q_{lat,hru}) \cdot area_{hru}] \quad \text{Equation 7}$$

Where V_{flowin} is the volume of water flowing into the pothole during the day (m^3), irr is the amount of water irrigation diversion during the day (m^3), n is the number of HRUs contributing water to the pothole, $fr_{pot,hru}$ is the fraction of the HRU area draining into pothole, $Q_{surf,hru}$ is the water surface runoff from the HRU on a given day (mm), $Q_{gw,hru}$ is groundwater flow generated in the pothole on a given day (mm), $Q_{lat,hru}$ is the water lateral flow generated in the pothole on a given day (mm), and $area_{hru}$ is the HRU area (ha). The whole HRUs for taro land use were assumed as pothole. It was also assumed that a maximum volume of water stored in pothole is 40 mm (depth) over the entire HRU with an initial volume of 10 mm (depth) and depth to impervious layer of 250 mm to make water ponding for taro cultivation(Arnold, *et al.*, 2012, Kakoo Oiwi, 2011, Miyasaka, *et al.*, 2003, Penn, 1997, Uchida, *et al.*, 2008). For irrigation water application, irrigation water diversion from reach and irrigation water schedule were defined in the management file of taro land use. The necessary input parameters are summarized in (Table 1). The flow in the reach is the factor that determines the diverted water from the reach. For instance, if the minimum flow value is high, the diverted water is low. Therefore, the irrigation diversion scenario was started with initial high value and decreased by 50%, 75%, and 90% respectively (Table 1 and Table 2) (Arnold, *et al.*, 2012, Fares, 2008, Gingerich, *et al.*, 2007, Xie and Cui, 2011).

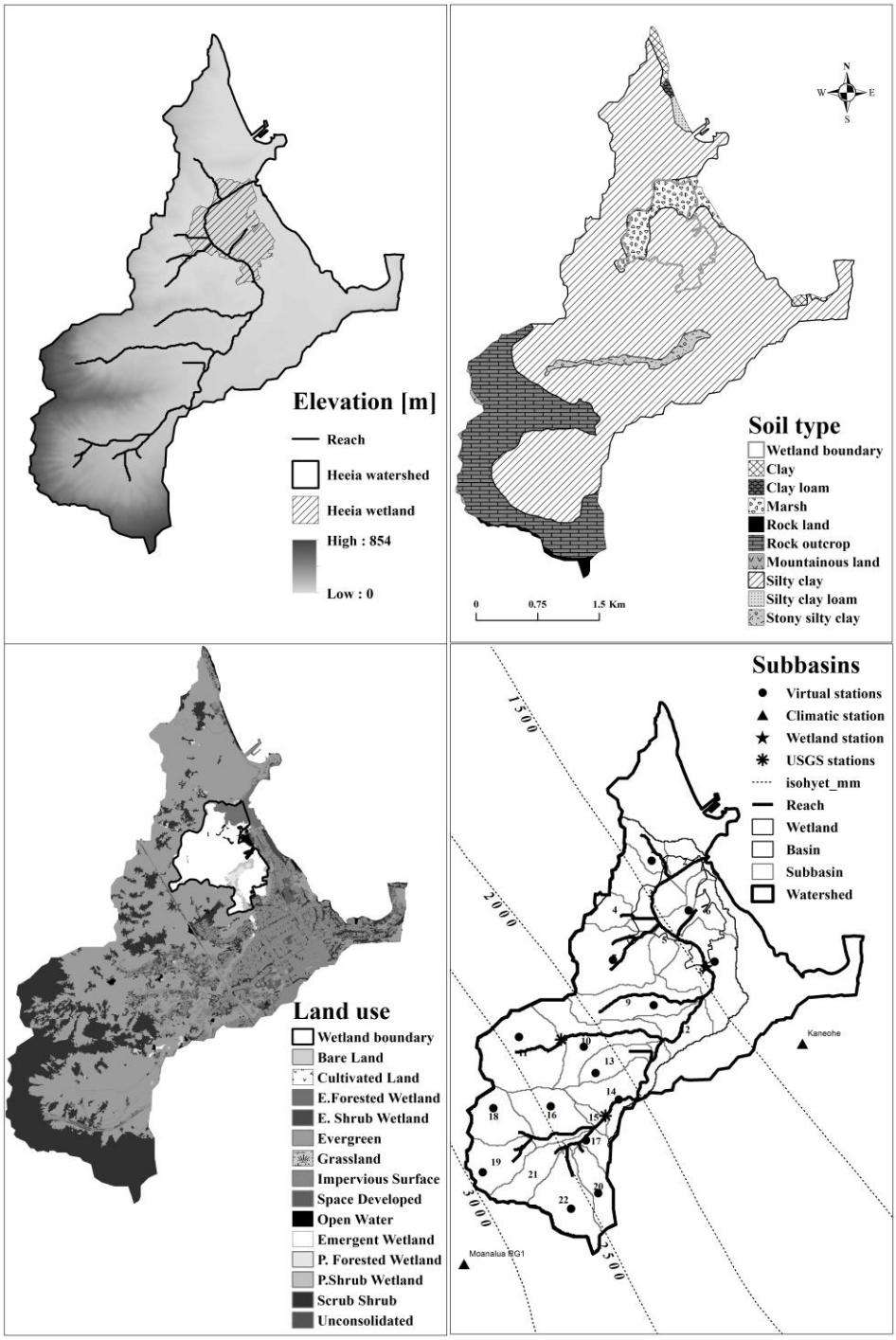

Figure 10: DEM (top, left) of the Heeia Watershed, land use (bottom left), soil type (top, right), and delineated sub-Watershed s with corresponding flow gauging locations and climatic stations (bottom, right)

.

Table 1: The minimum flow (m^3/s) in the reach for different scenarios of irrigation diversion.

Reach no.	Baseline	S1	S2	S3	S4
1	0	0.02	0.01	0.005	0.002
2	0	1.5	0.75	0.375	0.15
3	0	1.5	0.75	0.375	0.15
4	0	0.06	0.03	0.015	0.006
5	0	1.6	0.8	0.4	0.16
6	0	0.06	0.03	0.015	0.006
7	0	0.2	0.1	0.05	0.02
8	0	2	1	0.5	0.2
S1; scenario one (initial minimum flow)			S2; scenario two (decrease 50% of minimum flow)		
S3; scenario three (decrease 75% of minimum flow)			S4; scenario four (decrease 90% of minimum flow)		

Table 2: The annual irrigation diversion (mm/y) from each reach for different scenarios.

Reach no.	Baseline	S1	S2	S3	S4
1	0	0	45	255	875
2	0	0	0	0	1
3	0	1	2	0	103
4	0	1	3	8	134
5	0	3	21	62	1043
6	0	6	13	23	32
7	0	2	3	11	373
8	0	9	21	78	1325
Total	0	23	109	437	3886
S1; scenario one			S2; scenario two (decrease 50% of minimum flow)		
S3; scenario three (decrease 75% of minimum flow)			S4; scenario four (decrease 90% of minimum flow)		

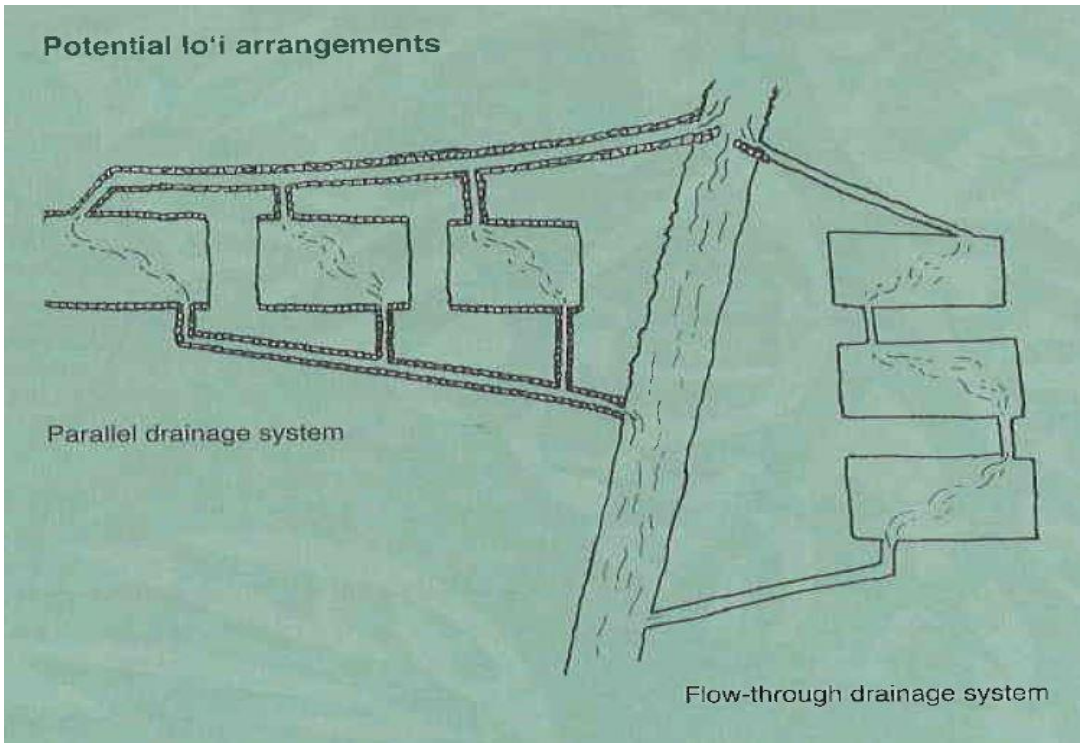

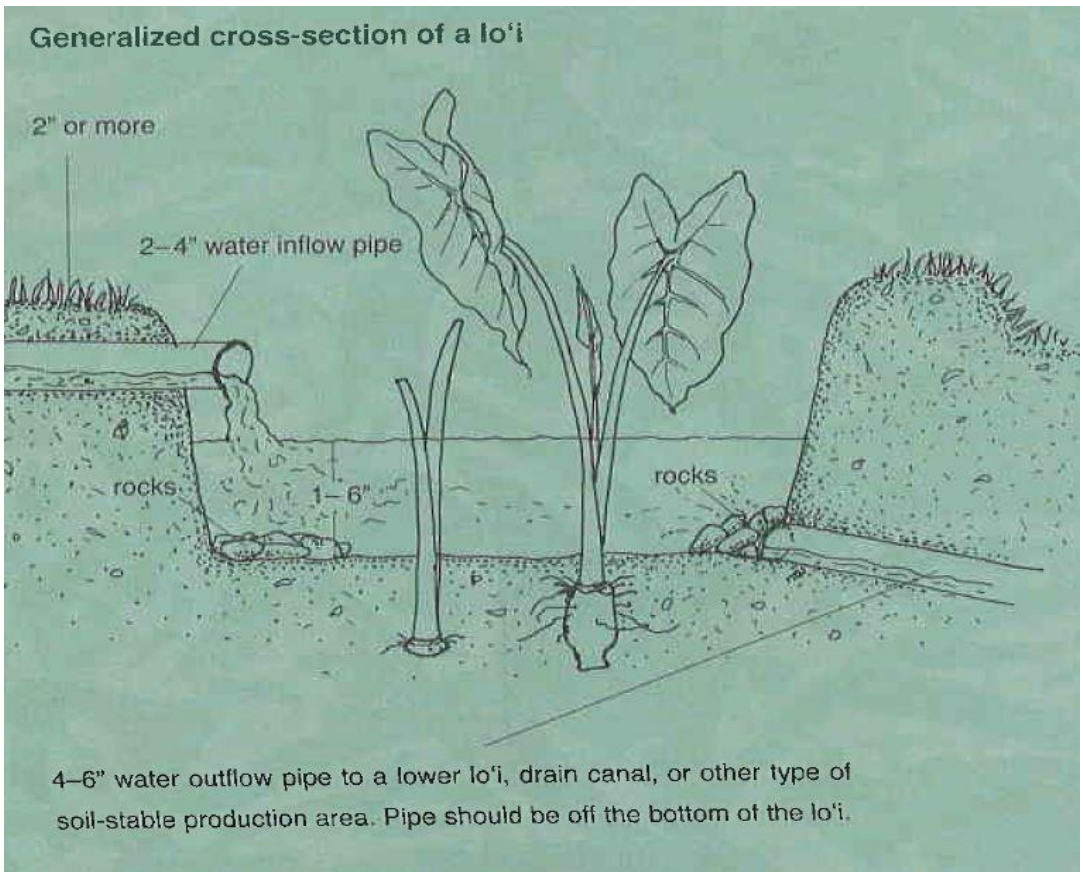

Figure 11: Management of the flooded taro patches (Uchida, *et al.*, 2008).

Figure 12: Biomass measurement of the wetland taro crop.

Table 3: Brief description of the variables in the SWAT plant growth database file of wetland taro.

Variable name	Code and values	Definition	Reference
OBJECTID	142	Land use number	(Arnold, et al., 2012)
ICNUM	142	Land cover/plant code	(Arnold, et al., 2012)
CPNM	TARO	Four character code of land name	(Arnold, et al., 2012)
IDC	6	Herbaceous perennial crop code	(Arnold, et al., 2012, Miyasaka, et al., 2003)
CROPNAME	Wetland Taro	Name of flooded Taro	(Gingerich, et al., 2007, Kakoo Oiwi, 2011)
BIO_E	47	Radiation-use efficiency of Herbaceous	(Arnold, et al., 2012, Miyasaka, et al., 2003)
HVSTI	0.01	Harvest index for optimal growth	(Kakoo Oiwi, 2011, Miyasaka, et al., 2003)
BLAI	2.5	Maximum potential leaf area index (LAI)	(Miyasaka, et al., 2003, Shih and Snyder, 1984)
FRGRW1	0.11	Fraction of the plant growing season	(Arnold, et al., 2012, Shih and Snyder, 1984)
LAIMX1	0.13	Fraction of the maximum LAI (first point)	(Arnold, et al., 2012, Shih and Snyder, 1984)
FRGRW2	0.24	Fraction of the plant growing season	(Arnold, et al., 2012, Shih and Snyder, 1984)
LAIMX2	0.91	Fraction of the maximum LAI (second point)	(Arnold, et al., 2012, Shih and Snyder, 1984)
DLAI	0.89	Fraction of growing season (decline leaf area)	(Arnold, et al., 2012, Shih and Snyder, 1984)
CHTMX	0.7	Maximum canopy height (meter)	Field measurement (Roberts, et al., 1993)
RDMX	0.6	Maximum root depth (meter)	Field measurement (Roberts, et al., 1993)
T_OPT	25	Optimal temperature for plant growth (^{0}C)	(Gingerich, et al., 2007, Penn, 1997)
T_BASE	21	Minimum temperature for plant growth (^{0}C)	Gingerich, et al., 2007, Penn, 1997)

3.3 Results and discussion

3.3.1 Sensitivity analysis

The sensitivity analysis (SA) indicated that CN2, CH_K2, ALPHA_BF, CH_N2, LAT_TTIME, SOL_K, GWQMN, RCHRG_DP, ESCO, SOL_AWC and CANMX were the sensitive parameters as they showed lower *P*-value and higher absolute *t*-statistics (Table 4). Although some of these parameters were not highly sensitive on model outputs, they were considered as their importance was noticed during model calibration. The SA identified the curve number at moisture condition CN2 as the highest sensitive parameter for the Heeia Watershed, which was probably due to its primary partitioning of hydrological simulation through its representation of the surface runoff generated from HRUs. The second sensitive parameter was the effective hydraulic conductivity of the main channel in the subbasin that controls water losses from streamflow to shallow aquifer. The third sensitive parameter was the baseflow alpha factor (ALPHA_BF), which controlled the recession curve of the streamflow hydrograph. This parameter was important for the Heeia Watershed because during dry season the flow depended on the contribution of the baseflow, which in turn had a strong correlation with ALPHA_BF. The other sensitive parameters include Manning's roughness coefficient, lateral flow travel time, saturated soil hydraulic conductivity, and the minimum depth for groundwater flow occurrence. These

parameters could affect the surface runoff processes and streamflow. In addition, these parameters were influenced by the soil type, land use, topography and aquifer characteristics.

Table 4: SWAT parameter sensitivity to daily streamflow at the Haiku station. Acronyms are explained in Table 5.

Parameter	**t-stat**	**P-value**	**Parameter**	**t-stat**	**P-value**
CN2	-50.73	0	SURLAG	1.289	0.198
CH_K2	34.071	0	OV_N	-1.031	0.303
ALPHA_BF	-16.563	0	EPCO	0.992	0.322
CH_N2	6.242	0	GW_DELAY	-0.686	0.493
LAT_TTIME	4.145	0	SLSUBBSN	0.677	0.499
SOL_K	2.69	0.007	SLSOIL	0.647	0.518
GWQMN	2.564	0.011	HRU_SLP	0.617	0.537
RCHRG_DP	-1.805	0.072	REVAPMN	0.505	0.614
ESCO	-1.672	0.095	GW_REVAP	-0.327	0.744
SOL_AWC	1.496	0.135	SOL_Z	-0.299	0.765
CANMX	1.411	0.159			

Table 5: Optimized parameter values for the Haiku and the Heeia Wetland stations.

Parameter	Description	Unit	Range		Calibrated	
			Min value	Max value	Haiku	Wetland
ALPHA_BF	Baseflow alpha factor	day^{-1}	0	0.005	0.0003	0.0045
CANMX	Maximum canopy storage*	mm	-0.4	0.4	0.1	-0.3
CH_K2	Effective hydraulic conductivity in main channel	mmh^{-1}	10	50	39	20.4
CH_N2	Manning's roughness coefficient		0.02	0.07	0.02	0.04
CN2	Curve number at moisture condition II**		-0.5	0.1	-0.49	-0.47
ESCO	Soil evaporation compensation factor		0.5	1	0.9	0.5
LAT_TTIME	Lateral flow travel time	day	10	90	81	18
RCHRG_DP	Groundwater recharge to deep aquifer		0	0.05	0.045	0.00015
GWQMN	Minimum depth for groundwater flow occurrence	mm	1	1000	137	774.5
SOL_K	Saturated soil hydraulic conductivity***	mmh^{-1}	-0.5	0.1	-0.4	-0.03
SOL_AWC	Soil water available capacity***		-0.2	0.3	-0.03	0.16
SURLAG	Surface runoff lag coefficient	day	0.5	2.5	1	
*Varies with land use; ** Varies with land use, soil & slope; ***Varies with soil type.						

3.3.2 SWAT model calibration, validation, and uncertainty analysis

The optimized parameter values (Table 5) that were calibrated for the Haiku and Heeia Wetland stations, were physically acceptable considering to the hydrological features of the Heeia Watershed (Figure 10). The statistical results analysis of daily streamflow simulation (Table 6) showed that the model performance was within the generally acceptable criteria for models evaluation especially under

scarcity of thee data and daily time steps approach. The table reported the goodness-of-fit statistics for different periods of calibration and validation in order to facilitate period event based evaluation. Overall, based on the recommended quantitative statistics (NSE, RSR, and PBIAS), the model simulation could be judged as satisfactory because the average of three criteria were 0.53, 0.66, and 5.9 respectively during the calibration and validation periods (Moriasi, *et al.*, 2007, Ndomba, *et al.*, 2008). The RMSE values, which were less than 50% RSR, the model performance rating was considered as the most stringent (very good) rating (Moriasi, *et al.*, 2007, Singh, *et al.*, 2005). The other goodness-of-fit statistics, (r) and (MBE) widely used to evaluate the hydrologic models performance and to describe the degree of collinearity between simulated and observed data. They were considered as acceptable values because the values of (r) and (MBE) were more than 0.5 and close to zero, respectively (ASCE, 1996, Van Liew, *et al.*, 2003). The low values of (r) for some simulation periods reflected the sensitivity of this criterion to high extreme values (outliers). Generally, the graphical comparison of the observed and simulated daily streamflow for the Heeia Watershed at the Haiku and the Wetland outlets showed that the SWAT reasonably tracked the trends of the hydrograph and its temporal evolution especially during validation periods for both stations (Table 13and Table 14). However, some peak events did not follow the trends of the hydrograph due to the lack of well-represented rainfall amounts for the Watershed. High spatial and temporal variability of rainfall within the Heeia Watershed had increased the uncertainty to represent the actual rainfall distribution within the entire Watershed in spite of using 15 virtual stations according to the isohyet contour lines (Giambelluca, *et al.*, 2011). The lack of well-represented rainfall amounts and the model sensitivity of rainfall input caused the weakness of model performance to simulate the daily stream flow. The weakness of the model was noticed in the underestimated or overestimated flows especially for peak events. The another weakness of the model performance was the derivative approach to estimate the down streamflow by using linear scaling factor (2.5) to the Haiku stream observation due to the absence of streamflow stations. The findings of SWAT model under scarce data was better than nothing to draw picture about the actual hydrologic processes within the Heeia Watershed in order to assess the impacts of restoration activities on the water resources.

The results of simulated and observed streamflow in daily time steps with 95PPU for the model were presented in (Figure 13 and Figure 14) and the performance indices in (Table 7). The derived results of 95PPU were shown that 96% of the observed data at the Haiku station during calibration period was

bracketed by the 95PPU, but it was 81% at the Wetland station. In addition, it was 96% at the Haiku station during validation period, while it was 95% at the Wetland station for the same period. These results indicated that SUFI-2 technique was capable of capturing the observations (Abbaspour, 2014).

The R-factor value for all periods closed to 1, and the value at Wetland station was less than Haiku station, which means the model was reliable to simulate the Heeia downstream flow (Khoi and Thom, 2015, Pervez and Henebry, 2015).

Table 6: The statistical summarized results of uncertainty analysis technique of the Heeia stream.

Station	Period	Time span	NSE	PIAS %	RSR	r	P-factor	R-factor
Haiku	Calibration	2002-2008	0.6	4.6	0.66	0.69	0.96	1.36
	Validation	2009-2014	0.51	8	0.7	0.54	0.96	0.89
Wetland	Calibration	2002-2008	0.51	13	0.63	0.67	0.81	0.81
	Validation	2009-2014	0.5	-2.59	0.67	0.5	0.95	0.67

Table 7: The statistical results for calibration and validation for the daily streamflow simulation at multi-sequential periods.

Station	Period	time span	NSE	RSR	PBIAS[%]	RMSE[m3/s]	MBE[m3/s]	r
Haiku	Calibration	2002-2003	0.6	0.56	36	0.05	-0.021	0.77
		2004-2006	0.57	0.64	6.584	0.08	0.006	0.55
		2006-2008	0.4	0.78	-31.282	0.04	-0.018	0.57
		2002-2008	0.6	0.66	4.593	0.06	0.003	0.69
	Validation	2009-2010	0.48	0.72	-4.19	0.08	-0.003	0.49
		2011-2012	0.54	0.68	2.21	0.07	0.001	0.51
		2013-2014	0.49	0.72	18.32	0.06	0.011	0.54
		2009-2014	0.51	0.7	8.13	0.07	0.005	0.54
Wetland	Calibration	2002-2003	0.74	0.48	17.8	0.11	0.027	0.84
		2004-2006	0.45	0.72	-6.348	0.11	-0.007	0.62
		2006-2008	0.49	0.68	22.43	0.15	0.04	0.6
		2002-2008	0.51	0.63	13.386	0.15	0.024	0.67
	Validation	2009-2010	0.5	0.61	-34	0.15	-0.04	0.45
		2011-2012	0.41	0.77	-0.77	0.2	-0.001	0.52
		2013-2014	0.61	0.62	27	0.09	-0.032	0.51
		2009-2014	0.5	0.67	-2.594	0.15	-0.003	0.5
		Average	0.53	0.66	5.879	0.11	0.007	0.6
NSE = Nash-Sutcliff efficiency; RSR = root mean squared error to observation standard deviation;								
PBIAS = percent bias; RMSE = root mean squared error; r = correlation coefficient; MBE = mean bias error.								

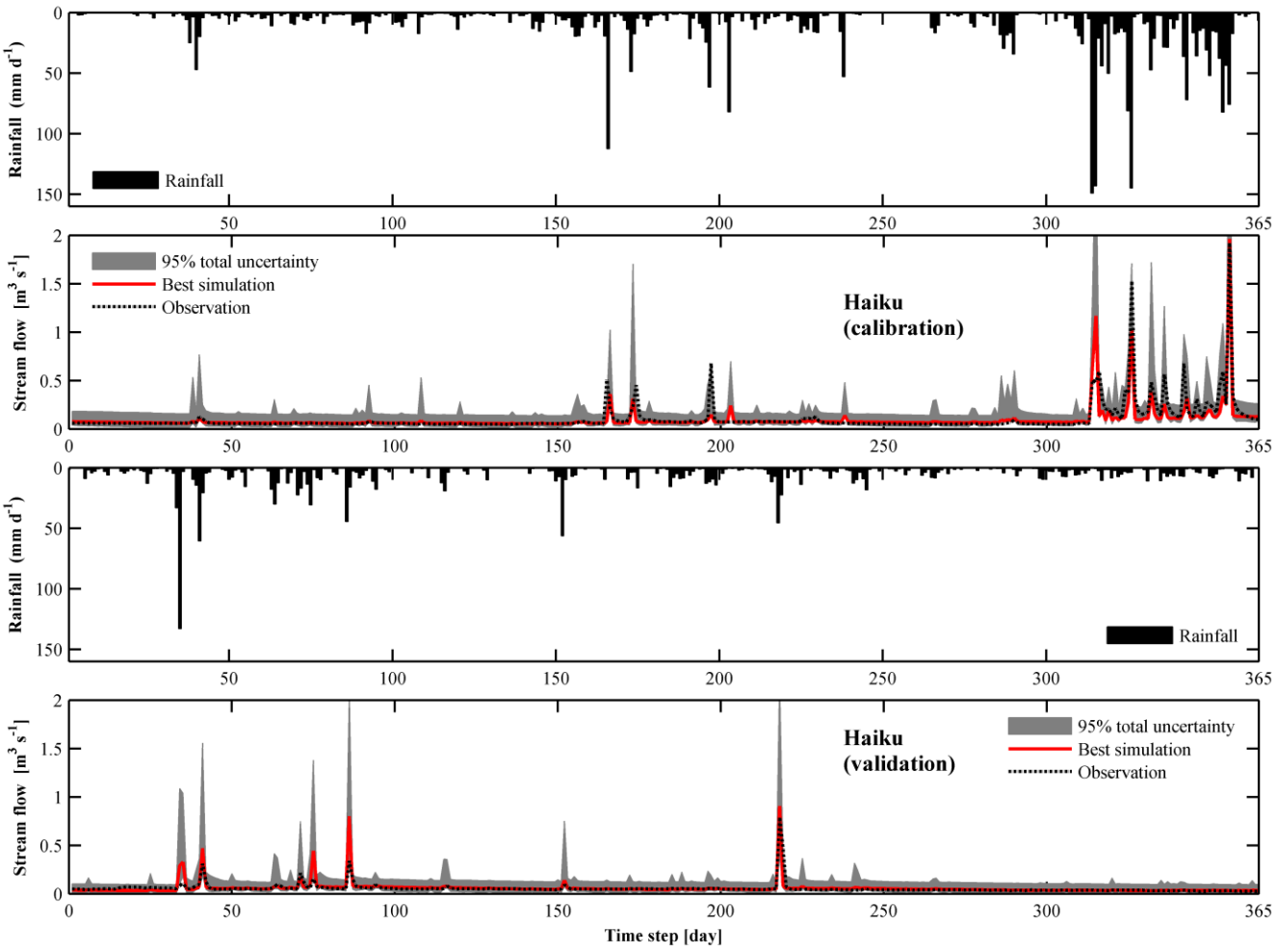

Figure 13: The areal average daily rainfall (panels 1 and 3) and the respective simulated and observed streamflow with 95% prediction uncertainty at the Haiku station for one year.

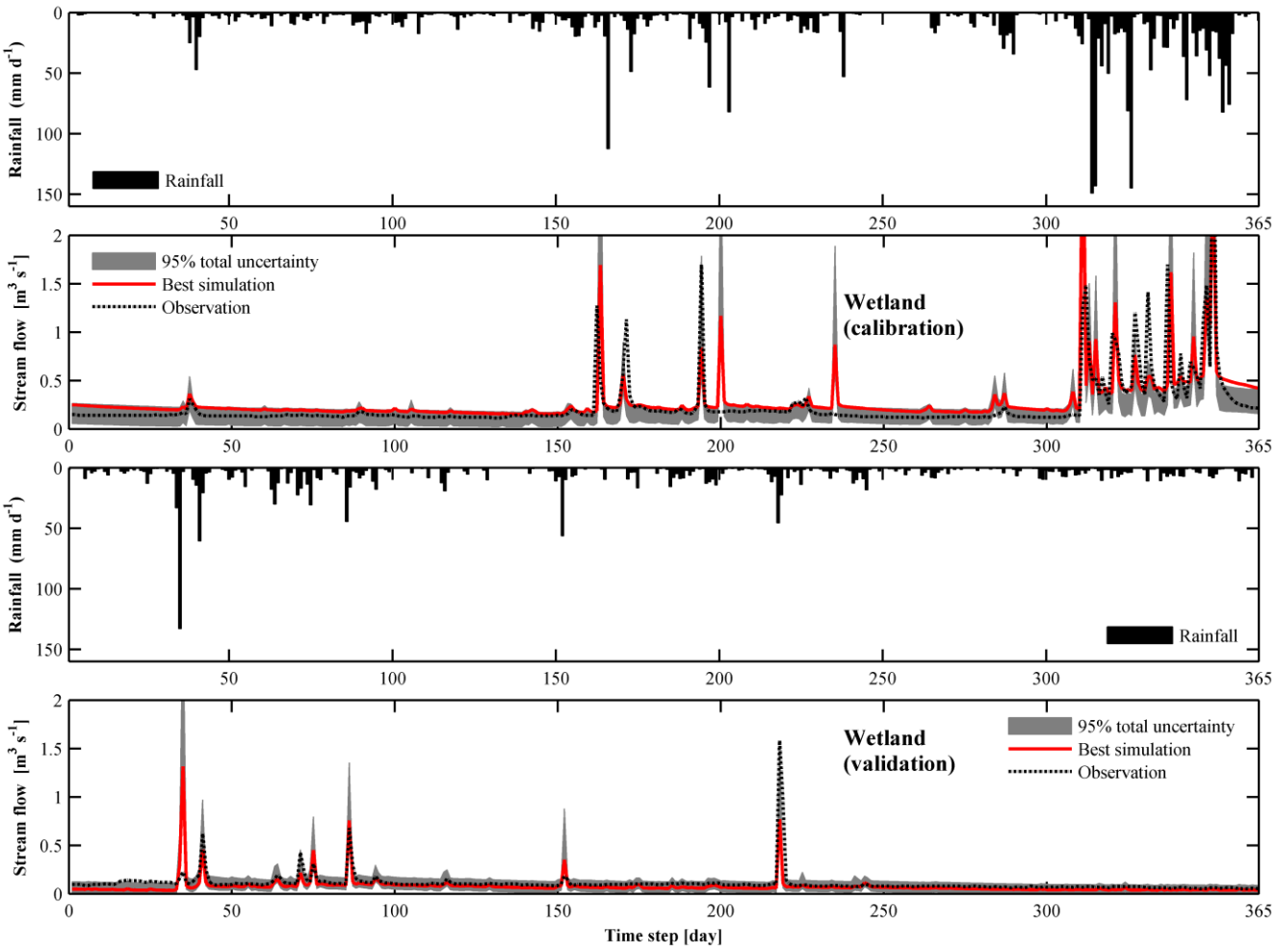

Figure 14: The areal average daily rainfall (panels 1 and 3) and the respective simulated and observed streamflow with 95% prediction uncertainty at the Wetland station for one year.

3.2.3 The Watershed water balance

The output of the baseline simulation indicated that the Heeia Watershed received average annual rainfall of 2042.6 mm (Table 8) during the period of 2002 -2014, while the Coastal Wetland received 1065 mm for the same period due to the spatial rainfall variability. The rainfall was greatest during wet season (Table 9). The rainfall was highly correlated with recharge (R^2 = 0.95) (Figure 15). The percent of recharge was accounted 34% of the annual rainfall that was consistent with previous studies in Hawaii (Izuka, *et al.*, 1993, Shade and Nichols, 1996, Takasaki, *et al.*, 1969).The average annual streamflow (surface runoff + baseflow + lateral flow+ seepage) was of 904 mm (Table 8). The baseflow contributed 87% of the average annual streamflow, while surface runoff contributed 13%. The results indicated that the streamflow was highly influenced by the groundwater discharge within the Heeia

Watershed (Takasaki, *et al.*, 1969). The contribution of the baseflow was very strong during dry season (May – October) and weak through wet season (November – April) (Table 9). In contrast, the streamflow was strongly influenced by surface runoff during wet season and less prominently during dry season. The average annual potential evapotranspiration (PET) was 1412.1 mm and actual evapotranspiration (ET) was 916 mm. Both PET and ET varied seasonally. The ET was substantially lower than PET during summer because of the lack of sufficient soil moisture (Osorio*, et al.*, 2014).

Table 8: The yearly water balance components (mm) of the Heeia Watershed.

year	rainfall	streamflow	Runoff	lateralflow	Baseflow	Recharge	soil moisture	ET	PET
2002	1696	519	84	257	160	474	124	914	1531
2003	1813	579	162	227	176	578	201	729	1072
2004	2925	1260	215	487	527	1297	220	909	1033
2005	2074	1072	89	354	604	823	163	886	1204
2006	2835	1535	268	474	763	1267	183	802	1167
2007	1793	815	62	235	503	545	220	890	1368
2008	1725	775	79	240	440	515	199	915	1458
2009	1946	898	89	313	476	639	146	979	1441
2010	1760	673	69	214	373	526	207	853	1651
2011	2308	1128	136	384	585	770	154	1115	1655
2012	1430	846	99	208	524	396	86	820	1697
2013	1983	788	118	264	390	557	147	963	1561
2014	2266	865	73	325	446	695	173	1139	1520
Average	2043	904	119	306	459	699	171	916	1412

Table 9: The average monthly (2002-2014) of water balance components (mm) of the Heeia Watershed.

Month	Rainfall	Streamflow	Recharge	Runoff	Lateralflow	Baseflow	Soil moisture	ET	PET
Jan	192	79	77	10	31	35	179	61	91
Feb	205	86	91	19	31	34	176	63	95
Mar	292	108	131	23	43	40	179	83	109
Apr	127	80	41	5	31	42	148	96	124
May	146	81	43	10	25	44	126	95	129
Jun	107	66	25	4	18	42	104	89	142
Jul	118	60	23	2	15	41	101	82	145
Aug	117	60	26	3	16	39	100	75	144
Sep	117	54	27	3	14	36	104	69	130
Oct	190	64	53	8	19	36	135	70	115
Nov	211	79	75	15	29	34	155	69	98
Dec	219	86	88	16	33	36	171	62	89

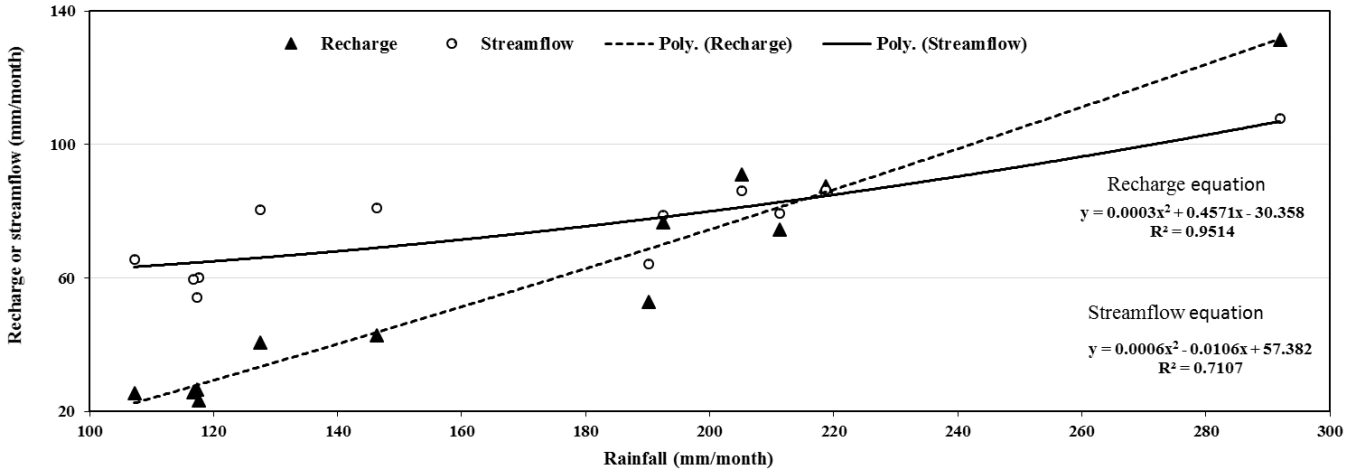

Figure 15: The relationship between the monthly averages (2002-2014) of water balance components (mm) of the Heeia Watershed.

3.3.3 The coastal wetland water balance

About 8 % of the Heeia Watershed is planned to be converted to taro field and impoundments (Kakoo Oiwi, 2011). The impacts of this change on water balance was evaluated at three spatial scales of the SWAT model, which included the hydrologic response units (HRUs), subbasins, and Watershed. Based on the land use map data (Figure 6), the coastal wetland was converted to taro cultivation and pond that occurs within the 8 subbasins of the SWAT model at the coastal plain. The expected impacts of converted land cover were illustrated in (Figure 16). The figure showed that the restoration was expected to impact the yearly average (2002-2014) of the WBCs. Specifically, the recharge will decrease due to the soil layer compaction under the taro patches to maintain ponding water in taro lo'i. However, the neighboring areas of the taro patches would get more recharge due to lateral seepage from the taro patches (Xie and Cui, 2011). The ET was expected to increase that may result in decrease of the other water balance components and increased the evaporation from the ponding water area (Figure 17). In addition, as it should be expected, conversion of existing Wetland (california grass) to taro cultivation would cause an overall decrease in total stream flow for the site, due to diversion of stream water for taro field irrigation and more evaporation from ponding water. However, in general, the change in the WBCs at Watershed scale was insignificant, which could be due to a small percent change in the restored land use area compared to the whole Watershed's area (Figure 17 and Table 10).

At Wetland scale, recharge was expected to decrease by 41 % under all irrigation diversion scenarios, which was probably due to taro cultivation and water ponding management. In contrast, the lateral flow and surface runoff would be increased about 76 % and 61%, respectively, for scenario 4, when 90% of the minimum stream flow in the main channel was diverted. For scenario 4, although baseflow was expected to decrease by up to 23%, stream flow was predicted to increase by 13%, which was due to considerable increase in surface runoff and lateral flow (Figure 17). It was also noticed that most of the WBCs were more influenced during the wet season as compared to the dry season (Table 11).

Finally, additional analysis at the Watershed scale indicated that the impact of land use change would have similar trends, the relative percent change was low compared to changes at subbasin and HRU (Table 11). That was reasonable considering the taro cultivation area, which was relatively small in comparison with the Watershed size. Another aspect of the research focused on the impact of land cover change on stream outflow for different scenarios of irrigation diversions. For baseline irrigation diversion was not applied (initial condition without taro cultivation and pond creation). The other scenarios applied irrigation diversions after restoration of taro cultivation and pond creation by rate 23, 109, 437, and 3886 mm/y respectively (Table 2). These scenarios were done by modifying the irrigation management parameter (FLOWMIN) of input file of the SWAT model, with different values started by initial value for each reach subbasin within wetland area and reduced by 50%, 75%, and 90% consequently for S2, S3,and S4 (Table 1).

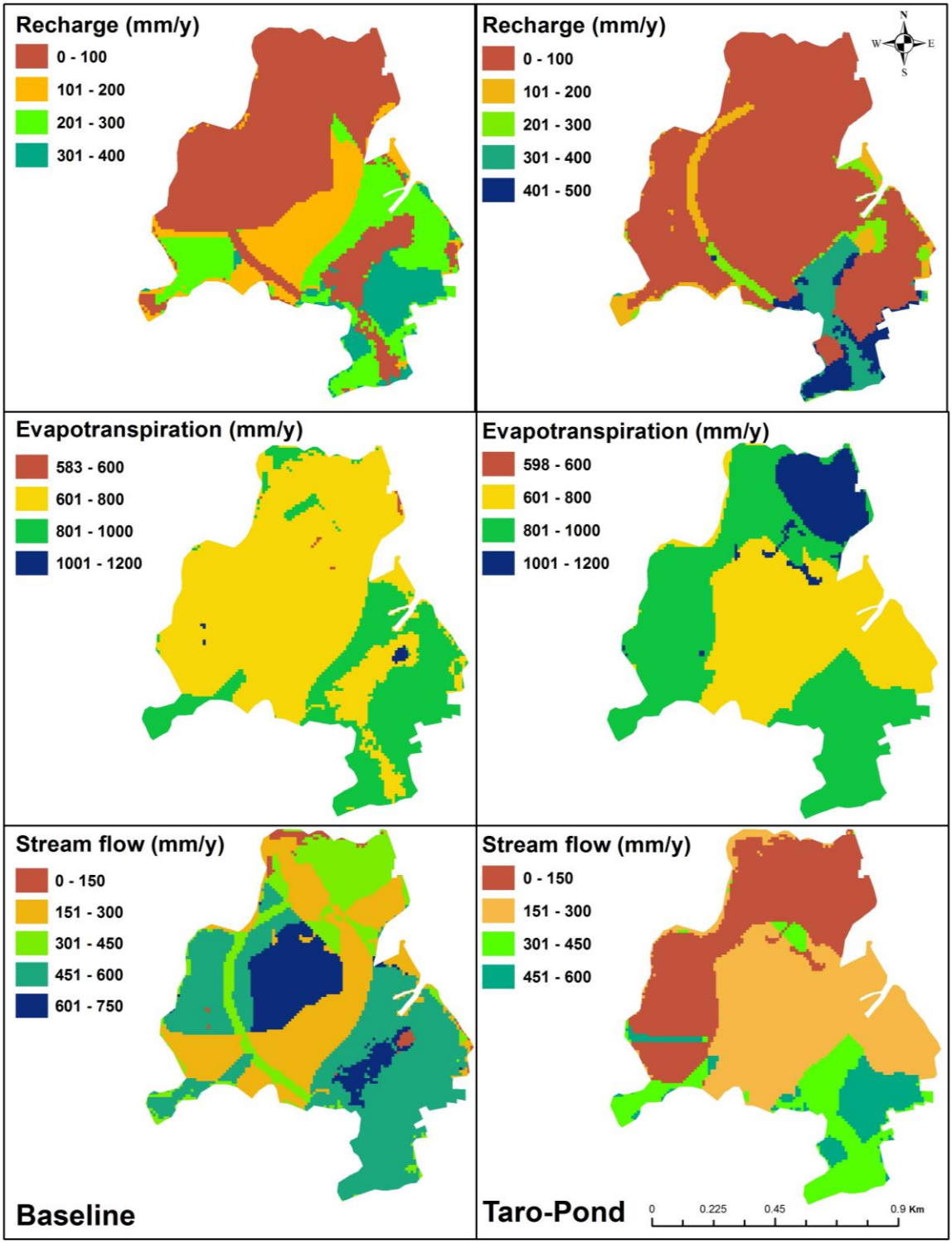

Figure 16: Yearly average WBCs maps of Hydrologic Response Units (HRUs) within the Heeia Wetland.

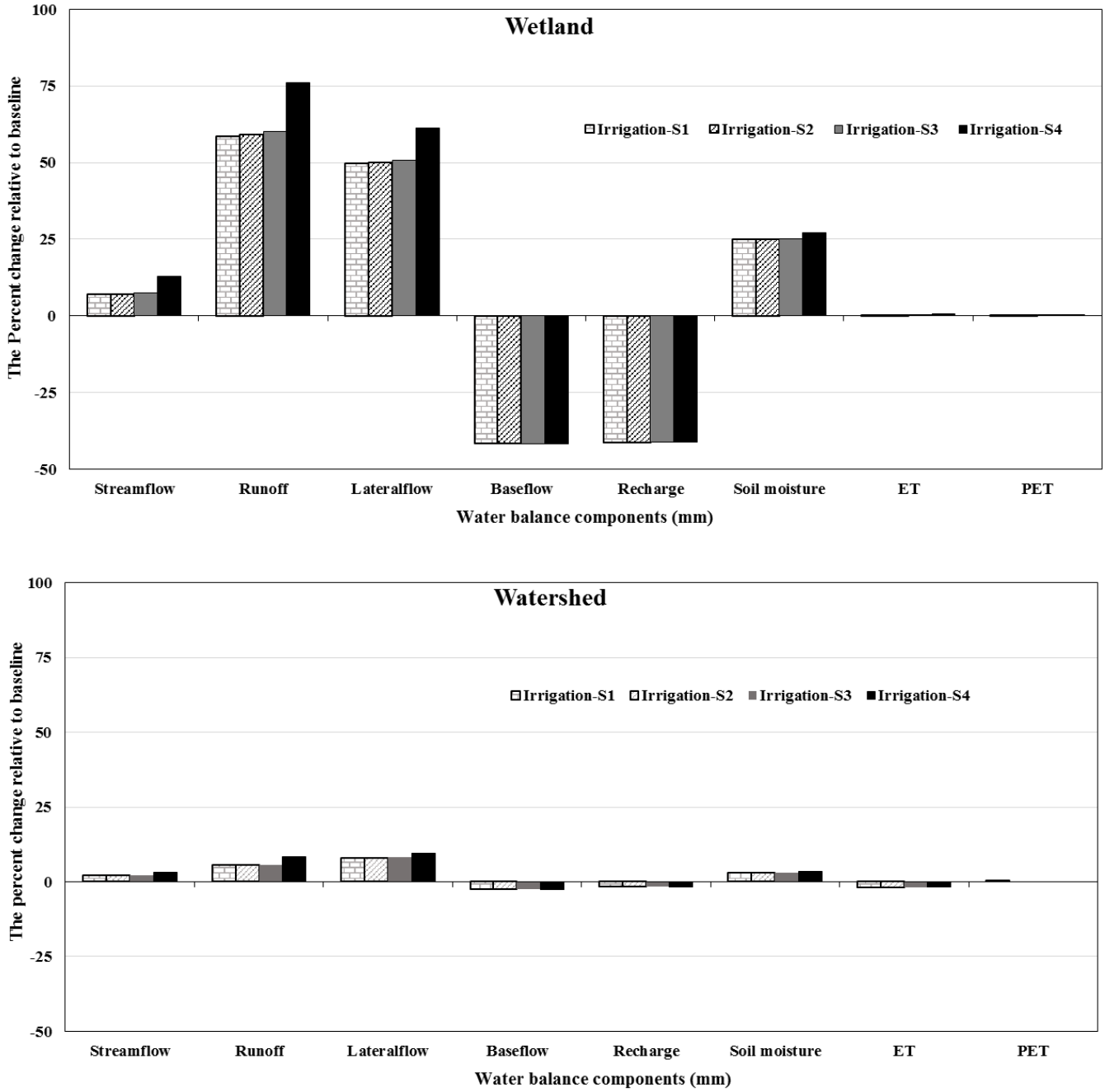

Figure 17: The percent change of yearly average (2002 – 2014) of WBCs relative to baseline for the Heeia Wetland and Watershed.

Table 10: The yearly average of WBCs (mm) for the Heeia Wetland and Watershed.

Scale	Scenario	Rainfall	Streamflow	Runoff	Lateralflow	Baseflow	Recharge	Soil moisture	ET	PET
Wetland	Baseline	1065	292	39	91	130	140	115	791	1533
	Irrigation-S1	1065	313	62	137	76	82	144	792	1534
	Irrigation-S2	1065	313	62	137	76	82	144	792	1534
	Irrigation-S3	1065	314	63	138	76	82	144	793	1534
	Irrigation-S4	1065	329	69	147	76	82	147	796	1534
Watershed	Baseline	2043	904	119	306	459	699	171	916	1412
	Irrigation-S1	2043	923	125	331	447	687	176	898	1412
	Irrigation-S2	2043	923	125	331	447	687	176	898	1412
	Irrigation-S3	2043	924	125	331	447	687	176	898	1412
	Irrigation-S4	2043	932	129	336	447	687	177	900	1412
S1 = Scenario one; initial minimum streamflow, S2 = Scenario two; (decrease 50% of minimum flow)										
S3 = Scenario three; (decrease 75% of minimum flow), S4 = Scenario four; (decrease 90% of minimum flow)										

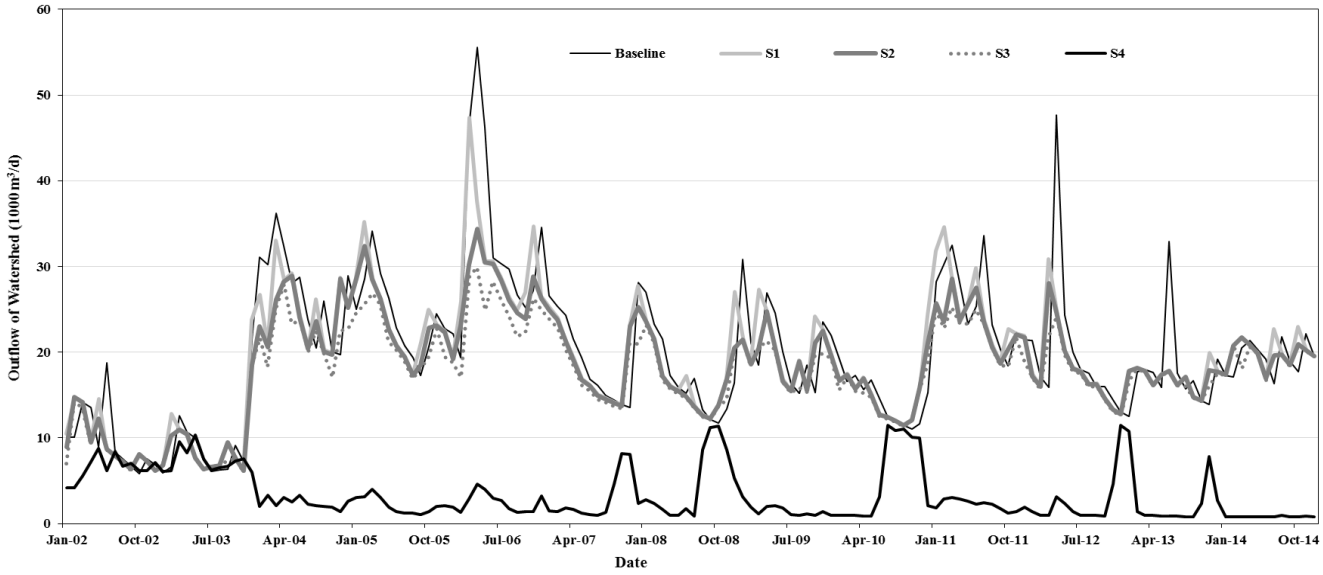

Figure 18: The monthly outflow of the Heeia Watershed for different scenarios of irrigation management.

Table 11: The percent changes in the seasonally WBCs relative to the baseline for the Heeia Wetland and Watershed.

Scale	Scenario	Season	Rainfall	Streamflow	Runoff	Lateralflow	Baseflow	Recharge	Soil moisture	ET	PET
Wetland	Irrigation-S1	wet	0.00	18.94	80.19	40.50	-42.07	-41.42	23.97	-4.31	-0.27
		dry	0.00	-12.22	13.18	84.99	-41.37	-43.07	57.46	5.53	0.26
	Irrigation-S2	wet	0.00	19.22	80.95	40.78	-42.07	-41.42	24.01	-4.29	-0.27
		dry	0.00	-12.17	13.32	85.22	-41.37	-43.07	57.49	5.54	0.26
	Irrigation-S3	wet	0.00	19.86	82.64	41.46	-42.07	-41.42	24.13	-4.26	-0.27
		dry	0.00	-11.94	13.79	86.15	-41.37	-43.07	57.60	5.57	0.26
	Irrigation-S4	wet	0.00	25.70	95.58	48.80	-42.07	-41.42	25.24	-3.94	-0.27
		dry	0.00	-5.62	35.46	108.34	-41.37	-43.07	59.95	6.21	0.26
Watershed	Irrigation-S1	wet	0.00	2.29	6.86	5.72	-2.49	-2.01	3.05	-2.66	-0.06
		dry	0.00	1.93	1.58	12.30	-2.69	-0.98	5.10	-1.36	0.05
	Irrigation-S2	wet	0.00	2.32	6.93	5.74	-2.49	-2.01	3.05	-2.66	-0.06
		dry	0.00	1.93	1.59	12.32	-2.69	-0.98	5.11	-1.36	0.05
	Irrigation-S3	wet	0.00	2.39	7.16	5.83	-2.49	-2.01	3.09	-2.65	-0.06
		dry	0.00	1.95	1.66	12.37	-2.69	-0.98	5.13	-1.35	0.05
	Irrigation-S4	wet	0.00	3.29	9.51	7.14	-2.49	-2.01	3.53	-2.50	-0.06
		dry	0.00	2.77	5.25	14.30	-2.69	-0.98	5.73	-1.12	0.05
S1 = Scenario one; initial minimum streamflow, S2 = Scenario two; (decrease 50% of minimum flow)											
S3 = Scenario three; (decrease 75% of minimum flow), S4 = Scenario four; (decrease 90% of minimum flow)											

3.4 Conclusions

The SWAT model used in this study to assess the impacts of the proposed Coastal Wetland Restoration plan on the WBCs. The model was developed using the available GIS and hydro-meteorological data. Majority of the climatic data were derived from the nearby watersheds and scaling techniques were used in order to capture the spatial variability of the climate data especially rainfall. Prior to the calibration, the SA was run. The model was calibrated and validated against the observed streamflow data. The model prediction uncertainty was also considered.

The SWAT model reasonably represented the temporal variability of the observed daily streamflow hydrograph. The simulated streamflow for upstream and downstream stations showed an acceptable performance and satisfactorily statistical evaluation values under hydrologic data scarcity. The findings showed that 34% of the annual rainfall of the Watershed (2042.6 mm) fed groundwater as recharge (699 mm), 44% of rainfall goes to streamflow (904 mm), and 45% annual rainfall was lost through evapotranspiration (916 mm). In addition, 87% of the annual streamflow came from baseflow (lateral flow and return flow). The baseflow was considered the main component of the downstream flow compare with surface runoff. The groundwater recharge was highly correlated with rainfall variation.

The impacts of Heeia Coastal Wetland restoration is expected to be significant at HRUs and subbasins within Wetland scale, but it is relatively low on the Watershed scale. Additionally, the land cover change (taro and pond) within the Coastal Wetland reduced the recharge and baseflow, while an increase in lateral flow and surface runoff was most likely to happen. The scenarios were aimed to achieve sustainable growth of taro without compromising the flow in the main stream that plays vital role for coastal health ecology. Based on the findings, the study proposed to use 50% of the minimum streamflow value for irrigation water diversion to irrigate taro field.

Chapter4 Assessment of the predicted water balance components of Heeia Coastal Wetland restoration under climate projections in Hawaii

4.1 Introduction

In this study, the LU and CL are considered as the determinant factors of the nutrient fluxes, thermal energy, and WBCs. These factors are also expected to affect each other through interaction processes effects (Dale, 1997, Loveland, *et al.*, 2012). In the Hawaiian Islands, the fossil evidence and human interventions indicate that the interactions among climate change, land use change, and biological invasions substantially aggravate the direct impacts of climate change (Benning, *et al.*, 2002). The conversion of wetlands to urban land use, the intensive agriculture, and the excessive using fossil fuels are examples of the human activities that aggravate the CL impacts. Consequences of these interaction are reflected on the implication of regional projects, such as strategies, the patterns of the coastal wetland restoration strategies and sustainable development plans of the water resources (Aumen, *et al.*, 2013, Conference, 2015, Gardner and Davidson, 2011, Keene, 2015, Pachauri, *et al.*, 2014). In such concerns, integrated hydrological modeling has a potential role to facilitate strategic decision making on environmental response and developing adaptation strategies to climate change and hazard mitigation policies. Such actions can ensure optimized allocation of water resource under a variable climate and land use changes (Pervez and Henebry, 2015, Safeeq, *et al.*, 2014).

The main consequences of climate change in the tropical pacific ecosystems include increase temperature and ET, alter rainfall and runoff, sea level rise, and elevate in atmospheric greenhouse gases which in turns affect the natural ecosystems (Keener, 2013, Xie, *et al.*, 2008). These future changes will affect the wetland ecosystem through introducing declines in the functional capacity and shifting the geographic location (Erwin, 2009). Therefore, climate change will make the wetland restoration and management more complex due to its effect on ecological and hydrological impacts interaction. The policymakers and restoration practitioners should take into account the potential impacts of climate change impacts during the implementation of the wetland restoration projects. However, climate change adaption and hazard mitigation strategies are still needed more studies due to the biggest unknowns of

the influence of global climate change on the dynamic hydrologic elements and nutrient fluxes (Paul, *et al.*, 2006).

Evidence of climate change impacts on the Hawaiian Islands has already observed. Some of these impacts are pronounced decrease in the groundwater recharge and increase in surface runoff, land sliding, increase soil erosion, and the coastal ecosystems degradation, such as coral reefs (Pritchard, 2010, Root, *et al.*, 2003). The observed and projected changes of the Hawaiian ecosystems invite the Hawaiian communities to better prepare for predicted effects of the global climate change effects on the water resources and ecosystem services. Particularly, the local expected impacts of climate change includes warming air temperatures of over 0.17 °C per decade, a decrease in the prevailing northeasterly trade winds, decline in rainfall amounts, decrease in groundwater discharge and total streamflow, increase in sea surface temperature have warmed between 0.07 up to 0.23 °C per decade. Additionally, the future projection indicates the trend of environmental warming by 1.3 to 2.7 °C by the end of the 21st century. Ocean acidity will be increased by 30%, sea level may be risen over 1.5 to 3.3 centimeters per decade and the projected rate of sea level rise about 0.3 to 1.0 meter by the end of the century. The consequences of these impacts are threats to human health (Eversole, *et al.*, 2014). These impacts will be increase the pathogens, spread invasive species, cause drought and heavy rains, reduce aquifer recharge and fresh water supplies, result changes in the ocean circulation, alter the nutrient distribution, impacts on marine biota, damage to infrastructure of low land areas, and cause beach loss(Eversole, *et al.*, 2014).

The studies also indicate that the combined effect of increasing groundwater withdrawals and overall decrease in precipitation are expected to decrease the base flow, and total streamflow of the Hawaiian Islands (Bassiouni and Oki, 2013, Timm and Diaz, 2009). In addition, the findings of the regional statistical downscaled of seasonal mean rainfall change in Hawaii, which was based on the recent Coupled Model Intercomparison Project phase 5 (CMIP5) global models results for two future representative concentration pathways (RCP4.5 and RCP8.5) for the main Hawaiian Islands, are supported the predicted impacts of climate change on the WBCs. The regional climate change was predicted that the wet windward sector will become wetter or remain stable in their seasonal rainfall, while the dry leeward sector will be strongest have increased drying trends (Timm, *et al.*, 2015). The seasonal rainfall anomalies reported by Timm et al., (2015) by the middle and late 21st century were

used to predict wet (November-April) and dry (May-October) season rainfalls values. In addition, the predicted average air temperature for the middle and late 21st century is expected to increase with very small spatial variations while the higher elevation regions in Hawaii Islands up to the 850 millibar are expected to get warmer (Diaz, *et al.*, 2011, Group, 2015, Kunkel, 2013, Safeeq and Fares, 2012). Another factor for climate change in the Hawaiian islands includes the variation in solar radiation due to variability in atmospheric transmissivity and cloud radiative properties (Wild, 2012). In the Hawaiian Islands, the historical solar radiation anomalies showed decreasing trend during the wet season whereas an increasing trend is most likely during the dry season (Longman, *et al.*, 2014).

Watershed models like SWAT coupled with a regional climate model (RCM) have been used to assess and examine the impacts of climate change on the WBCs (Jha, *et al.*, 2004, Pandey, *et al.*, 2016). The SWAT model is a useful tool in understanding the hydrologic response of wetlands to climate and land cover changes, which are considered as important factors of water resource planning and management (Feng, *et al.*, 2013).

Up to date, there are very limited hydrological studies for the windward side of the Oahu Island especially the Heeia Watershed, while there are a few hydrological modeling and climate change studies on the leeward side of Oahu Island (Safeeq and Fares, 2012, Sahoo, *et al.*, 2006). Therefore, the watershed model development and climate change assessment have become urgently needed and necessary for the windward side of Oahu Island. This study had been developed a SWAT model for the Heeia Watershed and will used the model to assess the impacts of both combined CL and LU effects on the WBCs.

4.2 Methodology

4.2.1 Climate change and wetland restoration scenarios

The calibrated and validated SWAT model (see chapter 3) was used to evaluate the combined effects of LU and CL projections on the WBCs at the Wetland and the Heeia Watershed scales. The model was used to simulate the climate change scenarios by manipulating the climatic input data of the SWAT model based on the recently statistically downscaled (250x250 m) seasonal rainfall anomalies reports for the Hawaiian Islands (Timm, *et al.*, 2015). The projected seasonal mean rainfall anomalies of Timm et al (2015) were reported over the representative 30 years for the middle (2041-2070) and late (2071-

2100) of 21st century under representative concentration pathways (RCP) 4.5 and 8.5 scenarios. Hereafter, the two periods were called 2050s and 2080s, respectively. In addition, the projected rainfall anomalies were spatially interpolated and made available as Geographic Information System (GIS) layers by Timm et al (2015) (see Figure 19 as an example). Consequently, the spatially interpolated eight GIS coverages were included two dry seasons (2050s, 2080s) and two wet seasons (2050s, 2080s) maps per each scenarios. Then due to the structure of the SWAT model to provide rainfall values and in order to capture the lower (minimum rainfall) and upper (maximum rainfall) anomalies per sub-basin, the sub-basins' observed daily rainfall values were perturbed based on the estimated lower and upper rainfall anomalies (%) (Figure 19). Such this approach has resulted in two additional scenarios, one for the lower limit and one for the upper limit for each of the RCP 4.5 and 8.5 scenarios (Table 12). In this study, the lower and upper bound rainfall were called rainfall min and rainfall max, respectively. The baseline rainfall values were increased or decreased by multiplying by those factors that were obtained from rainfall anomalies data. The perturbation values were implemented in the SWAT's sub-basin input files (Arnold *et al.*, 2011).

The temperature and solar radiation (Table 12), were varied during the modeling on the basis of many studies, which reported values about the Hawaiian Islands (Meteorology and CSIRO, 2011, Safeeq and Fares, 2012). Based on previous studies, the temperature and solar radiation was changed the temperature by increasing 1 ^{o}C (2050s) and 1.5 ^{o}C (2080s) for RCP 4.5 scenario, 1.5 ^{o}C for the 2050s and 2 ^{o}C for the 2080s for RCP 8.5 scenario, while the solar radiation was increased by 5% (2050s) to 10 % (2080s) for the RCP 4.5 scenario and 10% (2050s) to 15 % (2080s) for the RCP 8.5 scenario. The wet season solar radiation data were decreased by the same magnitudes.

The daily climatic data of the Watershed for the period 2002 to 2014 were used as baseline. The estimated output data included the lowest and highest impacts of combined climatic parameters (rainfall, temperature, and solar radiation) on the WBCs at Wetland and the whole Heeia Watershed scales. The combined effects of LU and CL scenarios of RCP 4.5 and 8.5 were simulated and formulated into eight combinations (Table 15). The analyses were done at monthly and yearly time scale steps.

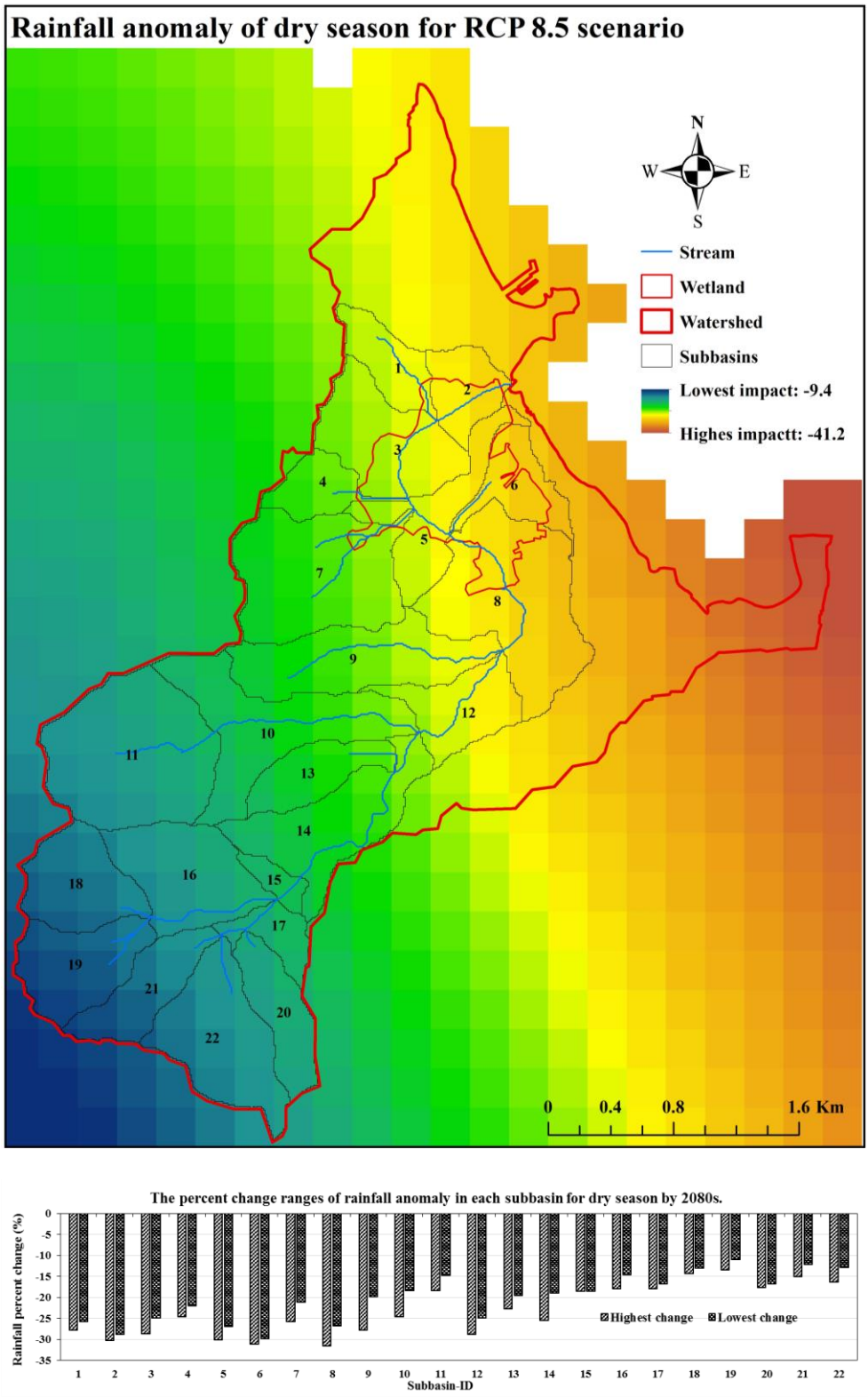

Figure 19: The projected rainfall anomaly adapted from (Timm et al. 2015) overlaid with the delineated subbasins (top) and the minimum and maximum rainfall change values within subbasins (bottom).

Table 12: The climatic adjusted variables in the subbasins general input file of SWAT model.

Climatic factor	RFINC(month) = Rainfall adjustment within the month (% change)							
Scenario name	MidRCP4.5max		MidRCP8.5max		LateRCP4.5min		LateRCP8.5min	
Subbasin_ID	Wet	Dry	Wet	Dry	Wet	Dry	Wet	Dry
1	-4.66	-13.96	-2.18	-19.42	-4.79	-16.62	-3.76	-27.79
2	-4.84	-15.51	-2.53	-21.69	-5.36	-18.16	-4.79	-30.21
3	-3.94	-13.65	-1.02	-18.76	-4.38	-17.32	-3.49	-28.72
4	-3.26	-12.32	0.17	-16.62	-3.05	-14.74	-1.28	-24.64
5	-3.92	-14.80	-1.52	-20.42	-4.95	-18.15	-4.32	-30.12
6	-4.71	-16.05	-2.57	-22.42	-4.85	-18.93	-4.51	-31.15
7	-2.84	-12.06	0.54	-16.03	-3.31	-15.60	-1.78	-25.80
8	-3.79	-14.70	-1.42	-20.25	-4.67	-19.40	-4.39	-31.61
9	-2.61	-11.47	0.79	-15.03	-3.60	-17.10	-2.42	-27.82
10	-2.24	-10.85	0.98	-13.80	-2.74	-15.17	-0.83	-24.61
11	-1.95	-9.21	1.50	-11.01	-1.14	-10.94	1.52	-18.33
12	-3.30	-13.88	-0.84	-18.91	-3.76	-17.82	-2.71	-28.89
13	-2.36	-11.36	0.63	-14.65	-2.22	-13.91	-0.04	-22.70
14	-2.26	-11.14	0.69	-14.26	-2.87	-15.70	-1.05	-25.42
15	-2.16	-10.90	0.75	-13.83	-1.22	-11.19	1.32	-18.48
16	-1.74	-9.15	1.56	-10.78	-1.09	-10.77	1.53	-17.89
17	-1.95	-10.12	1.05	-12.48	-1.12	-10.84	1.39	-17.93
18	-1.64	-8.42	1.79	-9.50	-0.42	-8.36	2.34	-14.27
19	-1.41	-7.55	2.11	-7.88	-0.24	-7.92	2.60	-13.52
20	-1.87	-10.08	0.92	-12.44	-1.12	-10.71	1.09	-17.70
21	-1.43	-8.09	1.95	-8.86	-0.56	-8.97	2.12	-15.07
22	-1.45	-8.35	1.71	-9.35	-0.88	-9.88	1.44	-16.39
Subbasin_ID	TMPINC(month) = Temperature adjustment within the month by the specified amount (°C)							
1	1.0	1.0	1.5	1.5	1.5	1.5	2.0	2.0
2	1.0	1.0	1.5	1.5	1.5	1.5	2.0	2.0
3	1.0	1.0	1.5	1.5	1.5	1.5	2.0	2.0
4	1.0	1.0	1.5	1.5	1.5	1.5	2.0	2.0
5	1.0	1.0	1.5	1.5	1.5	1.5	2.0	2.0
6	1.0	1.0	1.5	1.5	1.5	1.5	2.0	2.0
7	1.0	1.0	1.5	1.5	1.5	1.5	2.0	2.0
8	1.0	1.0	1.5	1.5	1.5	1.5	2.0	2.0
9	1.0	1.0	1.5	1.5	1.5	1.5	2.0	2.0
10	1.0	1.0	1.5	1.5	1.5	1.5	2.0	2.0
11	1.0	1.0	1.5	1.5	1.5	1.5	2.0	2.0
12	1.0	1.0	1.5	1.5	1.5	1.5	2.0	2.0
13	1.0	1.0	1.5	1.5	1.5	1.5	2.0	2.0
14	1.0	1.0	1.5	1.5	1.5	1.5	2.0	2.0
15	1.0	1.0	1.5	1.5	1.5	1.5	2.0	2.0
16	1.0	1.0	1.5	1.5	1.5	1.5	2.0	2.0
17	1.0	1.0	1.5	1.5	1.5	1.5	2.0	2.0
18	1.0	1.0	1.5	1.5	1.5	1.5	2.0	2.0
19	1.0	1.0	1.5	1.5	1.5	1.5	2.0	2.0
20	1.0	1.0	1.5	1.5	1.5	1.5	2.0	2.0
21	1.0	1.0	1.5	1.5	1.5	1.5	2.0	2.0
22	1.0	1.0	1.5	1.5	1.5	1.5	2.0	2.0
Subbasin_ID	RADINC(month) = Radiation adjustment within the month by the specified amount (MJ/m²-day)							
1	-0.18	0.25	-0.36	0.50	-0.36	0.50	-0.54	0.75
2	-0.18	0.25	-0.36	0.50	-0.36	0.50	-0.54	0.75
3	-0.18	0.25	-0.36	0.50	-0.36	0.50	-0.54	0.75
4	-0.18	0.25	-0.36	0.50	-0.36	0.50	-0.54	0.75
5	-0.18	0.25	-0.36	0.50	-0.36	0.50	-0.54	0.75
6	-0.18	0.25	-0.36	0.50	-0.36	0.50	-0.54	0.75
7	-0.18	0.25	-0.36	0.50	-0.36	0.50	-0.54	0.75
8	-0.18	0.25	-0.36	0.50	-0.36	0.50	-0.54	0.75
9	-0.18	0.25	-0.36	0.50	-0.36	0.50	-0.54	0.75
10	-0.18	0.25	-0.36	0.50	-0.36	0.50	-0.54	0.75
11	-0.06	0.09	-0.12	0.18	-0.12	0.18	-0.18	0.26
12	-0.18	0.25	-0.36	0.50	-0.36	0.50	-0.54	0.75
13	-0.18	0.25	-0.36	0.50	-0.36	0.50	-0.54	0.75
14	-0.18	0.25	-0.36	0.50	-0.36	0.50	-0.54	0.75
15	-0.06	0.09	-0.12	0.18	-0.12	0.18	-0.18	0.26
16	-0.06	0.09	-0.12	0.18	-0.12	0.18	-0.18	0.26
17	-0.06	0.09	-0.12	0.18	-0.12	0.18	-0.18	0.26
18	-0.06	0.09	-0.12	0.18	-0.12	0.18	-0.18	0.26
19	-0.06	0.09	-0.12	0.18	-0.12	0.18	-0.18	0.26
20	-0.06	0.09	-0.12	0.18	-0.12	0.18	-0.18	0.26
21	-0.06	0.09	-0.12	0.18	-0.12	0.18	-0.18	0.26
22	-0.06	0.09	-0.12	0.18	-0.12	0.18	-0.18	0.26

4.3 Results and discussion

4.3.1 Climate change scenarios

The relative sensitivity of WBCs to the baseline in terms of percent change for the yearly and monthly WBCs due to for the combined effects of rainfall, temperature, and solar radiation variables were assessed (Table 13) for both RCP 4.5 and 8.5 scenarios. Overall, the yearly average of WBCs would be projected to decrease in comparison with the baseline under both the RCP 4.5 and RCP 8.5 scenarios except PET. The relative percent change of PET would be projected to consistently increase due to increase in temperature and solar radiation during the dry season. However, the actual evapotranspiration decreased in comparison to the baseline value, which was most likely due to decrease in rainfall and thus limited soil moisture availability. Therefore, rainfall showed as the determinant factor for the negative effects of climate change impacts compared to against temperature and solar radiation changes. These results were consistent with previous studies (Erwin, 2009, Eversole, *et al.*, 2014, Safeeq and Fares, 2012). The effect of rainfall at the coastal region change would be a more pronounced at the coastal region, compared to the upstream regions (Figure 20 and Figure 21). Consequently, the relative changes in the WBCs, due to rainfall changes, were larger at Wetland than Watershed scales (Table 14). As should be expected, the results utilizing monthly time steps showed that the dry season caused more pronounced relative negative change in the WBCs than the wet season due to the variable rainfall, temperature, and solar radiation under both scenarios (RCP4.5 and 8.5) of climate change. The relative negative change in the WBCs was higher in the coastal wetland than further upland of the Watershed because of the variation in climatic parameters in both spatial and temporal scales (Giambelluca, *et al.*, 2011). Furthermore, the relative negative change in dry season for RCP 8.5 was higher than RCP4.5, especially for the late (2080s) period compared with the middle (2050s) period. These negative impacts were more pronounced for the seasonal change in recharge, surface runoff, lateral flow, and rainfall, especially for the Wetland compared with whole Watershed scale due to the variation in climatic parameters (Diaz, *et al.*, 2011, Longman, *et al.*, 2014, Meteorology and CSIRO, 2011, Safeeq and Fares, 2012, Timm, *et al.*, 2015). The high value of relative change in recharge compare to other components was due to the low value of recharge within the Wetland, with -100% relative changes in some instances for zero estimated recharge. The results showed that the

relative change in ET was expected to be positive during the wet season but negative during the dry season, which was in line with the rainfall change (Figure 20 and Figure 21).

The results indicated that the climate change effects were within the range of predictive uncertainties of the baseline. For instance, at the Haiku station, the 95PPU of climate change scenarios was within the 95PPU of the baseline, which indicated no pronounced impacts at upstream subbasins (Figure 22 and Figure 23). Consequently, the future climate change scenarios effect will be within the noise of model prediction uncertainty and may not have significant effect on the streamflow, except the middle 2050s and late 2080s period of RCP8.5 at Wetland station. The findings indicated that the amount of streamflow decreased particularly for the late 2080s of RCP 8.5 (Figure 22 and Figure 23).

Table 13: The yearly relative percent changes in the WBCs of the Heeia Wetland and Watershed relative to the baseline of RCP 4.5 and RCP8.5 scenarios.

Scale	Scenario	Scenario name	Rainfall	Streamflow	Runoff	Lateralflow	Baseflow	Recharge	Soil moisture	ET	PET
Wetland	Mid-max-RCP 4.5	S1wld	-7.78	-14.67	-12.06	-9.68	-19.03	-18.04	-22.30	-5.31	3.41
	Late-min-RCP 4.5	S2wld	-9.45	-17.62	-15.00	-11.35	-22.88	-21.73	-27.48	-6.48	5.21
	Mid-max-RCP 8.5	S3wld	-8.11	-13.47	-11.14	-8.82	-17.50	-16.33	-26.47	-6.12	5.21
	Late-min- RCP 8.5	S4wld	-13.20	-21.22	-18.79	-14.43	-26.78	-25.27	-36.46	-10.22	7.03
Watershed	Mid-max-RCP 4.5	S1wshd	-5.37	-8.76	-10.75	-6.55	-9.79	-8.87	-3.21	-1.56	3.43
	Late-min-RCP 4.5	S2wshd	-6.08	-10.09	-11.99	-7.35	-11.54	-10.21	-3.99	-1.67	5.24
	Mid-max-RCP 8.5	S3wshd	-4.40	-7.10	-6.97	-5.26	-8.43	-7.58	-3.09	-1.26	5.24
	Late-min-RCP 8.5	S4wshd	-8.02	-12.18	-12.90	-9.29	-14.03	-12.61	-5.67	-3.31	7.05

RCP = Representative Concentration Pathways; RCP 4.5 when radiative forcing 4.5 watt per square meters, carbon dioxide equivalent 650 part per million (PPM) and temperature anomaly 2.4 °C while RCP8.5 when radiative forcing 8.5 watt per square meters, carbon dioxide equivalent 1370 part per million (PPM) and temperature anomaly 2.9 °C (Moss, et al., 2010). wld = wetland; wshd = watershed
Mid = middle (2041-2070) and late (2071-2100) of twenty first century; max = maximum; min = minimum; ET = evapotranspiration; PET = Potential evapotranspiration

Table 14: The seasonally relative percent change in the (WBCs) of the Heeia Wetland and Watershed relative to the baseline of RCP 4.5 and RCP8.5 scenarios.

The climate change impacts for the monthly wet and dry season of Heeia Wetland											
Scenario	**Season**	**Scenario No**	**Rainfall**	**Streamflow**	**Runoff**	**Lateralflow**	**Baseflow**	**Recharge**	**Soil moisture**	**ET**	**PET**
Midmax4.5	wet	S1	-3.47	-10.53	-7.41	-5.15	-18.94	-12.11	-7.83	-1.86	2.71
	dry	S2	-22.52	-19.37	-33.11	-29.15	-14.87	-64.44	-20.94	-16.68	5.98
Midmax8.5	wet	S3	-1.64	-10.22	-5.59	-4.63	-19.75	-12.55	-8.77	1.01	3.79
	dry	S4	-20.20	-19.10	-30.63	-25.40	-15.83	-68.16	-21.64	-14.61	6.30
Latemin 4.5	wet	S5	-4.77	-14.84	-11.20	-8.19	-25.12	-18.45	-10.74	-0.09	3.79
	dry	S6	-18.22	-22.47	-28.70	-23.97	-21.21	-66.95	-21.65	-14.10	6.30
Latemin 8.5	wet	S7	-4.16	-16.64	-11.30	-8.65	-29.53	-20.84	-13.73	0.04	4.81
	dry	S8	-30.05	-28.98	-44.47	-37.06	-24.68	-84.61	-31.25	-22.46	8.72
lowest impact %	wet		-1.64	-10.22	-5.59	-4.63	-18.94	-12.11	-7.83	1.01	4.81
Highest impact %	wet		-4.77	-16.64	-11.30	-8.65	-29.53	-20.84	-13.73	-1.86	2.71
lowest impact %	dry		-18.22	-19.10	-28.70	-23.97	-14.87	-64.44	-20.94	-14.10	8.72
Highest impact %	dry		-30.05	-28.98	-44.47	-37.06	-24.68	-84.61	-31.25	-22.46	5.98
The climate change impacts for the monthly wet and dry season of Heeia Basin											
Scenario	**Season**	**Scenario No**	**Rainfall**	**Streamflow**	**Runoff**	**Lateralflow**	**Baseflow**	**Recharge**	**Soil moisture**	**ET**	**PET**
Midmax4.5	wet	S1	-2.30	-7.38	-6.70	-4.44	-10.28	-4.92	-3.21	1.16	2.92
	dry	S2	-10.19	-10.63	-22.58	-10.45	-9.33	-18.96	-7.30	-4.02	3.82
Midmax8.5	wet	S3	0.83	-4.76	-0.06	-1.96	-9.08	-1.67	-3.15	2.82	4.12
	dry	S4	-12.61	-10.27	-27.20	-11.36	-7.81	-22.67	-9.41	-4.95	6.08
Latemin 4.5	wet	S5	-2.07	-8.30	-6.85	-4.68	-12.16	-5.35	-4.19	2.11	4.12
	dry	S6	-12.38	-12.50	-27.03	-12.28	-10.96	-22.60	-9.71	-5.09	6.08
Latemin 8.5	wet	S7	-0.06	-8.80	-3.16	-4.35	-14.99	-3.94	-5.43	2.96	5.31
	dry	S8	-20.49	-16.74	-41.40	-18.43	-13.13	-34.77	-14.73	-8.99	8.36
lowest impact %	wet		0.83	-4.76	-0.06	-1.96	-9.08	-1.67	-3.15	2.96	5.31
Highest impact %	wet		-2.30	-8.80	-6.85	-4.68	-14.99	-5.35	-5.43	1.16	2.92
lowest impact %	dry		-10.19	-10.27	-22.58	-10.45	-7.81	-18.96	-7.30	-4.02	8.36
Highest impact %	dry		-20.49	-16.74	-41.40	-18.43	-13.13	-34.77	-14.73	-8.99	3.82

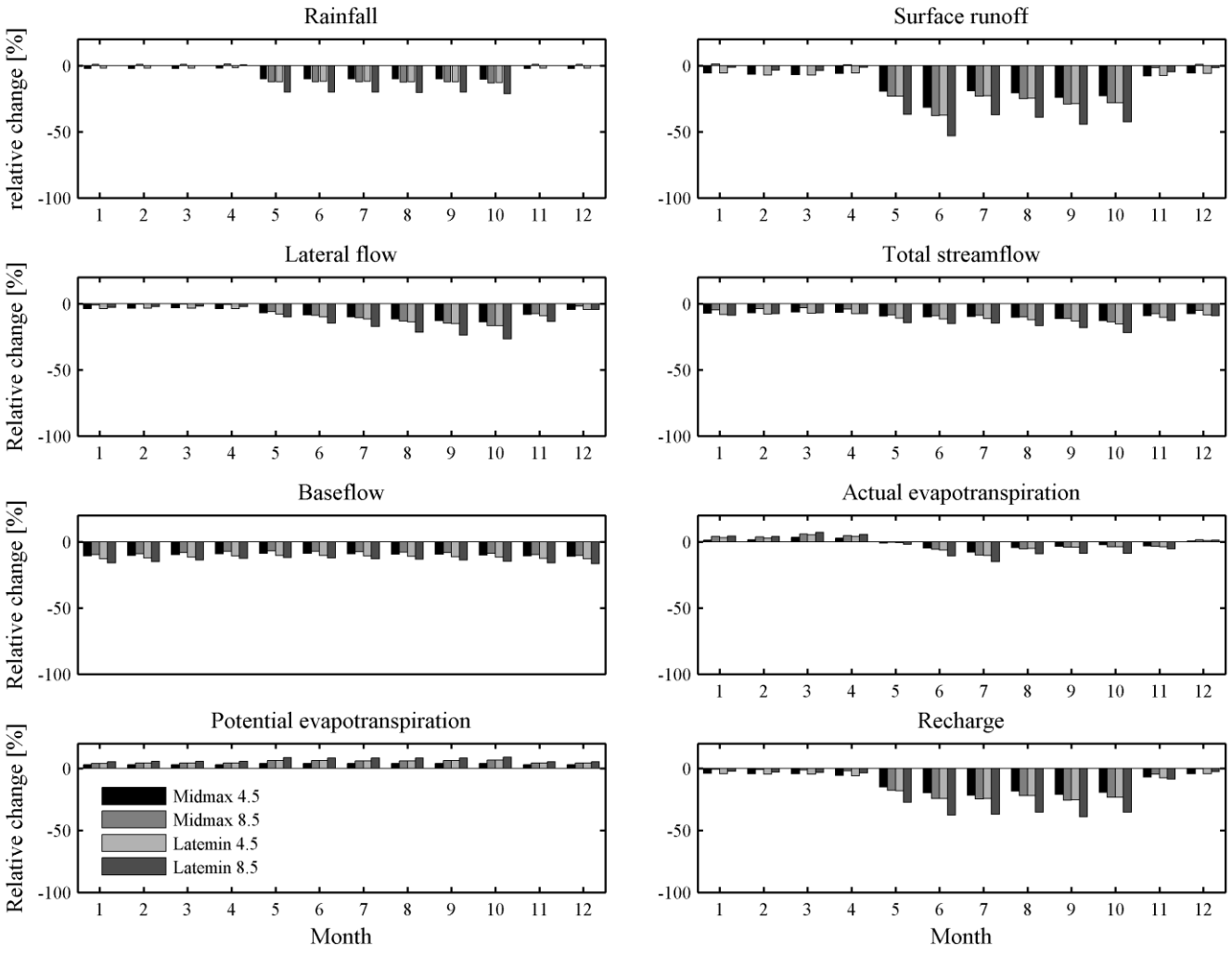

Figure 20: The monthly relative percent change in (WBCs) of the Heeia Watershed relative to the baseline of RCP 4.5 and RCP8.5 scenarios.

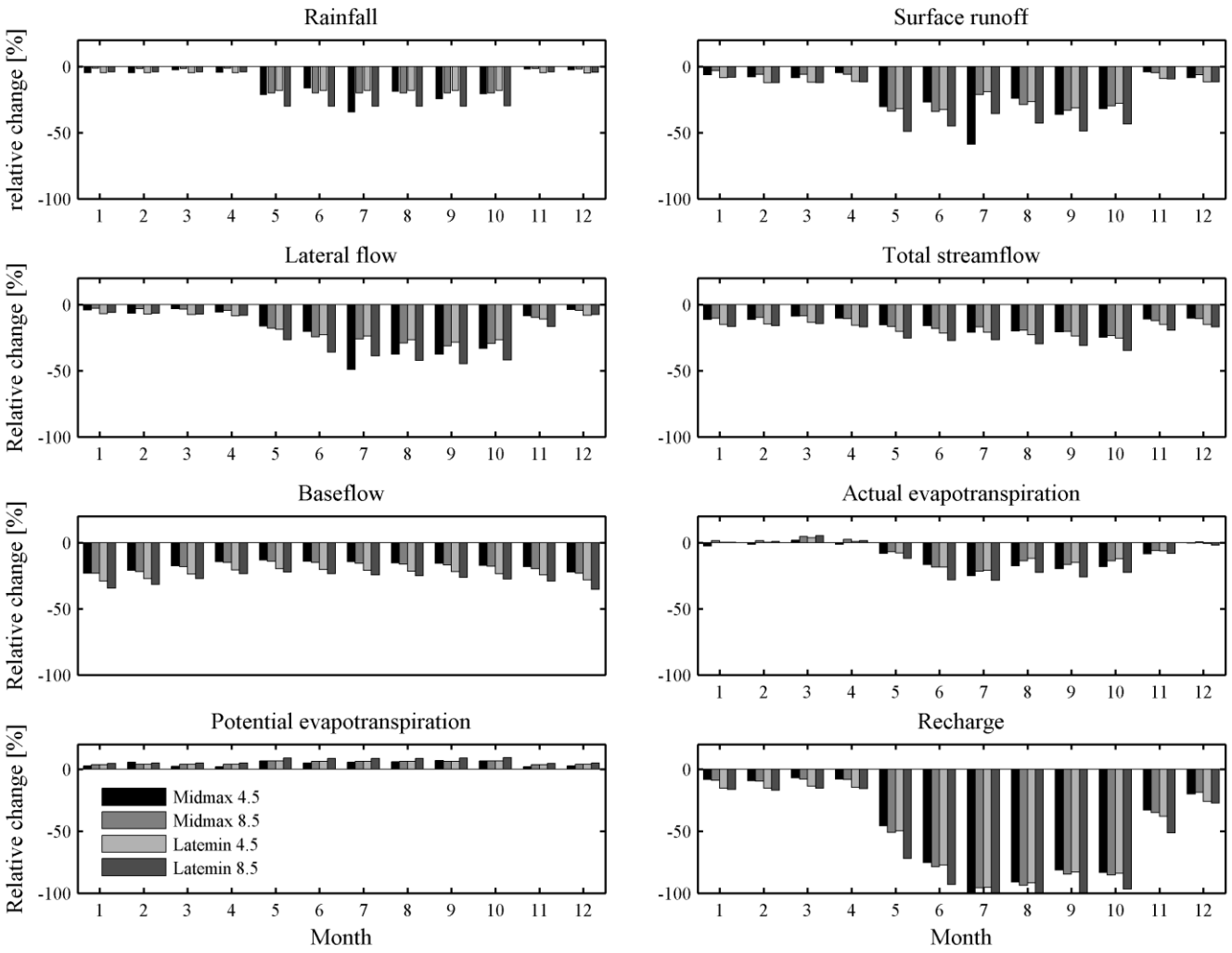

Figure 21: The monthly relative percent change in (WBCs) of the Heeia Wetland relative to the baseline of RCP 4.5 and RCP8.5 scenarios.

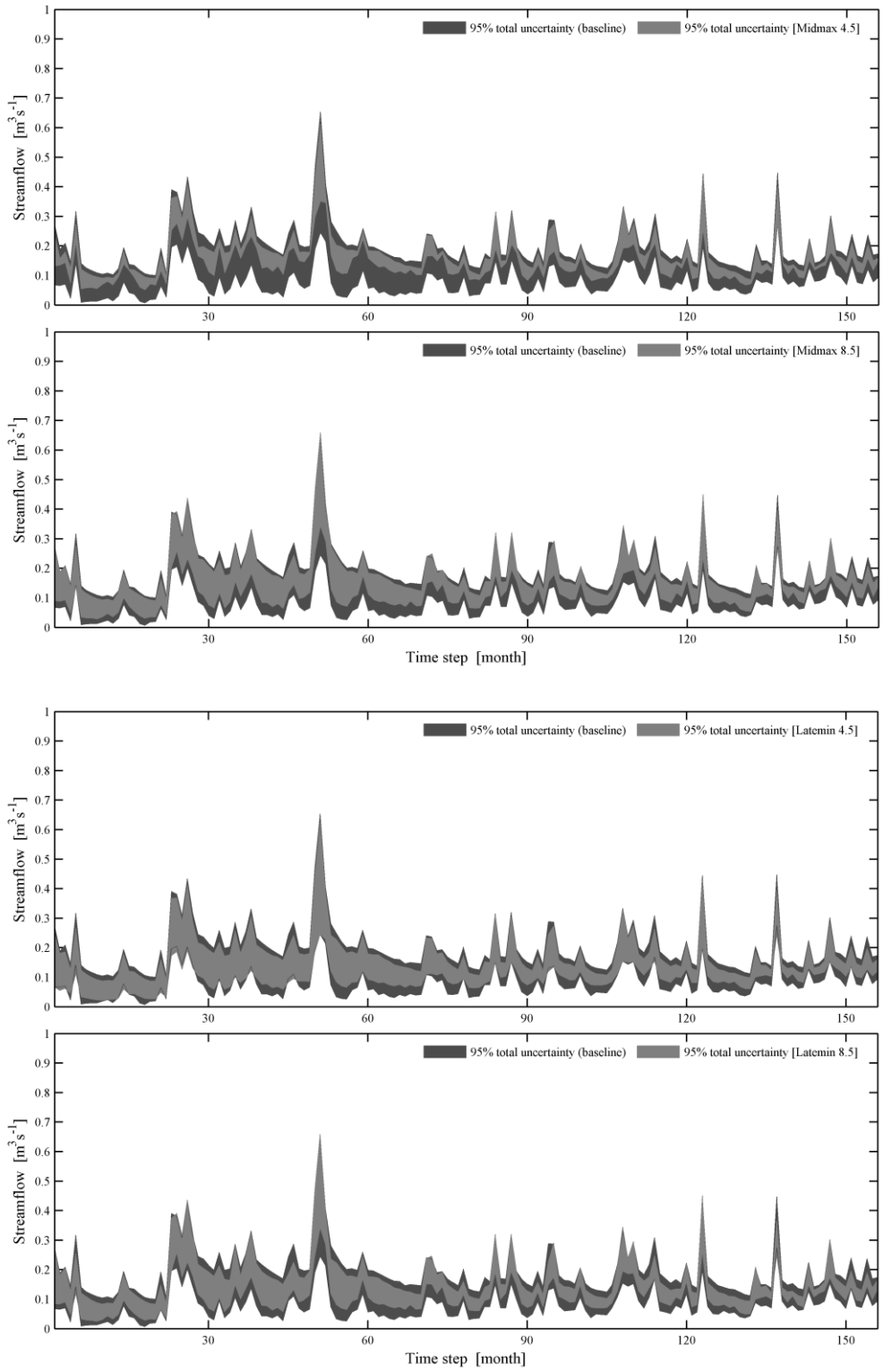

Figure 22: The monthly 95% streamflow prediction uncertainty for the thirteen years of baseline and as a result of rainfall, temperature, and solar radiation changes for RCP 4.5 and 8.5 scenarios at the Haiku station.

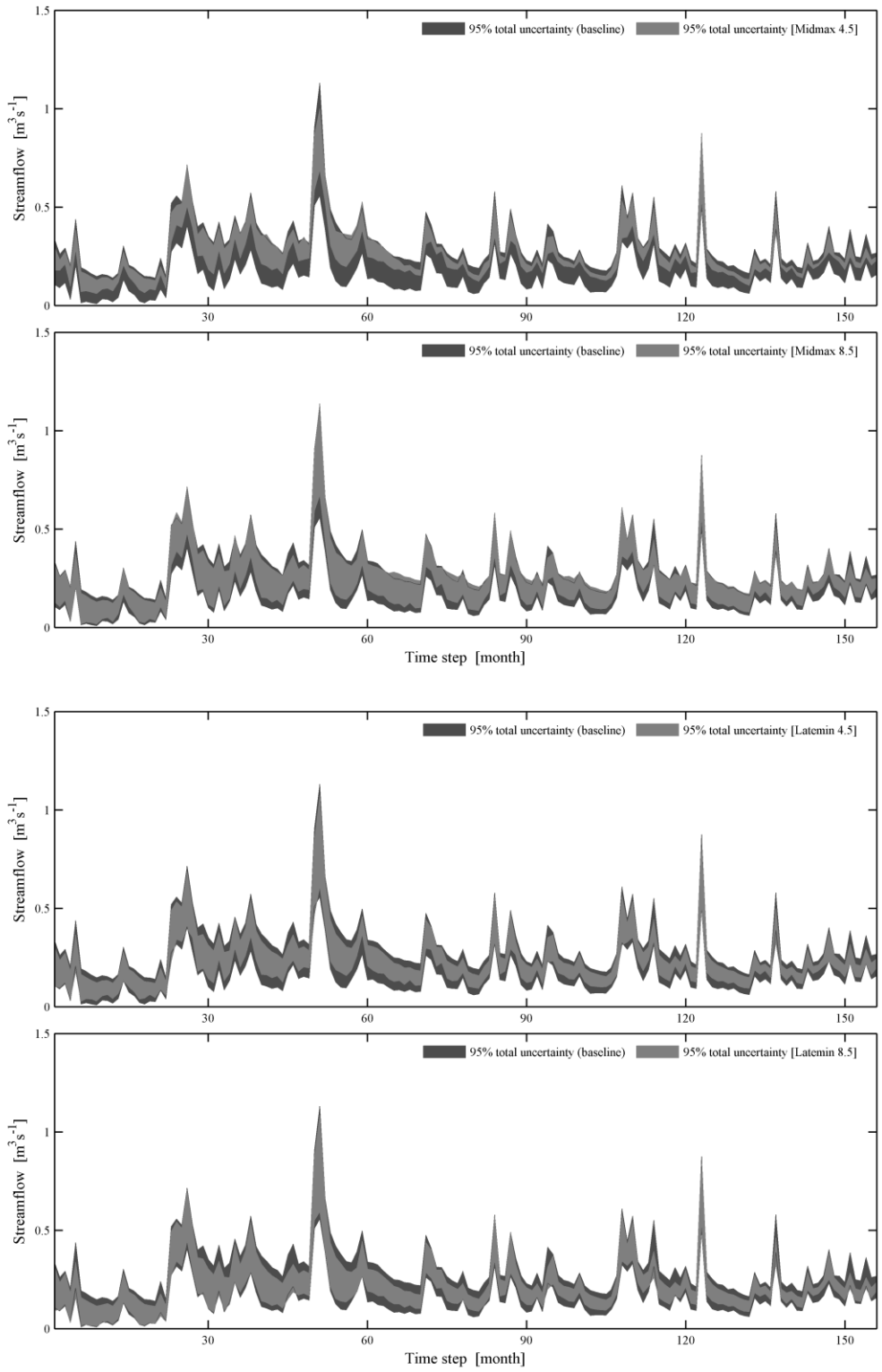

Figure 23: The monthly 95% streamflow prediction uncertainty for the thirteen years of baseline and as a result of rainfall, temperature, and solar radiation changes for RCP 4.5 and 8.5 scenarios at the Wetland station.

4.3.2 Combined effects of climate change and wetland restoration on the WBCs

The simulated WBCs were analyzed on monthly average basis for both Wetland and Watershed scales under four combined climate change and LU scenarios. Also, taro field irrigation water requirement from streamflow diversion was set at 50% of minimum stream reach flow (Table 15). Considering LU, results showed that there were generally an increase in surface runoff and lateral flow for both Wetland and Watershed scales. This could be mainly due to the taro cultivation and ponding of water, especially during wet season, which will dominate the effects of CL scenarios (Table 14 and Table 15). In contrast, the recharge and baseflow were expected to decrease due to the combined effects of CL and LU (Figure 24and Figure 25). This was probably due to the setting of the impervious layer at a depth of 25 cm below surface of taro patches (Uchida, *et al.*, 2008), These changes become more pronounced in the late 2080s period especially during the dry season. The results in Figure 24 and Figure 25 indicate that the total streamflow was more correlated to changes in rainfall than other components (temperature and solar radiation). In addition, the trend of the total streamflow was compatible with surface runoff, while the lateral flow was inversely proportional to surface runoff and total streamflow. The results stressed the effect of LU on increasing the lateral flow especially during dry season compared with CL scenarios (Figure 20 and Figure 21). The results indicated that the baseflow was considered the main component of streamflow especially during dry season for all scenarios in spite of the decrease after LU (Figure 23 and Figure 24). The soil moisture content is expected to increase after LU for all CL scenarios due to the ponding water in taro patches and creating a pool. The trend of potential evapotranspiration was in the decline behavior, especially during the dry season (Figure 29). It was not possible to illustrate the trend of monthly actual evapotranspiration for all scenarios due to the coupled interaction between the LU and climatic projections (Figure 29).

Table 15: The seasonally percent change in the (WBCs) of the Heeia Wetland and Watershed relative to the baseline of RCP 4.5 and RCP8.5 scenarios with applied irrigation management.

The combined climate change and restoration (S2) impacts for the monthly wet and dry season of Heeia Wetland											
Scenario	**Season**	**Scenario No**	**Rainfall**	**Streamflow**	**Runoff**	**Lateralflow**	**Baseflow**	**Recharge**	**Soil moisture**	**ET**	**PET**
LUs2_Midmax4.5	wet	S1	-4.15	4.60	57.72	28.03	-54.19	-50.57	13.54	-4.80	2.30
	dry	S2	-14.63	-28.89	-16.64	51.68	-51.82	-73.63	32.22	-4.01	4.15
LUs2_Midmax8.5	wet	S3	-4.15	4.60	57.72	28.03	-54.19	-50.57	13.54	-4.80	2.30
	dry	S4	-14.63	-28.89	-16.64	51.68	-51.82	-73.63	32.22	-4.01	4.15
LUs2_Latemin 4.5	wet	S5	-4.77	1.38	52.54	25.16	-56.75	-52.52	11.00	-3.92	3.22
	dry	S6	-18.22	-32.73	-24.11	43.72	-54.06	-80.57	24.98	-7.08	6.54
LUs2_Latemin 8.5	wet	S7	-4.16	-1.12	50.21	22.49	-59.13	-53.70	7.32	-3.06	4.14
	dry	S8	-30.05	-39.78	-41.95	22.98	-56.00	-91.59	13.95	-15.31	8.97
lowest impact %	wet		-4.15	4.60	57.72	28.03	-54.19	-50.57	13.54	-3.06	4.14
Highest impact %	wet		-4.77	-1.12	50.21	22.49	-59.13	-53.70	7.32	-4.80	2.30
lowest impact %	dry		-14.63	-28.89	-16.64	51.68	-51.82	-73.63	32.22	-4.01	8.97
Highest impact %	dry		-30.05	-39.78	-41.95	22.98	-56.00	-91.59	13.95	-15.31	4.15
The combined climate change and restoration (S2) impacts for the monthly wet and dry season of Heeia Basin											
Scenario	**Season**	**Scenario No**	**Rainfall**	**Streamflow**	**Runoff**	**Lateralflow**	**Baseflow**	**Recharge**	**Soil moisture**	**ET**	**PET**
LUs2_Midmax4.5	wet	S1	-2.46	-5.75	-0.87	0.34	-13.09	-6.75	-0.34	-1.65	2.80
	dry	S2	-10.92	-9.61	-22.42	-0.41	-12.29	-21.17	-3.29	-5.16	3.90
LUs2_Midmax8.5	wet	S3	0.56	-3.53	6.09	2.38	-12.56	-3.72	-0.33	0.03	3.95
	dry	S4	-13.85	-10.01	-27.36	-2.52	-11.40	-26.00	-5.86	-6.15	6.19
LUs2_Latemin 4.5	wet	S5	-2.36	-7.07	-1.27	-0.44	-15.32	-7.28	-1.40	-0.64	3.95
	dry	S6	-13.38	-11.93	-26.94	-3.08	-14.25	-25.28	-6.22	-6.30	6.19
LUs2_Latemin 8.5	wet	S7	-0.52	-8.12	2.18	-0.82	-18.70	-6.09	-2.71	0.35	5.10
	dry	S8	-22.02	-16.94	-41.52	-10.86	-16.90	-38.15	-11.81	-10.30	8.51
lowest impact %	wet		0.56	-3.53	6.09	2.38	-12.56	-3.72	-0.33	0.35	5.10
Highest impact %	wet		-2.46	-8.12	-1.27	-0.82	-18.70	-7.28	-2.71	-1.65	2.80
lowest impact %	dry		-10.92	-9.61	-22.42	-0.41	-11.40	-21.17	-3.29	-5.16	8.51
Highest impact %	dry		-22.02	-16.94	-41.52	-10.86	-16.90	-38.15	-11.81	-10.30	3.90
LUs2 = wetland restoration for scenario-2 (decrease 50% of minimum flow).											

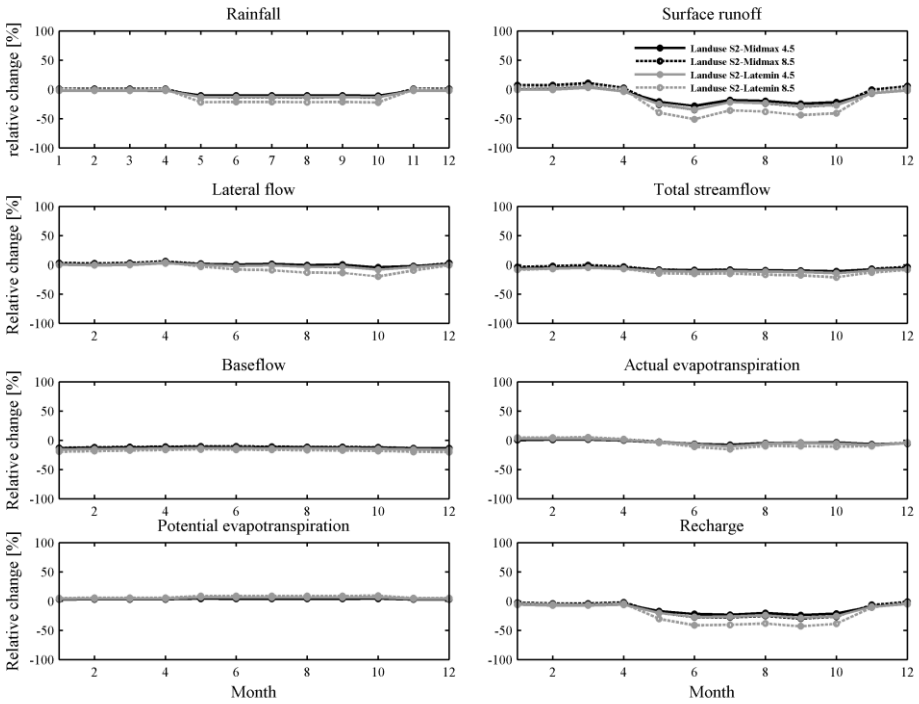

Figure 24: The monthly relative percent change in (WBCs) of the Heeia Watershed relative to the baseline of combined climate change and wetland restoration scenarios.

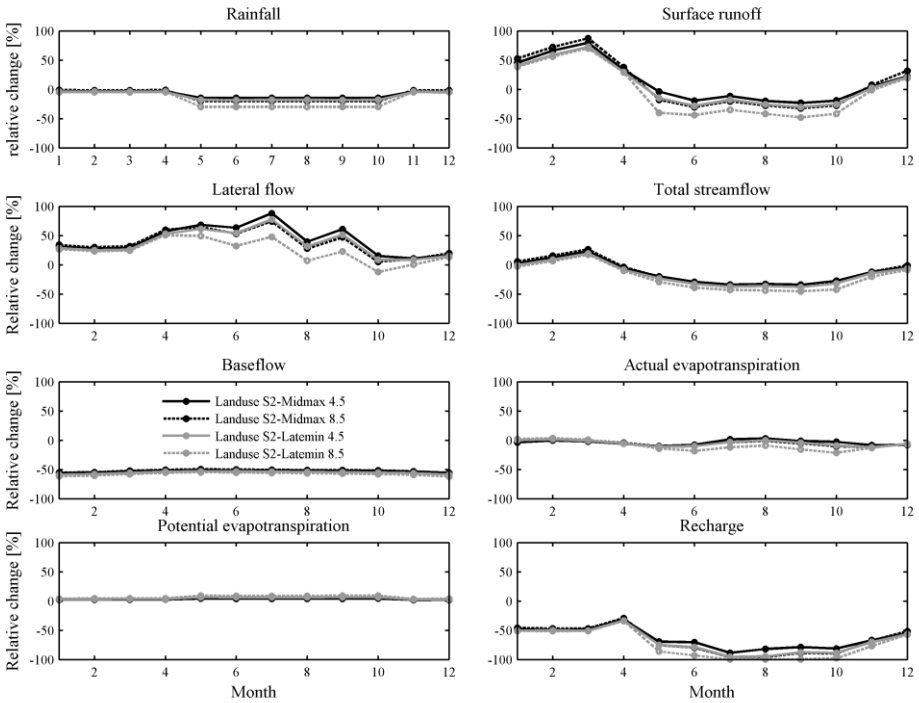

Figure 25: The monthly relative percent change in (WBCs) of the Heeia Wetland relative to the baseline of combined climate change and the Wetland restoration scenarios.

4.4 Conclusions

The combined effects of wetland restoration and climate change may have profound impacts on the WBCs in Heeia Wetland. These impacts reflect on the fresh water availability within coastal region, which have a vital role in both ecological health and human well-being. In this study, the SWAT model was developed to capture the unique characteristics of Hawaiian Islands in terms of volcanic soil, initial infiltration rate, and other special hydrogeological features. The model successfully and satisfactorily simulated the stream flow in both upstream and downstream segment of the watershed in spite of hydrological data scarcity and the absence of taro crop in the SWAT data base. The SUFI-2 technique was used to estimate the sensitivity and uncertainty for different climate change scenarios.

The results showed the changes in the WBCs, were, as expected driven by the combined effects of CL and LU. The spatial and temporal rainfall variation was the determinant factor of the relative negative impact on the WBCs. Recharge and baseflow were the highly sensitive components to the combined effects of LU and CL especially during dry seasons. Moreover, the downstream flow significantly dependent on the groundwater discharge during dry season compared with other stream components. The relative decrease as resulting of the LU were higher than CL on recharge, baseflow, soil moisture content, and streamflow especially during the dry seasons. The WBCs were more impacted in the late of the 2080s than 2050s periods. The CL effects were within the range of the predictive uncertainties of both baseline and future climate change scenarios except the middle 2050s and late 2080s period of RCP8.5 at the Wetland Station. The uncertainty analysis indicates that the streamflow will decline during the late 2080s period of RCP 8.5 in the Wetland station, while it will increase in the middle 2050s of RCP 8.5.

Considering the importance of evaluating the hydrological changes after LU, this study can be extended to examine the effect of restoration processes on the water quality and sustainable Wetland Restoration Management.

Chapter5 Assessing fresh submarine groundwater discharge in the Heeia Coastal Shoreline via integrated hydrological modeling approach

5.1 Introduction

The Heeia coastal zone in Hawaii is a typical example of groundwater dependent ecosystems due to the presence of boundary interface among the Island of Oahu's largest fishpond, the largest federally designated wetland, and the Kaneohe Bay's greatest sheltered water body of coral reefs (Dulai, *et al.*, 2016, Jokiel, 1991). Understanding the processes that take place at the boundary of terrestrial and marine environments are crucial in preserving native ecosystems and saving marine biodiversity (Wilder, *et al.*, 1999). Fresh water flows play vital roles in preserving the native adjacent ecosystems. For instance, the growth of diverse groups of plankton in water bodies like ocean, lakes, and wetland, is highly influenced by the availability of nutrients and light. The importance of plankton is obvious through providing a crucial source of food to large aquatic organisms and reducing the greenhouse emission in the coastal zone (Libes, 2011). Assessing the freshwater discharge and associated nutrient fluxes into the ocean by streams, rivers, and FSGD has been getting great attentions among researchers, managers, and policymakers especially who focus on the coastal environmental health (UNESCO, 2004). Therefore, quantifying the volumetric freshwater discharge through surface runoff and SGD in coastal zones, is needed to understand the comprehensive relationships between coastal hydrology processes and ecosystems.

In the Hawaiian Islands, the groundwater gradient slope between the coastal aquifer and ocean is considered the indispensable driver of fresh water and nutrient fluxes through SGD process (McGowan, 2004). FSGD is a significant hydrological process and an important component of water budget that transports considerable amount of fresh water and dissolved nutrients from coastal aquifer to the nearshore marine environment. The transport of nutrients highly depends on the amount of aquifer groundwater storage and head that determine the hydraulic flow gradient from land to ocean (Burnett, *et al.*, 2006, Duarte, *et al.*, 2010, Moore, *et al.*, 2009). The positive impact of FSGD on marine ecosystems is achieved through decreasing the salinity level and altering the pH gradient in coastal waterways,

which enables the organisms to maintain their sustainable productivity (Duarte, *et al.*, 2010, Libes, 2011, McGowan, 2004).

Estimating SGD is very challenging due to the fact that the flow magnitude can vary spatially and temporally, which in turns depend on the site hydrogeological framework features, climate variability, and human activities. Generally, SGD for fresh groundwater and recirculated seawater, is estimated by direct field measurement, using geochemical tracers, and hydrological models (Burnett, *et al.*, 2006). Field measurements of SGD are most adequate for small scale assessment. Alternatively, the water balance approach has been used for estimating SGD across coastal shoreline (Shade and Nichols, 1996), but it is very simplified, ignores density dependent groundwater flow, and is subjected to large error in estimating recharge (Zhang, *et al.*, 2002). Due to the complicated interactions at the interface of land and ocean, estimating SGD needs integrated modeling that considers the surface and ground water hydrology interact with ocean circulations. The integrated hydrological model approach of distributed MODFLOW model and semi-distributed SWAT model is thus considered a more representative estimation of the freshwater discharge fluxes along the coastline for large scale with temporal and spatial variability (Andersen, *et al.*, 2007, Hugman, *et al.*, 2015). Moreover, integrated hydrogeological models can be used to estimate the FSGD values under current and future conditions of sea level, land use, and climate changes (McCoy and Corbett, 2009). FSGD is influenced by the impacts of climate and land use changes through sea level rise, increased evapotranspiration, and decreased recharge as a resultant of both negative effects (Bishop, *et al.*, 2015, Kløve, *et al.*, 2014). Due to the complicated interactions at the interface of land and ocean, estimating SGD needs integrated modeling that considers the surface and ground water hydrology interact with ocean circulations.

In this study, the SWAT model (Arnold, *et al.*, 1998).and the MODFLOW model (McDonald and Harbaugh, 1988) were utilized in estimating FSGD. In addition, the another objective of the study assessment also included evaluating the consequences of the Heeia Wetland restoration, climate change, and sea level rise on the volumetric FSGD across the coastal shoreline of Heeia Watershed.

5.2 Methodology

In order to assess SGD, first, a MODFLOW model was developed for the Heeia Watershed. The recharge coverage of the study area, which used as an input to MODFLOW, was estimated by SWAT model (see Chapter 3). The SWAT also was used to estimate the recharge under Heeia future wetland

restoration, climate change, and combination of both factors impact. Additionally, the MODFLOW also was run considering future sea level rise. Then, FSGD was estimated for both steady and transient conditions. Finally, volumetric FSGD was quantified as the source of fresh groundwater flow across the coastal shoreline of the Heeia Watershed under different scenarios.

5.2.1 MODFLOW model description

The USGS MODFLOW model is a grid based, fully distributed, and USGS modular 3D groundwater flow model. The model numerically simulates saturated flow by solving the three-dimensional groundwater flow equation for porous media using a cell centered finite-difference approach (McDonald and Harbaugh, 1988). MODFLOW is interfaced with Groundwater Modeling System (GMS), where the input data of MODFLOW are generated and the model execution is performed by GMS. The main steps of setting up MODFLOW model includes the planning, conceptualization, verification, calibration, validation, and predictive scenarios (Barnett, *et al.*, 2012).

5.2.2 Data and MODFLOW 2005 set-up

The first step in setting up the model was importing a digital maps of the site to determine the containing location of water sources, wells, layer parameters, such as hydraulic conductivities, recharge zones, and model boundary conditions. An Oahu regional groundwater model developed by Whittier, et al. (2010) was used as reference for developing the Heeia MODFLOW model. The Heeia MODFLOW model simulated an area of 21.7 square kilometers, which encompassed aquifer in the Heeia Watershed and some a part of Kaneohe Bay. The area was extend into the ocean to more accurately simulate the flow boundary condition therein. The modeled area was variably discretized into 3680 cells of refined grid. The grid size was decreased toward the central and active portion of the model domain and increased toward the model boundary. The grid was rotated 150 degrees to achieve a better fit with active coverages of the conceptual model and reduce the number of inactive cells in the formulation. Two modeled material-layers units were used to represent the major hydrogeological unit features in the study area, which were with subdivided into twenty MODFLOW layers; one the top and bottom units were represented by one layer and nineteen layers, respectively. The latter unit was used to represent unit two, which divided the study domain into two dike zones (marginal and complex) (Figure 26). The top unit contained the free water-surface of an unconfined aquifer that is directly affected by surface hydrological processes, such as recharge. The second layer material was represented by the bed-rock

layer and the bottom boundary of the model, which is located at 2000 meters below sea-level. The two layers were assumed to have homogenous vertical conductivity because of the information scarcity of the lava layers (Izuka, *et al.*, 1993, Whittier, *et al.*, 2010).

Three types of boundary conditions were used to specify the groundwater flow paths within model domain, which included specified flux, head-dependent flux, and no flow boundary. The ground surface and ocean upper boundaries were represented with specified flux. The coastal shoreline was represented by specified-flux at the east boundary (Figure 27). The drain and groundwater seeps were simulated as head-dependent boundary conditions. The outer model boundary arcs were defined as no-flow boundaries based on the simplified assumption that assumed the groundwater flow divides coincide with major surface water divides and the hydraulic gradient was equal zero at no-flow boundary (Robinson, *et al.*, 1997). The Heeia stream was simulated as drain and was divided into two reach groups, the upstream group (before the Haiku USGS gauging station) and the downstream group (after Haiku station) representing the rest of the stream. In addition, the Heeia Wetland was simulated as drain because it represented the drainage basin of the Heeia stream (Kakoo Oiwi, 2011). The groundwater level at the boundary and the parameters of coverage setup were derived from simulated initial steady state conditions of the Oahu regional groundwater modeling of Whittier *et al*. (2010).

The Heeia Watershed was delineated into 22 subbasins by the SWAT model that represented the polygons of recharge coverage for MODFLOW model. The estimated daily recharge for predevelopment period, was derived from the 46% of the recorded rainfall at Mauka station (1950-1959) based on the water budget approach (Nichols, *et al.*, 1997, Shade and Nichols, 1996). The rainfall (predevelopment) was recorded at the old NOAA National Climatic Data Center (NCDC) Mauka station (GHCND: USC00513113). The estimated daily recharge output of the SWAT model (recorded rainfall in other stations see chapter 3) was used as input for the MODFLOW transient simulation and validation during post development period. In addition, for model calibration, the filtered baseflow by using the Water Engineering Time Series PROcessing tool (WTSPRO), was used as observed groundwater flow at Haiku Station for the period of 1950 to 1959 (pre-development) and from 2005 to 2014 (post-development) (Willems, 2004). For downstream, due to lack of streamflow data, MODFLOW was calibrated and validated by using the groundwater head observed in piezometers at the wetland and a previously derived baseflow scale factor (Leta, *et al.*, 2016). The predevelopment period was considered

the baseline scenario of FSGD assessment. Moreover, it is considered as verification of the assumed model boundary conditions in comparison with post development period (anthropogenic effects).

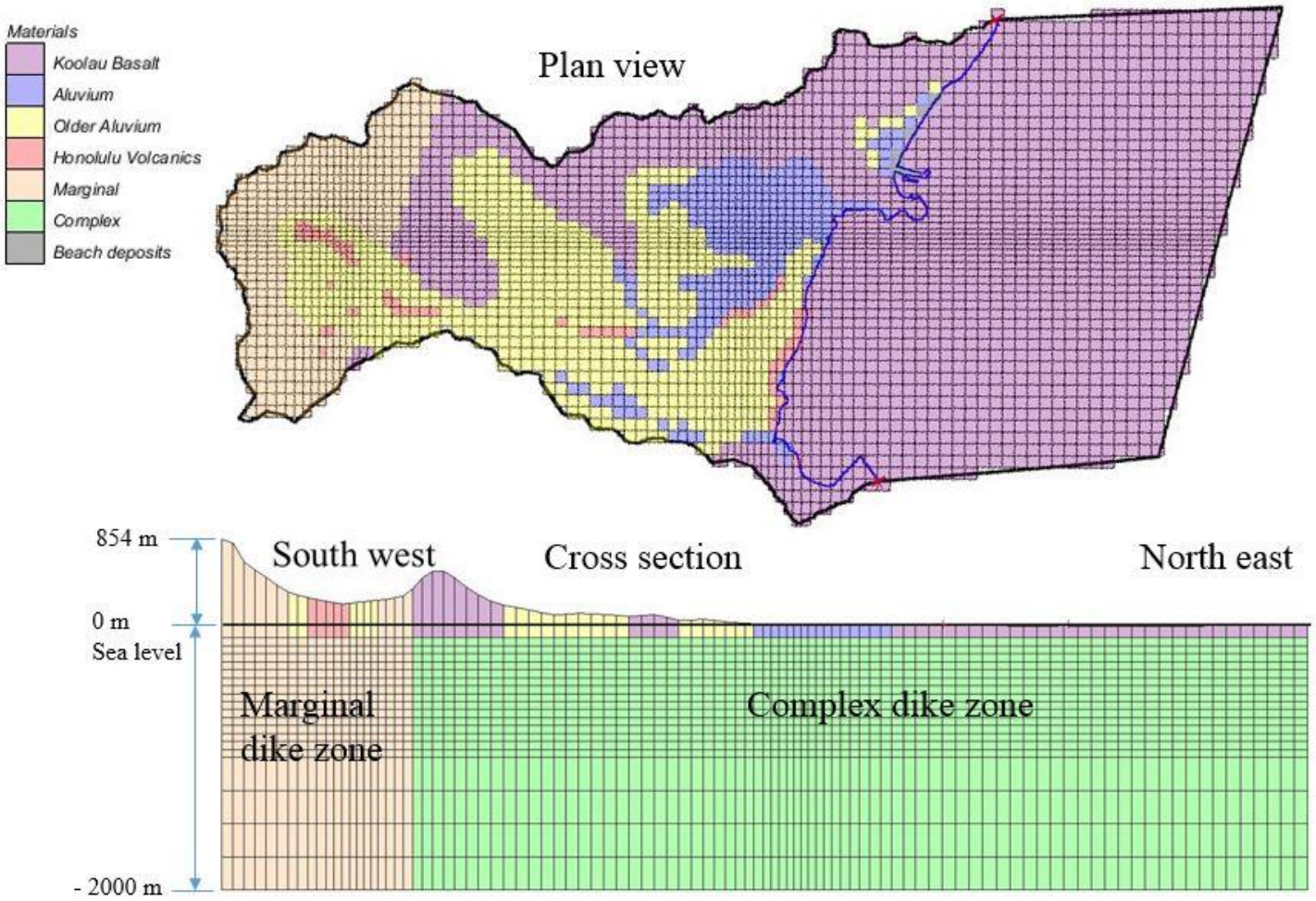

Figure 26: Plan and cross sectional view with hydrogeological materials of the Heeia MODFLOW model.

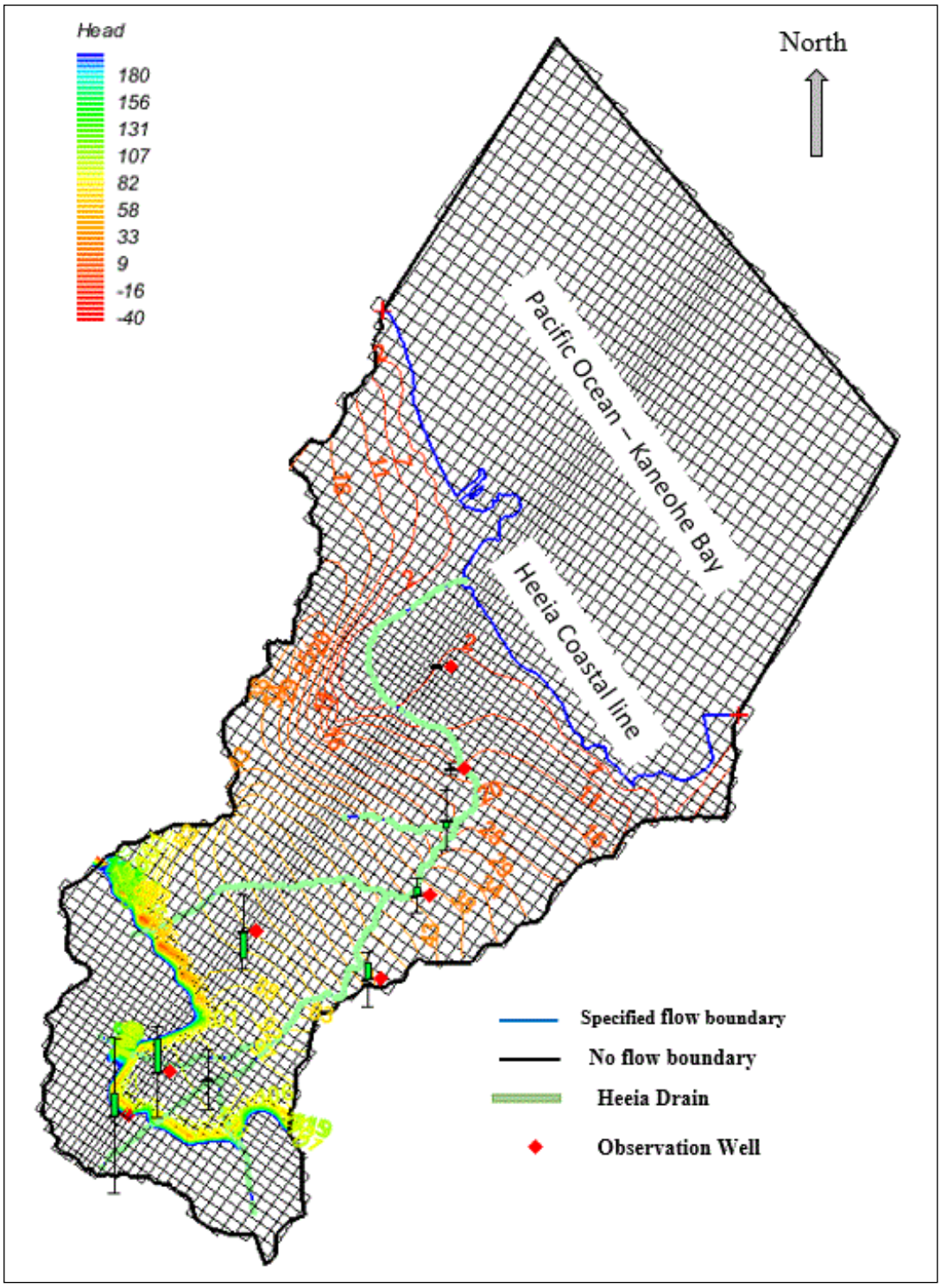

Figure 27: The boundary conditions of MODFLOW model of the Heeia unconfined aquifer.

5.2.3 MODFLOW model calibration and validation

The MODFLOW model was calibrated under steady state conditions by using automated parameter estimation approach through an inverse PEST model that interfaces with the GMS software. The inverse model was systematically adjusted with the input parameters until minimizing the difference between the computed and observed parameters values (Doherty and Hunt, 2009). The calibrated parameters include drain conductance, horizontal, vertical, and anisotropic hydraulic conductivity of the aquifer (Table 16).The MODFLOW model was developed to simulate both the steady state and transient conditions of groundwater flow in the Heeia unconfined aquifer. Under steady state conditions, water inflows are equal to outflows at equilibrium conditions resulting in no change in groundwater storage. In addition, input data and output results do not change over time. In contrast, calibration of the transient MODFLOW model of groundwater flow represented the dynamic system, in which variable inflows, outflows, and groundwater storage change with time. Therefore, it was considered as the primary step for discussing the spatial and temporal distribution of FSGD under different stress periods. The model was performed run by using daily timesteps and stress period for predevelopment and post development periods at two flow stations and two observed water level piezometers.

The MODFLOW model under transient condition and the SWAT model outputs were used as essential information to assess FSGD through the Heeia Coastal Shoreline. Moreover different scenarios were used to assess FSGD in daily stress periods and timesteps. The main factors and forces that drive and influence FSGD, include sea level rise, groundwater recharge, land use and climate changes, and hydraulic head gradient across the ocean-aquifer interface (Church, 1996, Mulligan and Charette, 2009). Based on the projected sea level rise of Hawaii, the sea level was increased by 0.12, 0.4, and 1.1 meters to represent the middle and the end of twenty first century, respectively (Rotzoll and Fletcher, 2013)(Figure 32: The daily sea level rise scenarios calculated based on RCP 8.5 projected for the Heeia Watershed based on levels observed between 2005 and 2014. The average annual values of recharge, discharge, pumping wells, and other groundwater flow system processes the same that were used during steady state calibration and validation. The steady state calibration used the calibration targets method of average initial groundwater level data in 7 wells and two stations of measured streamflow data within the Heeia Watershed. The transient model was calibrated using the historical Haiku stream flow data that were recorded between the periods of 1950 to 1959 for predevelopment. Then the model was

validated for the period of 2005 to 2014 for post development. The transient model calibration was started using the calibrated steady state model and estimated hydraulic conductivities, storage coefficient, and drains conductance. Daily timesteps and one stress period for each day were used for both predevelopment and post development periods.

5.3 Results and discussion

5.3.1 SGD simulation under steady state conditions

The results of the sensitivity analysis of the simulated model outputs indicate that the simulated head and drain flow were highly affected by changes in horizontal anisotropic hydraulic conductivity of older alluvium material (HANI_60), recharge in the mountain zone (RCH_80), horizontal hydraulic conductivity of older alluvium (HK_30), and drain conductance (Figure 26). On the other hand, the calibrated results indicated that the computed head was highly correlated with observed head and the steady state condition a model formulation was satisfactory (Figure 29). In addition, the ratio of standard error of model residual (1.5) to the range of observation (7) was 0.2 (Table 17) indicating good model fit (Kuniansky, *et al.*, 2004).

The results of MODFLOW model under steady state conditions indicated that the baseflow and FSGD comprised of 70% and 30% of recharge, respectively during predevelopment period (Table 18).The relative decreasing of post development relative to the baseline (predevelopment period) in recharge, baseflow, and FSGD, were 33%, 37%, and 53%, respectively under steady state conditions. The FSGD declined significantly due to decrease in recharge and increase in groundwater withdrawals (Table 18). On the other hand, the predicted future scenarios of recharge assessment according to the SWAT outputs (chapter 3 & 4) for scenarios of the wetland restoration (LU), climate change (CL), and combined effects declined by 2%, 13%, and 15% respectively at the end of twenty first century under RCP 8.5 climatic projections. These would be lead to FSGD decline by 0.3 %,1.9 %, 2.4 %, 9.6 %, respectively due to wetland restoration, climate change, combined effect of climate change and wetland restoration, and combined wetland restoration, climate change, and sea level rise (SLR) by 1.1 meter (Rotzoll and Fletcher, 2013). The outputs of MODFLOW model illustrated that FSGD is highly sensitive to the recharge rate, groundwater withdrawals, sea level rise, and climate change (Table 18).

Table 16: The calibrated parameters of steady state MODFLOW model.

MODFLOW

	ID	Name	Color/Pattern	Transparency (%)	Horizontal k (m/d)	Vertical k (m/d)	Horiz. anisotropy	Vert. anisotropy (Kh/Kv)
All								
1	4	Koolau Basalt		70.0	0.49982	0.1	0.09921	0.74271
2	5	Aluvium		70.0	0.5992108	0.1	0.0723	2.3689
3	6	Older Aluvium		70.0	1.074	0.1	0.97	0.1
4	8	Honolulu Volcanics		70.0	0.56755	0.1	0.5721	0.74271
5	9	Marginal		70.0	0.000195136	0.1	0.40834	0.1
6	3	Complex		70.0	0.000206	0.1	0.05257	0.5
7	1	Beach deposits		70.0	0.74696644	0.1	1.328475	3.0

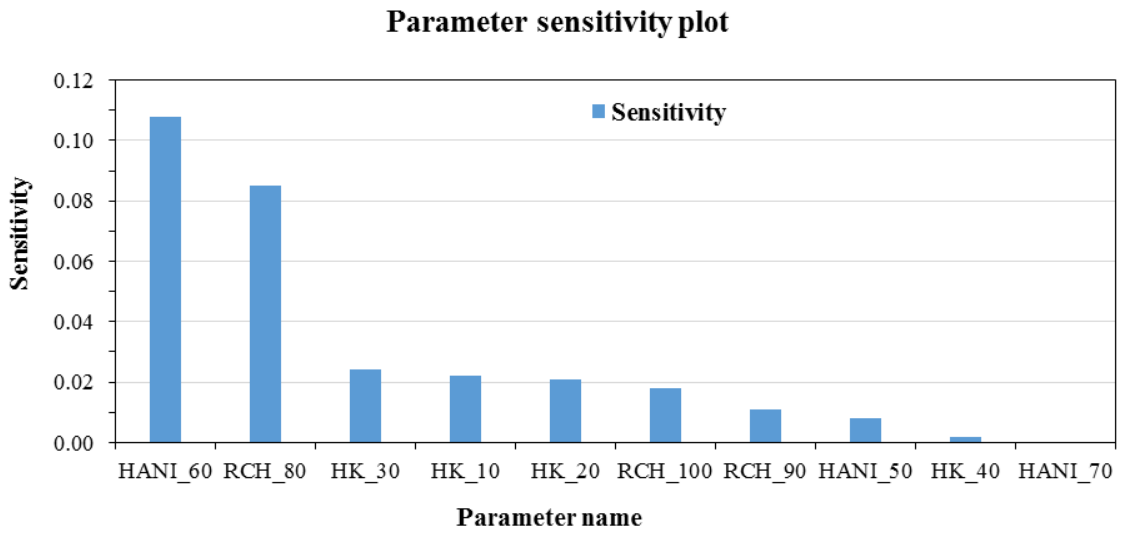

Figure 28: Parameter sensitivity of MODFLOW model to simulated groundwater head and baseflow. Parameter abbreviation are explained in text.

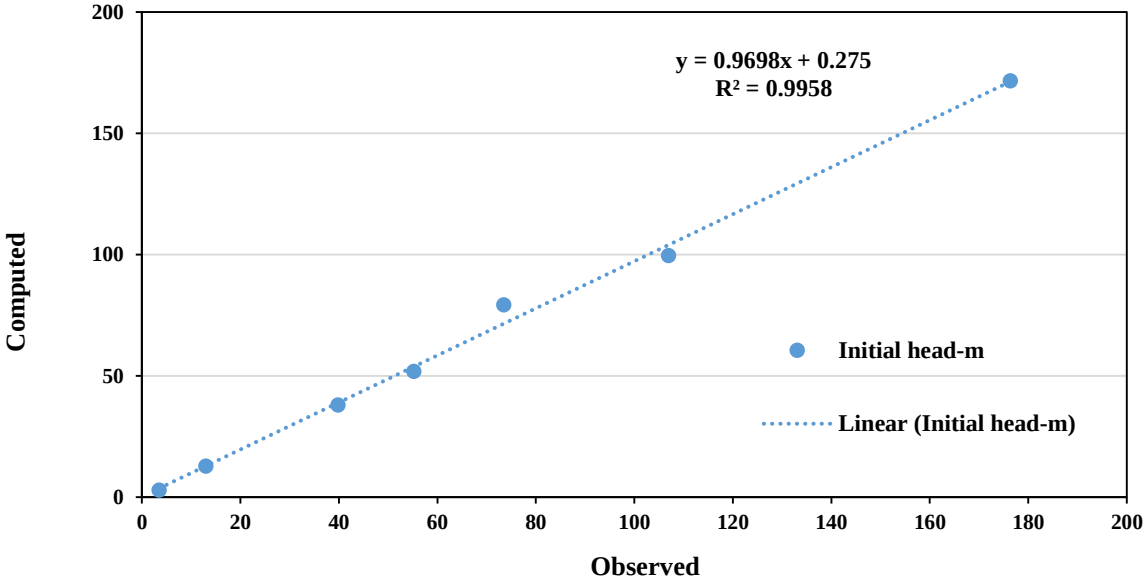

Figure 29: Regression plot for steady state simulation of computed and observed groundwater heads in 7 wells and 2 stream gauging points in the Heeia Watershed.

Table 17: The statistical analysis of the computed and observed groundwater head within MODFLOW model domain.

Observed well name	Initial head-m	Head interval	Standard deviation	Computed head	Residual head
Weather st.	2.98	0.3	0.15	3.46	-0.48
StreamDiversion_piezo	12.79	1.4	0.71	12.95	-0.16
Kaneohe_well_lowland	38.01	3.8	1.94	39.82	-1.81
Kaneohe_well_upland	51.82	6	3.06	55.23	-3.41
Iolekaa_well	79.25	8	4.08	73.49	5.76
Haiku_well	99.58	10	5.10	106.97	-7.39
Haiku_DOT_well	171.6	17	8.67	176.32	-4.72

Table 18: The flow budget of groundwater system under steady state conditions with different scenarios: LU- wetland restoration, CL-climate change, SLR-sea level rise scenarios as described in the text.

Steady state-groundwater flow (m^3/d) budget						
Flow rate	predevelopment	development	Future			
			LU-effect	CL-effect	Combined LU&CL-effects	Combined LU&CL&SLR-effects
Recharge	21694	14628	14336	12727	12434	12434
Baseflow	15205	9900	9617	8058	7780	8007
Pumping Wells	0	1677	1677	1677	1677	1677
SGD, m3/d	6489	3051	3042	2992	2977	2759
SGD, m3/d/m	0.91	0.43	0.43	0.42	0.42	0.39
LU : land use change, CL : climate change, SLR : sea level rise.						

5.3.2 MODFLOW model evaluation under transient conditions

The results of the statistical error analysis of simulated baseflow, illustrated that the model performance was within the generally acceptable criteria under scarcity of data and daily time steps approach (Table 19). Overall, based on the recommended quantitative statistics (NSE, RSR, and PBIAS see description in Table 19), the model simulation can be judged as satisfactory because the average of three criteria are 0.65, 0.59, and 4.28 respectively during the calibration and validation periods (Moriasi, *et al.*, 2007, Ndomba, *et al.*, 2008). The other goodness-of-fit statistics, (r) and MBE widely used to evaluate the hydrologic model performance and to describe the degree of collinearity between simulated and observed data are considered as acceptable values because they are more than 0.5 and close to zero, respectively (ASCE, 1996, Van Liew, *et al.*, 2003). Generally, the graphical comparison of observed and simulated daily baseflow for the Heeia aquifer at the Haiku and the wetland outlets indicated that the MODFLOW model reasonably tracked the trends of the hydrograph (Figure 30). In addition, the model was calibrated based on two years of observed groundwater levels at the Heeia stream diversion piezometer and piezometer of the Heeia weather station within wetland. The green calibration targets next to the different timesteps were used to match computed values the observed values (Figure 31).

Table 19: The statistical results for calibration and validation for the daily baseflow simulation at sequential periods.

Simulation	Station	Period	Time span	NSE	RSR	PBIAS[%]	RMSE[m3/s]	MBE[m3/s]	r
Predevelopment	Haiku	Calibration	1950-1959	0.74	0.51	-1.172	0.01	0.00033	0.86
	Wetland	Calibration	1950-1959	0.62	0.62	2.814	0.01	0.00604	0.81
Postdevelopment	Haiku	Validation	2005-2014	0.56	0.66	-5.228	0.01	-0.00365	0.87
	Wetland	Validation	2005-2014	0.68	0.56	7.928	0.01	0.00614	0.92
NSE = Nash-Sutcliff efficiency; RSR = root mean squared error to observation standard deviation;									
PBIAS = percent bias; RMSE = root mean squared error; r = correlation coefficient; MBE = mean bias error.									

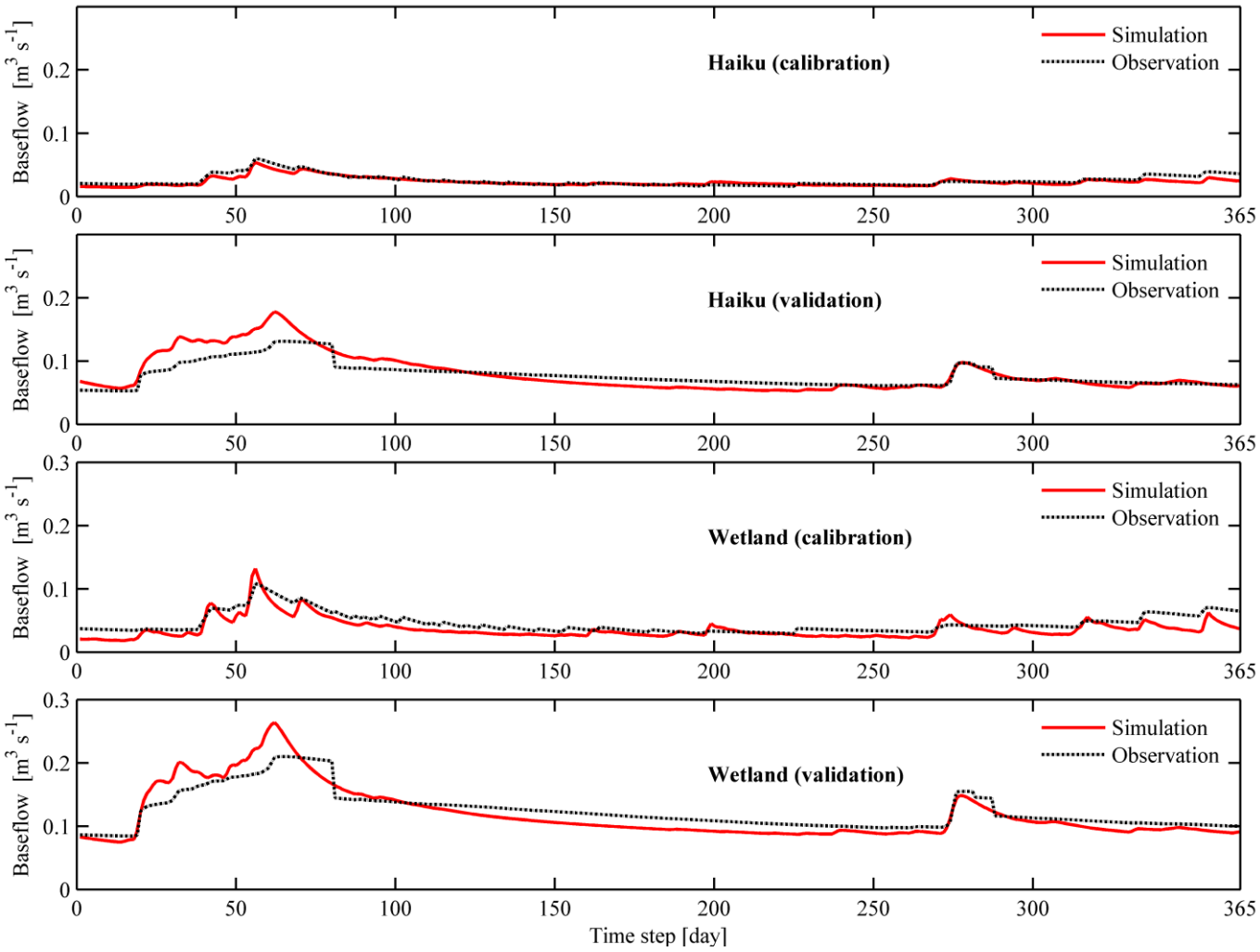

Figure 30: The respective simulated and observed baseflow at Haiku and Wetland stations over one year. The years 1951 and 2006 were used for calibration and for validation, respectively

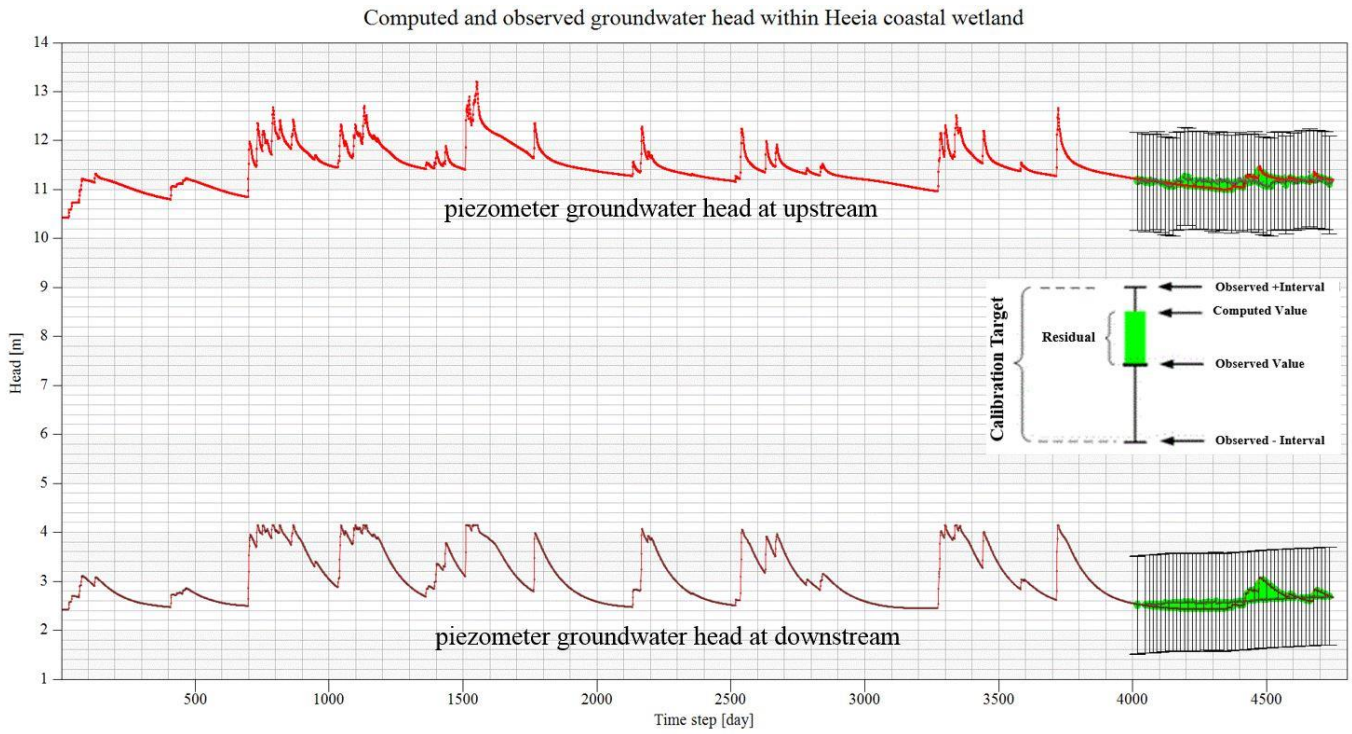

Figure 31: Measured and computed groundwater levels at different timesteps of post development period.

5.3.3 FSGD assessment under different scenarios

The daily FSGD was highly sensitive to sea level rise especially during dry season (Figure 33). Compared to the middle century (SLR=0.4 m), FSGD magnitude will decrease 10% approximately by the end of century when SLR equal 1.1 m, is reached. In contrast, based on the previous research, the recirculated SGD will increase due to increase in sea level rise (Lee, *et al.*, 2013). Another scenario assessed the combined effects of the Heeia Wetland restoration, climate change projection, and sea level rise at the end of century on the FSGD fluxes (Figure 34). The relative negative impacts of wetland restoration, climate change (RCP 8.5) and combined change on FSGD during wet season would be 1%, 9%, and 15%, respectively. In contrast, during dry season the relative changes were 2%, 13%, 46% respectively. The low effect of wetland restoration is most likely related to the low percentage of restored area (7%) of the whole Watershed. It is clear that FSGD experiences the most negative impact value during the dry season. In spite of decreasing FSGD magnitude with time (Figure 35), it still remained responsible for between 1.5 to 3.5 times more the amounts of fresh water delivered to the Kaneohe Bay than by total the Heeia Stream flow (Figure 36). Generally, the flux of FSGD to the coastal ocean especially on the windward side of Oahu Island was expected to be high due to increased

recharge rate, porous basalt with high hydraulic conductivity, and steep seaward hydraulic gradient in shallow unconfined coastal aquifer (Izuka, *et al.*, 1993, Vaksvik, 1935). The findings demonstrated that the FSGD was considered to be important source of freshwater to the coastal shore at the windward side of Oahu, which were consistent with finding of other researchers (Dulai, *et al.*, 2016, Knee, *et al.*, 2016). The decline in FSGD fluxes during the post development period (Figure 35) period are due to anthropogenic effects through increasing demand for freshwater and the likely effect of decreasing recharge rate because of due to climate change impact (Gingerich and Oki, 2000, Timm, *et al.*, 2015). The FSGD fluxes were highly influenced by recharge rate increase (Figure 37) where the linkage is that due to increase causing higher in the groundwater levels, which in turn increase and the respective hydraulic gradient especially in steep topography like the Heeia Watershed, forces the increase of FSGD fluxes (Lau and Mink, 2006, Macdonald, *et al.*, 1983). The average percent of FSGD from rainfall, recharge, and baseflow are about 3%, 11%, and 18% respectively (). In addition, the results illustrated that the FSGD had reasonable correlations ($r^2 \geq 0.5$) with baseflow (Figure 38). On the other hand, FSGD fluxes had significant exponential regression relationship with groundwater head at the Heeia stream diversion piezometer before entering the wetland (Figure 39). The coefficient of determination (R^2) was 95%. This function was demonstrated the strong relationship between groundwater head and FSGD fluxes. The exponential function can be used as approach to estimate FSGD fluxes for temporal scale transient condition depending on the observed head in coastal wetland.

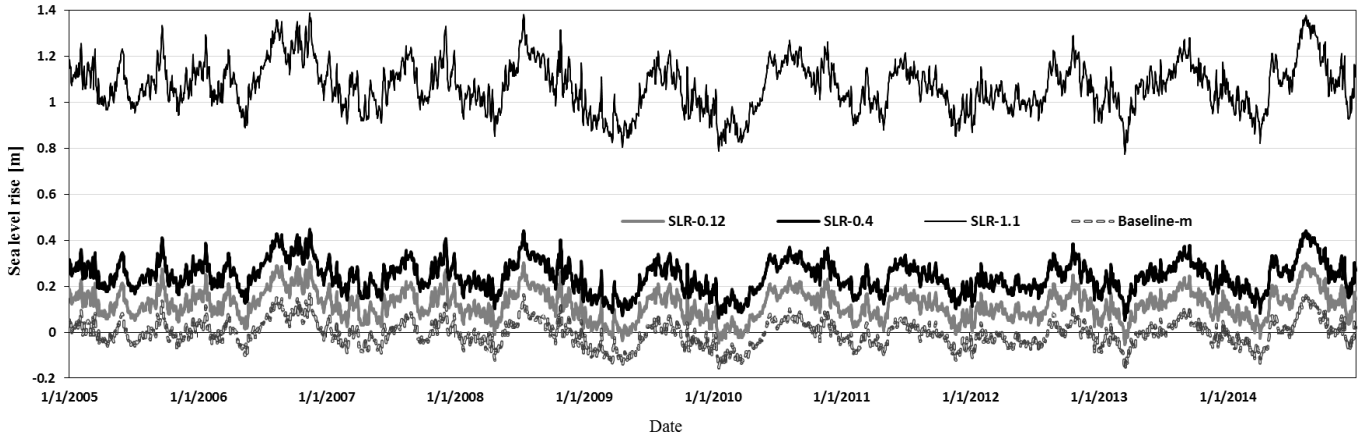

Figure 32: The daily sea level rise scenarios calculated based on RCP 8.5 projected for the Heeia Watershed based on levels observed between 2005 and 2014.

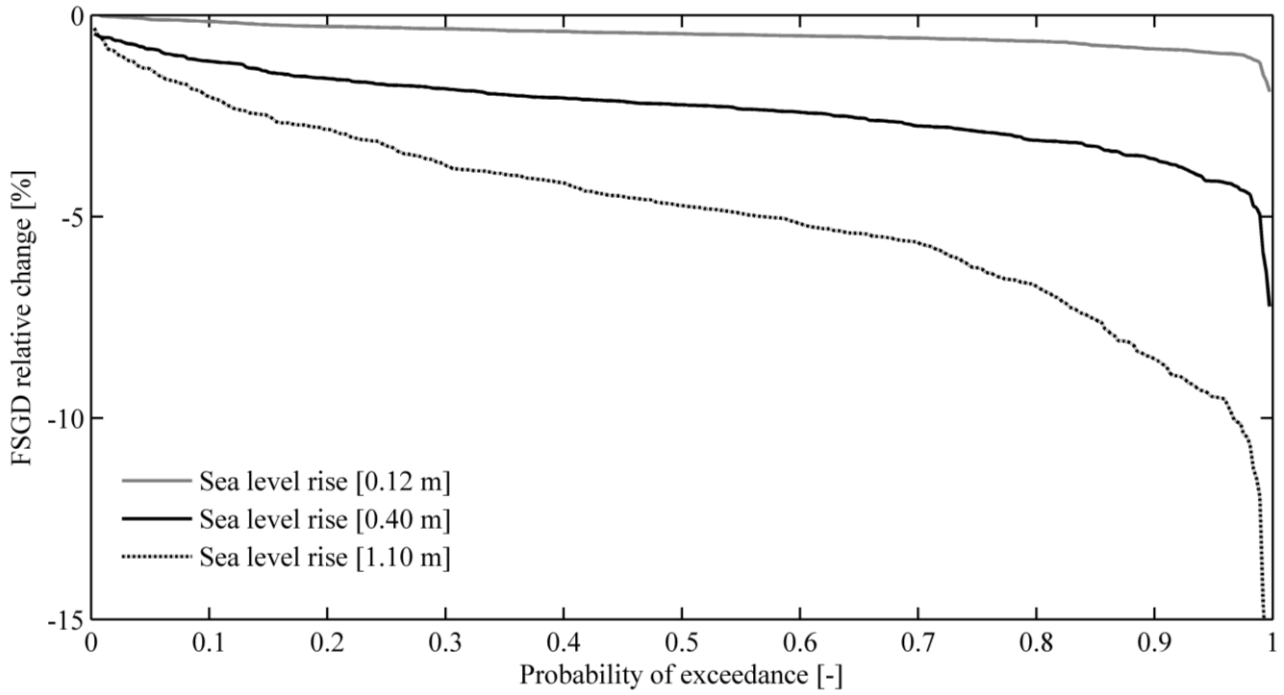

Figure 33: The daily relative percent change in FSGD as a result of sea level rise.

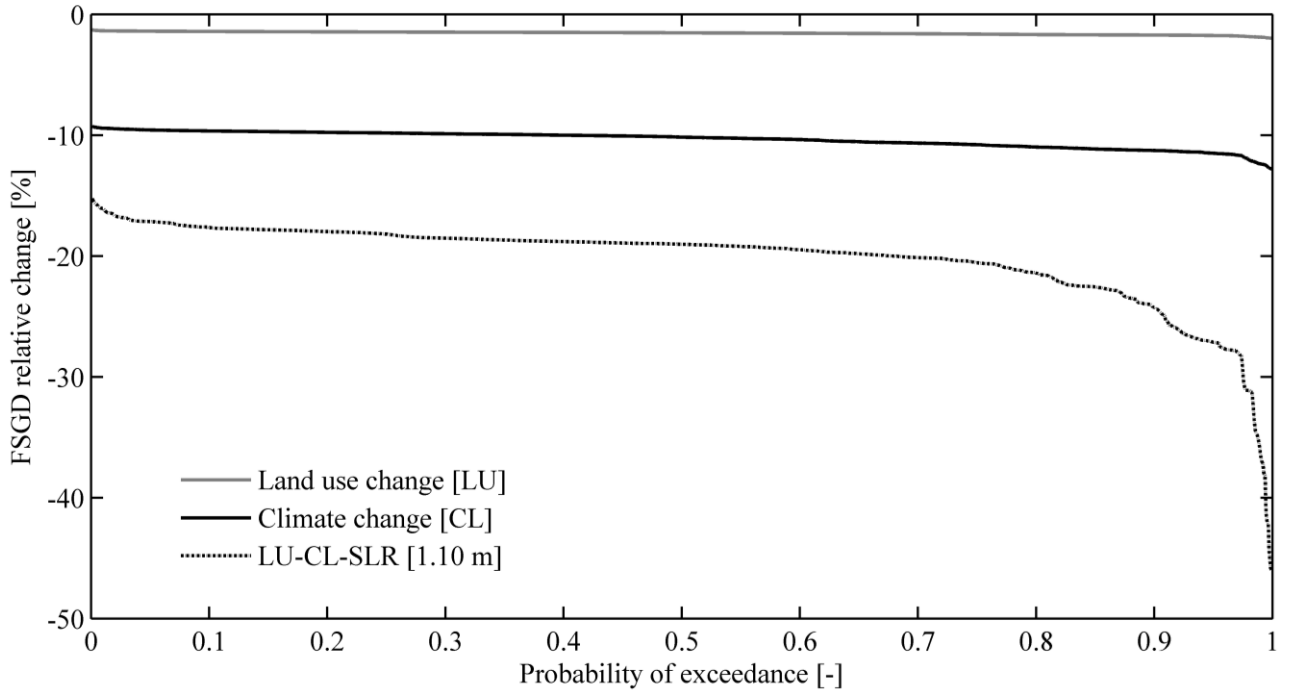

Figure 34: The daily relative percent change in FSGD duration curve under different scenarios of land use change, climate change, and sea level rise.

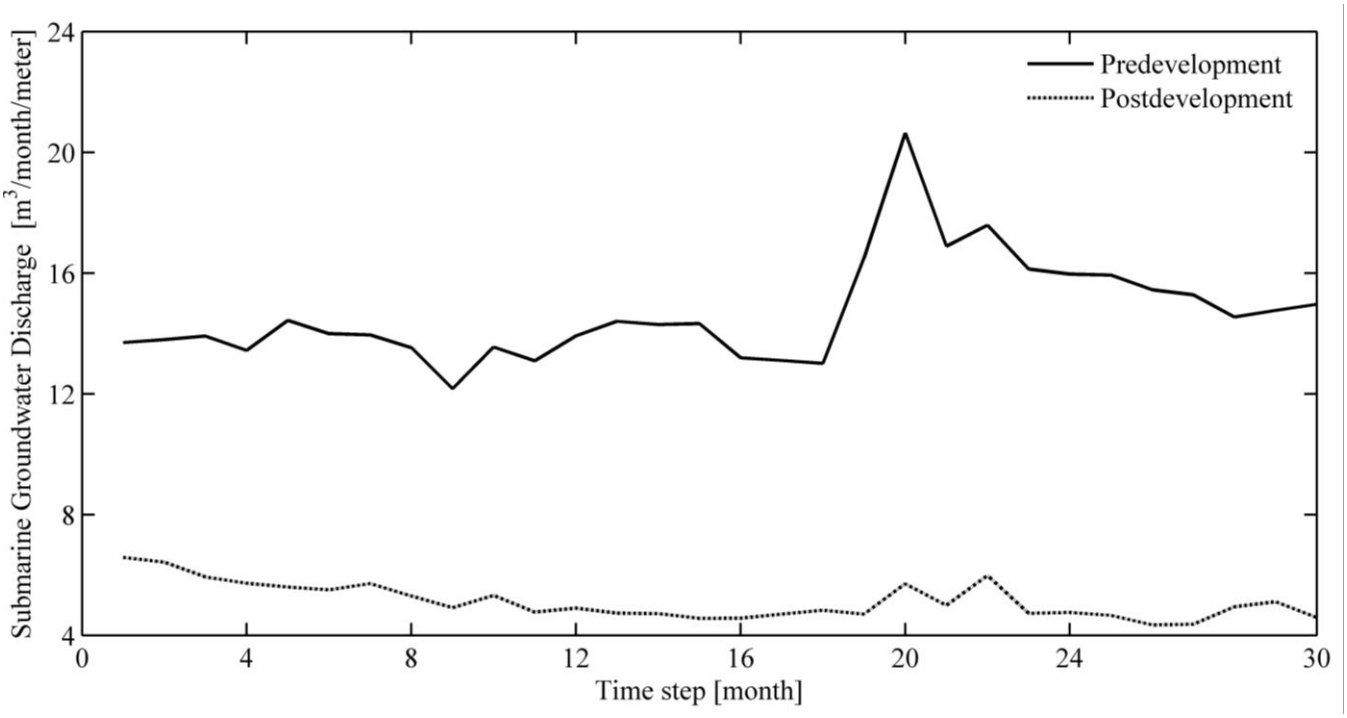

Figure 35: The temporal variability of FSGD across the Heeia Coastal Shoreline (7136 meter).

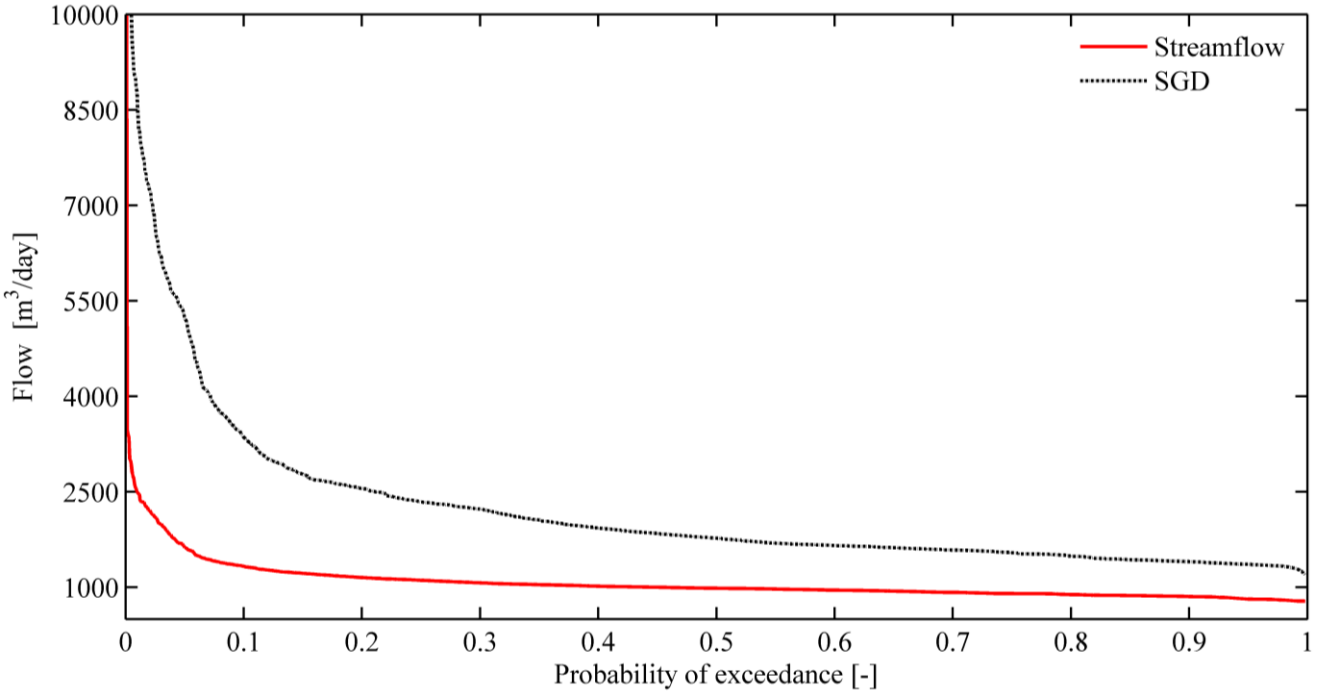

Figure 36: The flow duration curve of FSGD across the Heeia Coastal Shoreline and total the Heeia stream flow estuary.

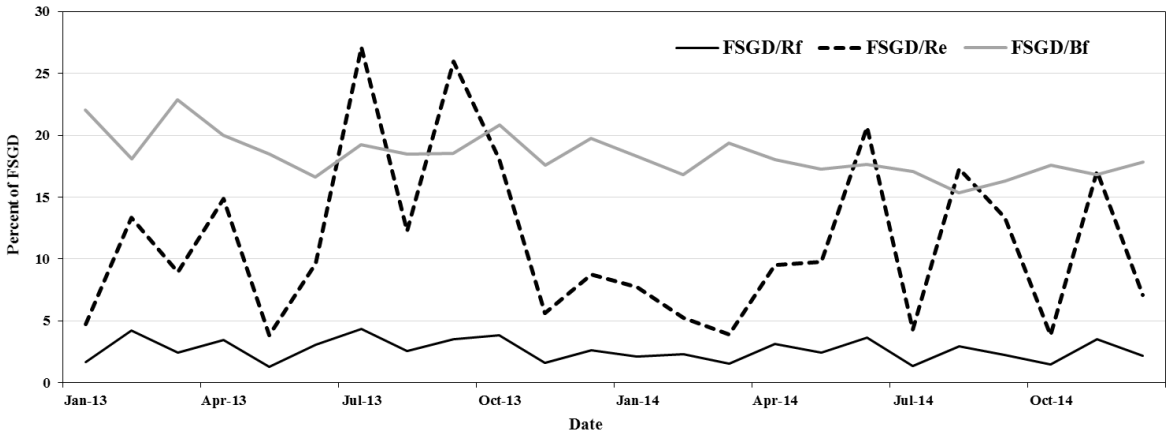

Figure 37: The monthly baseline percent of FSGD from annual average WBCs, rainfall (Rf), recharge (Re), and baseflow (Bf).

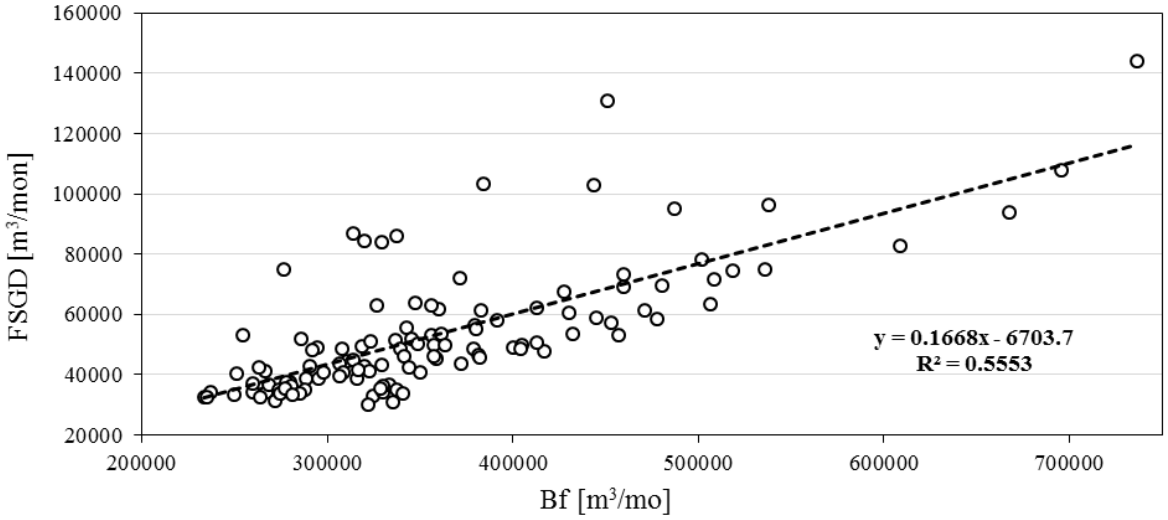

Figure 38: The relationship between monthly groundwater discharge (Bf) and FSGD fluxes across the Heeia Coastal Shoreline.

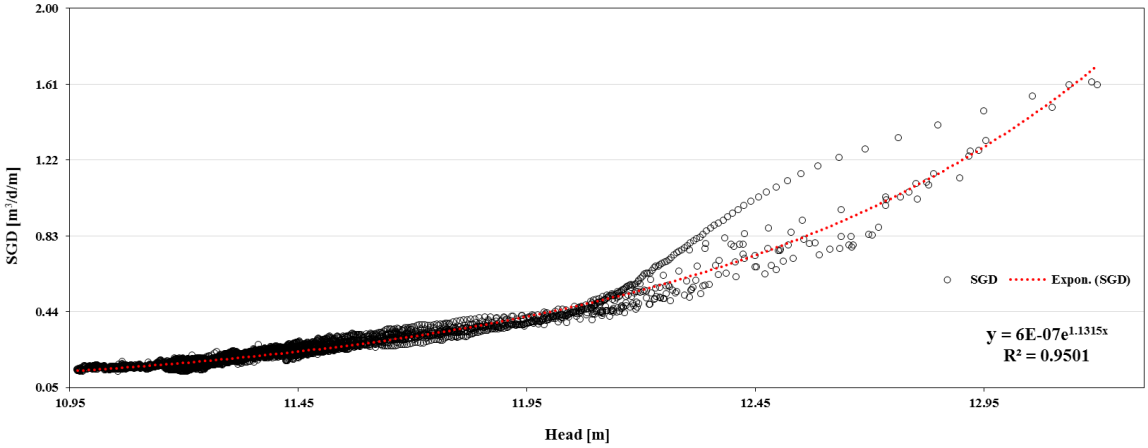

Figure 39: The relationship between coastal groundwater head of coastal aquifer and FSGD fluxes across the Heeia Coastal Shoreline

5.4 Conclusions

Integrated hydrological modeling was used in this study to assess the FSGD fluxes across the Heeia Coastal Shoreline. The calibrated and validated MODFLOW model under transient and steady state conditions with SWAT model outputs for recharge were used as the tools for FSGD assessment. The MODFLOW model was developed to simulate the groundwater system of shallow unconfined aquifer within the Heeia Watershed. The model was calibrated and validated based on filtered baseflow at Haiku stream flow and virtual Wetland stations and measured groundwater head within the Heeia Watershed. The MODFLOW model reasonably represented the groundwater head and discharge of shallow unconfined coastal aquifer with an acceptable performance and satisfactorily statistical evaluation values under hydrological data scarcity. Under steady state conditions, the findings showed that FSGD was significantly influenced by anthropogenic effects, recharge rate, and climate change impact, especially at the end of twenty first century. The average decline in FSGD flux during the post development relative to the predevelopment period, would be about 53% due to considerable decrease in recharge by 33% and increase in groundwater withdrawals. In addition, the average FSGD fluxes will be expected to decrease by 0.3 %, 2 %, and 10 % due to wetland restoration effect, climate change impact, and combined wetland restoration, climate change, and sea level rise (1.1 m) effects, respectively. Under transient conditions, the findings showed that the FSGD was significantly influenced by sea level rise, recharge rate, groundwater head at the coastal aquifer, and climate change impact, especially at the end of the twenty first century. The respective average annual decline in FSGD fluxes during the scenarios of sea level effect, were 0.5%, 2%, and 5% due to increasing the sea level by 0.12 m and 0.4 m for the midcentury and 1.1 m for end century. The average decline in FSGD fluxes during the scenarios of wetland restoration, climate change and combined wetland restoration, climate change, and sea level rise (1.1 m) effects, were 1.6 %, 10 %, and 20 %, respectively.

Finally, the findings suggested that FSGD fluxes during post development were about 1.5 to 3.5 times larger than the fresh water delivered to the Kaneohe Bay via the total Heeia stream flow. Moreover, the FSGD fluxes were significantly influenced by recharge, sea level rise, and groundwater withdrawals during dry season more than wet season. It was found that the percent of FSGD to recharge was low during wet season, but it was high during the dry season due to the low percent of recharge to rainfall ratio especially at the highest exceedance probability. In addition, the findings indicated that FSGD had

reasonable correlations with baseflow. On the other hand, The FSGD had significant exponential relationship with groundwater head for the coastal unconfined aquifer. This relationship could be used as an approach to continuously estimate FSGD from groundwater head with coastal wetland.

Chapter6 Modeling density dependent groundwater flow, dissolved silicate fluxes, and heat transport in Heeia coastal aquifer of Oahu, Hawaii via an integrated hydrological modeling approach.

6.1 Introduction

The Heeia coastal aquifer provides a vital role in determining coastal environmental health. However, yet it is vulnerable because it may have been facing challenges related to seawater intrusion due to inundation of lowland in the coastal zone (Diersch and Kolditz, 2002, Rotzoll, *et al.*, 2010). The density differentials among fresh, brackish, and saline waters at the ocean-aquifer interface is considered to be the deterministic main factor for affecting seawater intrusion and nutrient fluxes into the ocean (Simmons, 2005). Therefore, any change in the hydrostatic equilibrium between at the freshwater-seawater interface invades can force seawater into the coastal unconfined aquifer (Barlow, 2003). For instance, if the groundwater level in the Heeia coastal unconfined aquifer is lowered by one meter, the fresh-saltwater interface will rise by 40 meters according to the Ghyben-Herzberg theory (De Wiest, 1998). The seawater intrusion and inundation of lowland in coastal zone are likely to be further aggravated by future climate change, sea-level rise (SLR), and continued population growth (Luoma and Okkonen, 2014).

Specifically for the study area, due to the presence of lowland in coastal zone, the shallow unconfined aquifer is particularly susceptible to salt water intrusion through inundation process, especially during storms, rising sea level, tsunami, hurricanes, and decline groundwater level (Guha, 2010, Izuka, *et al.*, 1993). In contrast, the hydrogeological upper aquifer setting, characterized by perennial groundwater flow and high level aquifer in dike zone, of the Heeia coastal aquifer has a relatively natural barrier (freshwater lens floating on top of seawater) against seawater intrusion under normal conditions, but the barrier will collapse during storms, tsunami, and sea level rise (Keener, 2013, Takasaki, *et al.*, 1969). On the other hand, the hydrogeological setting of freshwater lens is able to support the Heeia Coastal Shoreline and fishpond by providing cold fresh groundwater, DSi, and other nutrient fluxes, which sustain the normal marine organisms' lifespan and recover the overall coastal environmental health (Dulai, *et al.*, 2016, Libes, 2011, Mink, 1964). Additionally, studies that document by many researchers

mentioned that the FSGD is considered to be as a large main contributor of freshwater and nutrient fluxes across land-ocean interface include (Burnett, *et al.*, 2006, Kelly, *et al.*, 2013, Swarzenski, *et al.*, 2016). For example, in one coastal site of Hawaii, Swarzenski et al. (2013) found that concentration of DSi was 36 times higher in SGD than in ambient seawater (Swarzenski, *et al.*, 2013).

The high concentration of DSi and low salinity provide a clear signal of freshwater discharge across the coastline, especially in the Hawaiian Islands, where groundwater is the main source of DSi as the result of weathering basaltic bed rocks and volcanic ash (Street, *et al.*, 2008, Visher and Mink, 1964). DSi level and distribution within aquifer and its fluxes into the coastal ocean has been getting great attention among researchers, managers, and policymakers, especially who those focusing on the coastal environmental health. DSi has a significant effect on the structural component of marine and terrestrial organisms, and invasive grass uptake (Blecker, *et al.*, 2006, Schopka and Derry, 2012).

The hydrogeological setting of the Heeia aquifer enhances the presence of cold groundwater within the coastal wetland and ocean shoreline, which maintains the suitable temperature for taro growth and decreases the metabolic rate of fish population and marine organisms (Hanna, *et al.*, 2008, Libes, 2011). The mountain regions of Heeia Watershed are considered the source of cold water for coastal wetland and shoreline zones (Mink, 1964). The aerial infrared photo of a groundwater plume that discharges into the shoreline of Oahu Island appeared as a brighter image because the showed a clear FSGD signal because it was colder than ambient seawater (Kelly, *et al.*, 2013, Lau and Mink, 2006). More recently, studies have documented that the shallow groundwater temperatures have been significantly influenced by regional surface air temperatures and shifting in climate change (Menberg, *et al.*, 2014). Therefore, assessing the dynamical pertinent variables processes, such as heat transport, dissolved silicate fluxes, and seawater intrusion across the Heeia coastal aquifer-ocean interface are important aspects for preserving coastal environmental health. An integrated hydrological model approach that consists of a coupled distributed MODFLOW 2000 and MT3DMS in that couples SEAWAT computer program and linked with semi-distributed watershed SWAT model outputs is used. This is considered as a representative estimation of SEAWAT is a three dimensional, variable-density, saturated ground-water flow for simulation of sea water intrusion. It will also be used for assessing DSi and heat transport under temporal and spatial variability conditions. Estimating the species transport across coastal aquifer-ocean interface is very challenging due to the fact that the flow magnitude can vary spatially and temporally,

which in turns depends on the hydrogeological framework, climate variability, human activities, and SLR.

This study aims to assess the density dependent groundwater flow and species transport across the Heeia coastal aquifer-ocean interface under different scenarios of dynamic variables land use and climate changes. This information is needed in order to support the strategic plans for water resources management in this and similar sites in Hawaii. The objectives will be achieved by developing and coupling the above mentioned numerical models.

6.2 Methodology

In order to assess the density dependent groundwater flow and species transport across the Heeia coastal aquifer-ocean interface, the MODFLOW model was first developed for the Heeia coastal zone. The recharge coverage of the study area, which was used as input to MODFLOW, was estimated by the SWAT model (see Chapter 3). The SWAT estimated the recharge under Heeia future wetland restoration, climate change, and a combination of both factors. Additionally, MODFLOW 2000 was run for both steady and transient conditions. The SEAWAT model combines MODFLOW and the solute transport MT3DMS model was initialized to combine with MODFLOW model before initializing SEAWAT model in modeling density dependent flow. In this study. The SEAWAT model was run to assess the salt water intrusion, DSi fluxes, and heat exchanger fluxes into the wetland and coastal ocean under different scenarios of climate change, wetland restoration, and sea level anomalies.

6.2.1 Data and MODFLOW 2000 model set-up

The MODFLOW model described in Chapter 4, was used with the same set up, but the area was clipped to only cover the Heeia close to the coastal zone (Figure 40). The MODFLOW model simulated an area of 3.9 square kilometers, which encompassed the Heeia coastal zone, fishpond, and some a part of the aquifer covered by the Kaneohe Bay. The modeled area was variably discretized into 817 cells of refined grid. The grid size was decreased toward the central and active portion of the model domain and increased toward the model boundary. The grid was rotated 212 degrees to better fit with active coverages of the conceptual model. Three types of boundary conditions were used to specify the groundwater flow paths within model domain, which include specified flux, head-dependent flux, and no flow boundary. The ground surface boundary represented with specified flux. The Kaneohe Bay and

the Heeia fishpond represented with specified head. The Heeia downstream and Wetland simulated as drain with head-dependent boundary conditions. The southern west arc simulated as specified flux boundary, which represented the upland of the Heeia Coastal Wetland The outer model boundary arcs defined as no-flow boundaries based on the simplified assumption, which assumed the groundwater flow divides coincide with major surface water divides and with zero head gradient at no-flow boundary (Robinson, *et al.*, 1997). The Heeia Wetland and downstream were simulated as drains. The Heeia coastal zone was delineated into 9 subbasins by the SWAT model, which represented the polygons of recharge coverage for the MODFLOW model. The estimated daily recharge output of the SWAT model, was used as input for the various MODFLOW transient simulations and validation. In addition, the observed piezometric groundwater heads at the wetland were used for model calibration and validation.

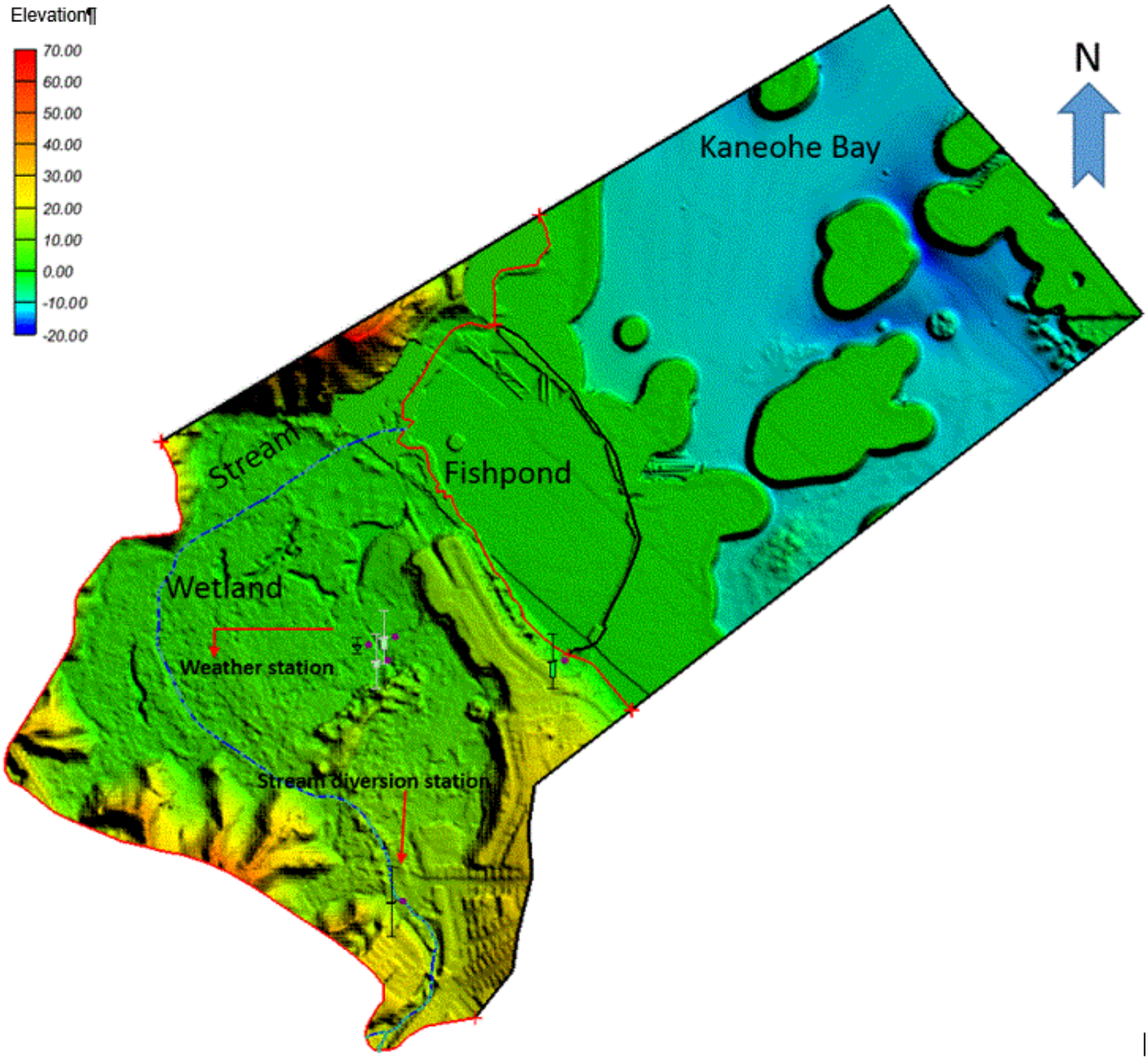

Figure 40: LiDAR digital map of the Heeia coastal zone.

6.2.2 MT3DMS model description and initialization

The MT3DMS Version 5 is a modular three dimensional multispecies transport model. It is able to simulate advection, dispersion, and chemical reaction processes in groundwater systems. It has ability to calculate concentration and mass fluxes at observation location and other active feature objects within

the model domain (Zheng, 2006). The MT3DMS version 5.2 was initialized to combine with MODFLOW before SEAWAT model initialization. The sea water intrusion, DSi, and heat were defined as transported species in groundwater system. The advection, dispersion, and chemical reactions were selected to represent the possible processes that influence the species in the groundwater system. Appropriate time stepping information were set for mass fluxes and concentrations of each solute simulations.

6.2.3 SEAWAT model description and initialization

The SEAWAT model (Figure 41) version 4 computer program is a coupled version of MODFLOW 2000 version 1.18.01 and MT3DMS version 5.2 designed to simulate three dimensional, variable density, saturated groundwater flow, and multi-species transport (Langevin, *et al.*, 2008). It has become a powerful tool to simulate the fluid density as function of the solute concentration and hydraulic head gradient through the dispersion and advection processes. The model has an ability to estimate the sequences of the current seawater intrusion and future behavior under various groundwater management scenarios, which is important for the sustainable qualitative and quantitative management of the groundwater resources in the coastal aquifers (ARIS, 2010, Guha, 2010, Hughes, *et al.*, 2016).

SEAWAT-2000 model was run for a long term simulation under constant boundary conditions for species concentration (salt, DSi, and temperature) until quasi-steady state species concentration were reached (Figure 41). Each final species-concentration distribution for different model layers was assigned as the initial condition for the respective transient variable-density groundwater flow and species transport simulations, which covered the period between from 2012 to 2014. The model also accounted for total dissolved salt (TDS), DSi, and cold groundwater temperature values that ranged, respectively, from 0.1 g/l, 0.024 g/l, and 22 ^{o}C for fresh water at the southern west boundary, to 35 g/l, 0.002 g/l, and 28 ^{o}C for seawater at the northern east boundary, respectively. Such data were compiled base on the initial a survey of the Heeia Watershed and coastal zone (Table 20 and Figure 42). The salinity of recharge is neglected, because of its very small effect, compared to the main source of salinity (seawater intrusion). The model was constructed to assess the seawater intrusion, DSi fluxes, and cold groundwater effects on the coastal shore line and wetland under various scenarios of climate change, land cover, and SLR.

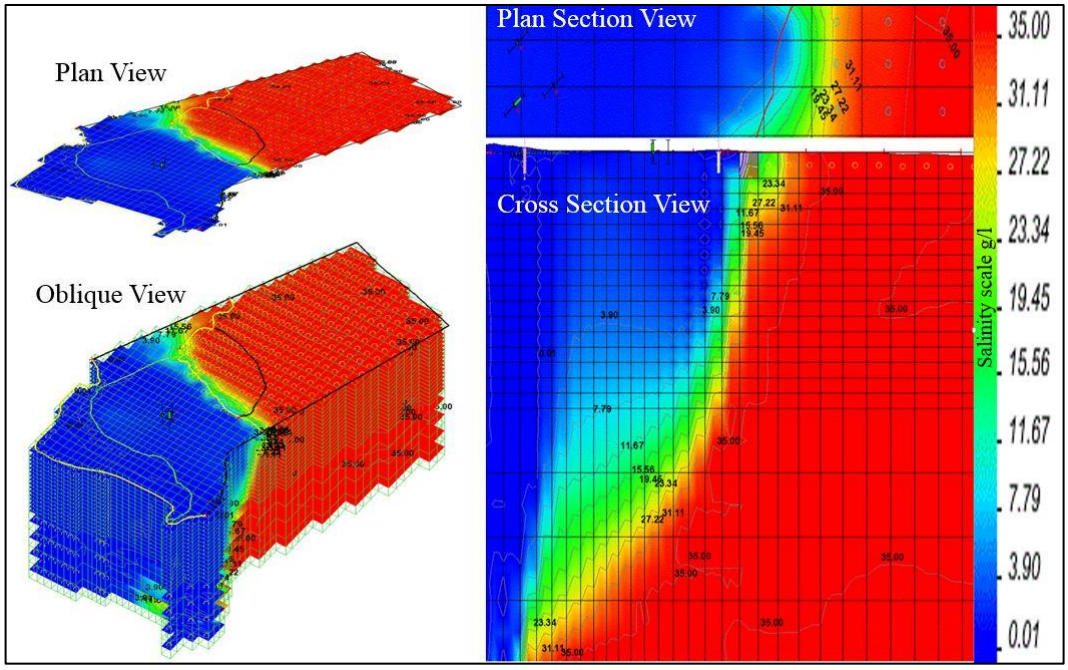

Figure 41: The SEAWAT model construction of fresh-seawater interface in Heeia coastal aquifer.

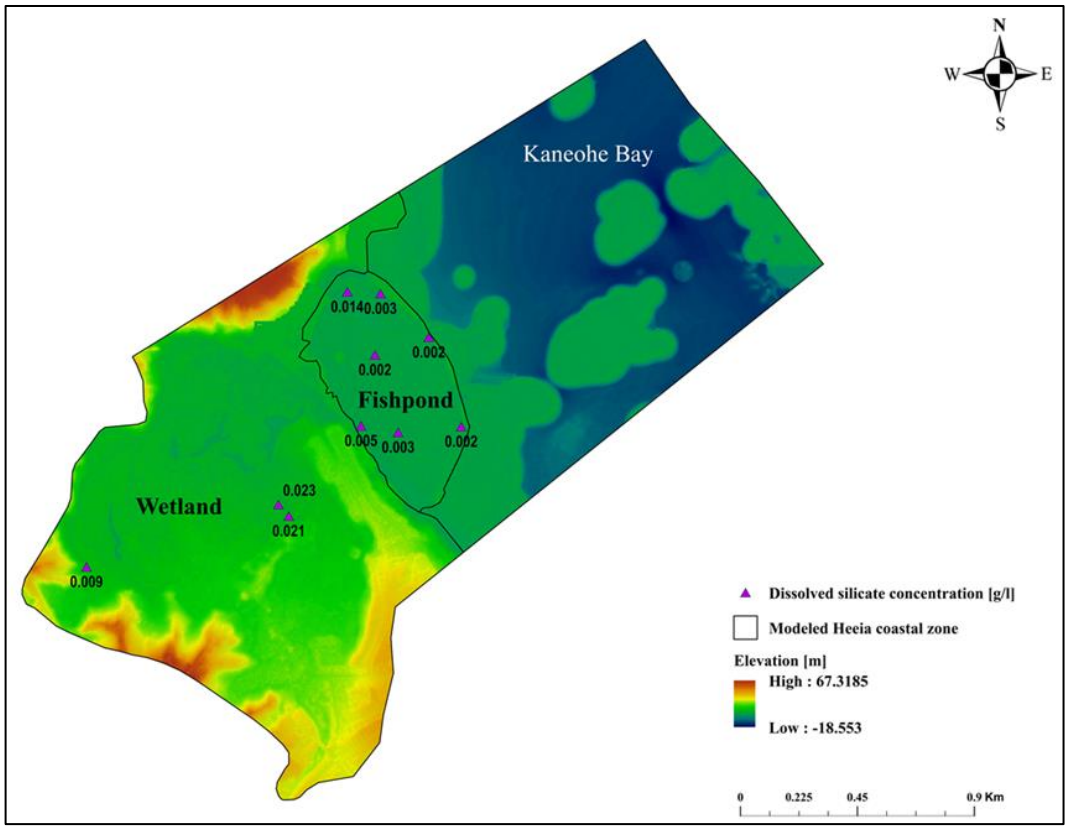

Figure 42: The measured dissolved silicate distribution within the Heeia coastal zone.

Table 20: The initial survey results of simulated species within the Heeia Watershed and coastal zone.

Site name	Location	Coordinates		Concentration [gm/l]		degree [°C]
	symbol	X	Y	Dissolved silicate	Total dissolved salinity	Temperature
Heeia fishpond	L1	623426	2370733	0.005	30	24.65
Heeia fishpond	L2	623268	2371014	0.021	11.5	25.91
Heeia fishpond	L3	623373	2371249	0.014	20.6	25.63
Heeia fishpond	L4	623480	2371006	0.002	32.6	25.48
Heeia fishpond	L5	623569	2370708	0.003	32.2	25.20
Heeia fishpond	L6	623812	2370730	0.002	33.4	24.61
Heeia fishpond	L7	623687	2371074	0.002	32.9	24.70
Heeia fishpond	L8	623501	2371242	0.003	32.4	24.91
Wetland weather station	L9	623108	2370430	0.023	0.22	21.46
Wetland second bridge	L10	623148	2370386	0.021	0.57	22.44
Wetland uphill road	L11	622369	2370190	0.009	0.28	20.74
Heeia stream	L12	621143	2367583	0.012	0.344	18.8
Kapuna_1 springs	L13	622067	2368130	0.051	0.125	21.0
Kapuna_2 springs	L14	622067	2368130	0.063	0.138	21.71
Baskerville surfacewater	L15	622782	2369503	0.044	0.114	20.02
Iolekaa well	L16	621757	2368571	0.058	0.116	21.79
Haiku well	L17	621145	2367581	0.049	0.088	19.32
Haiku tunnel	L18	621145	2367581	0.035	0.08	18.52

6.2.4 Scenarios

6.2.4.1 Salt water intrusion

Because of a growing awareness about the importance of coastal zones, a three dimensional density dependent groundwater model (the developed model SEAWAT) was developed as a predictive and interpretive tool used to investigate the probability that the Heeia coastal zone will be affected by seawater intrusion under various conditions. The calibrated transient simulations of SEAWAT model were satisfactory according to the calibration targets of groundwater head, salt concentration, DSi concentrations, and the daily groundwater temperature records. Following calibration, various scenarios were completed. These had been assessing the effects of SLR by 0.4 m, 1.1 m, and a combined effect of climate change, wetland restoration, and SLR by 1.1 m on the salt distribution at the transition zone. The distribution considered both horizontal and vertical scales based on the wetland restoration impact and climate projections of Hawaii Islands.

6.2.4.2 Dissolved silicate

Globally, DSi [$(SiO_4)^{-4}$] is one of the essential elements of biogeochemical cycles in the coastal zones (Frings, *et al.*, 2016, Libes, 2011). It plays a vital role in the preservation of diverse endangered and endemic diverse organism's structure (Sun, *et al.*, 2007). In Hawaiian Islands, DSi is one of the main products of basaltic rocks weathering, which is an essential element to construct the forms structural components of marine organisms, terrestrial organisms, and many diverse plants (Derry, *et al.*, 2005, Dulai, *et al.*, 2016). Three scenarios will consider the distribution of DSi in the Heeia costal aquifer and the coastal shore of Kaneohe Bay, as well as DSi fluxes under various scenarios of sea levels, climate change and wetland restoration effects. The wetland restoration scenario includes the converting the current California grassland (DSi uptake rate of 8.4 kg/hec) to taro (DSi uptake of 0 kg/hec) and their effects on DSi fluxes and mass balance (Blecker, *et al.*, 2006, Derry, *et al.*, 2005, Guntzer, *et al.*, 2012).

6.2.4.3 Heat transport

Heat transport by groundwater flow involves the combined processes of conduction (heat diffusion) and advection (heat transferred by bulk groundwater flow). Transport and fate of species, including heat, is mainly controlled by head gradient as it controls various physical and chemical processes. Under density dependent flow conditions, the species concentrations, or temperatures, affect the hydraulic head

as well. Densities affect values of hydraulic parameters (e.g., conductivity) and physical transport parameters (e.g., the dispersion and molecular coefficients).

Specifically in the Heeia coastal zone, simulations were done under an initial average ocean water temperature (28 °C) representing the warm seawater, while the fresh groundwater within coastal shallow aquifer representing the source of cold fresh water (22°C). This natural setting has a positive effect on the taro cultivation within coastal wetland, preventing seawater encroachment, and decreasing the metabolic rate of some kinds of fish and other marine organisms. The coldest groundwater is concentrated in the mountain zones due to low temperature, high recharge, and high level of groundwater, which is impounded by geological dike barriers (Mink, 1964). Groundwater temperature is generally close to the average air temperature above the land surface within a narrow range of variation year-round (Figure 43).

For heat transport simulation by the SEAWAT model analyses, three simulations were done. The first simulation was used to examine the case with no temperature effects, where the seawater density is only a function of salinity under thermal equilibrium conditions (no temperature effect). The second simulation (temperature effect) was aimed at investigating the effect of cold groundwater discharge on seawater density due to heat energy reduction during warmer sea water-cold groundwater interface. The analysis utilized an assumed a linear regression inverse relationship of slope about (-0.375). The third simulation was focused on the heat conduction, heat sorption by solid phase, and heat retardation due to taro cultivation where heat transfer between warm water of taro ponding and cold groundwater. The SEAWAT model by adding a chemical reaction was utilized in this analysis. The simulation was conducted by assigning a value of 0.00017 for the thermal distribution coefficient (slope of the linear isotherm) to make set the value of the retardation factor about (2). The thermal energy reduction (kilojoule per cubic meter of groundwater flow) was calculated according to the Fourier's Law of heat fluxes calculation by using thermal conductivity of (0.58 w/m.^{0}K) for fresh groundwater. The thermal energy reduction (Kj/day) divided by groundwater discharge at the southern west or northern east model boundary to obtain the thermal energy reduction (Kj) per on cubic meter of groundwater discharge (Langevin, 2009).

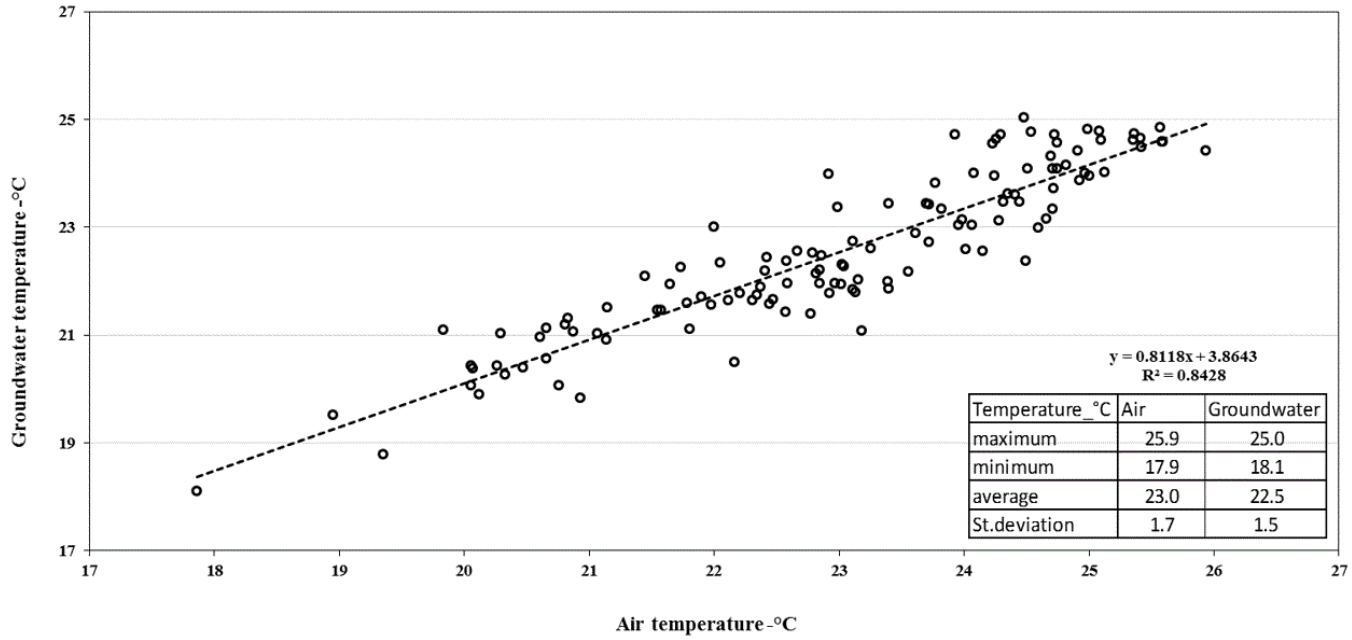

Figure 43: Regression plot between air temperature above earth surface and groundwater of the Heeia weather station.

6.3 Results and discussion

6.3.1.1 SEAWAT results

The model was manually calibrated by using a calibration target approach and adjusting the sensitive parameters, through a trial-and-error approach until an acceptable match between observed and computed outputs was achieved. Table 21, includes the calibrated parameters of the transient analysis. Figure 44 illustrated the matching between the observed and computed head within the Heeia coastal aquifer. Figure 45 represented the significant correlation between observed groundwater head and the computed head by SEAWAT model. Figure 46 indicated the observed and computed salinity of groundwater within coastal aquifer. Although observed values showed salinity fluctuation, the computed salinity values did not reflect such characteristics. This was likely due to less variability in density value within freshwater aquifer. Similarly, the computed temperature showed constant value while observed values indicated noticeable fluctuation.

Table 21: The calibrated parameters of the transient condition of SEAWAT model.

Name	Color/Pattern	Transparency (%)	Horizontal k (m/d)	Vertical k (m/d)	Horiz. anisotropy	Vert. anisotropy (Kh/Kv)	Specific storage (1/m)	Specific yield	Long. disp.	Porosity
Koolau Basalt		70.0	0.0002	0.1	20.938714	0.51624705	0.0000107	0.071	40.0	0.1
Aluuvium		70.0	0.0125	0.1	20.938714	0.51624705	0.0000152	0.05	40.0	0.15
Older Aluuvium		70.0	0.0119	0.1	20.938714	0.51624705	0.0000152	0.04	40.0	0.15
Honolulu Volcanics		70.0	0.0022	0.1	20.938714	0.51624705	0.0000107	0.031	40.0	0.1
Complex		70.0	0.0016	0.1	1.0	0.0016	0.0000305	0.035	40.0	0.05

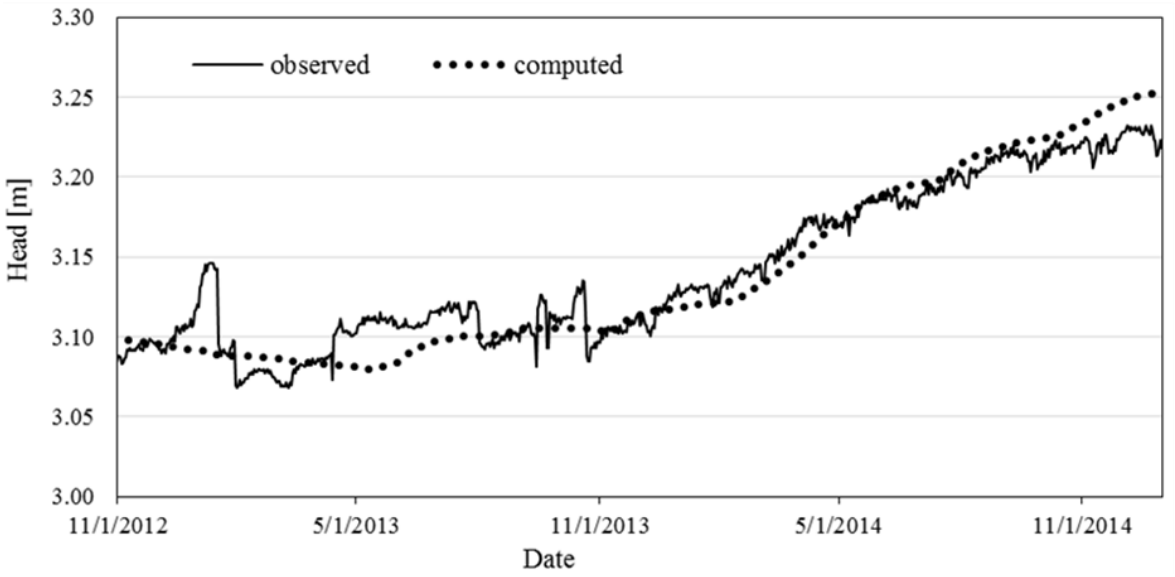

Figure 44: The observed and computed head of weather station piezometer (Schlumberger levelogger sensor).

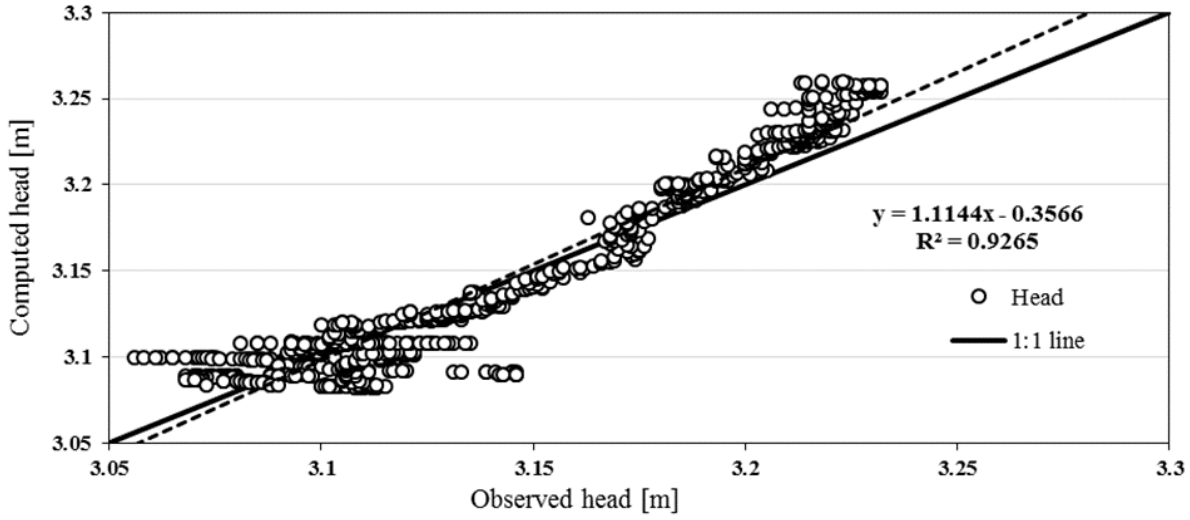

Figure 45: The observed and computed groundwater head of weather station piezometer (Solinst levelogger sensor).

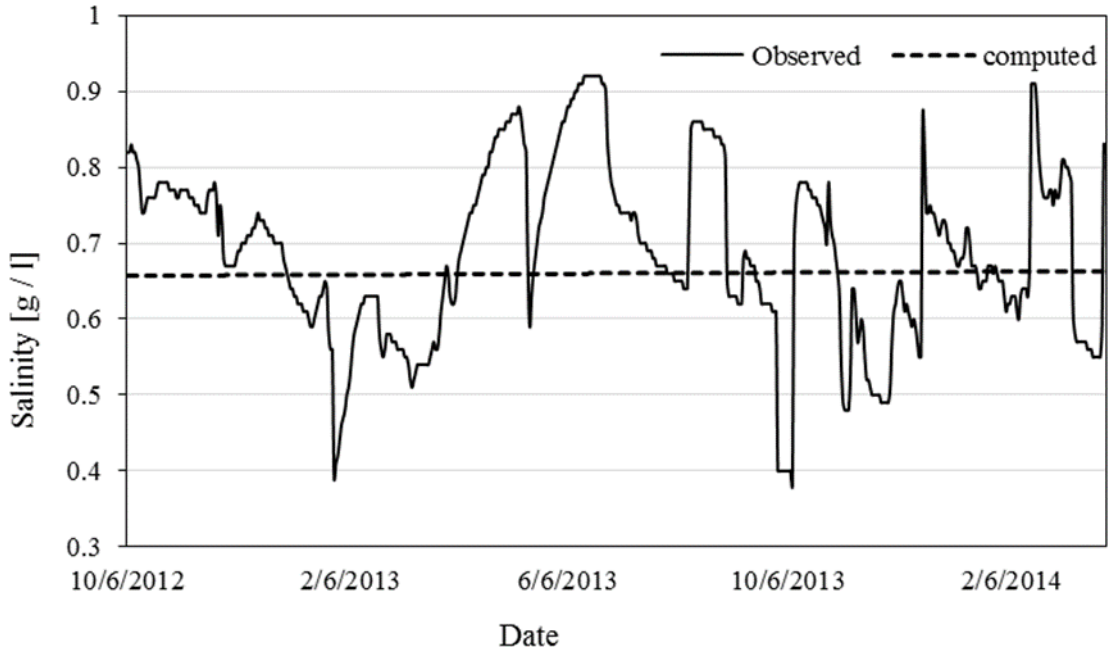

Figure 46: The observed and computed groundwater salinity of weather station piezometer (Solinst levelogger sensor).

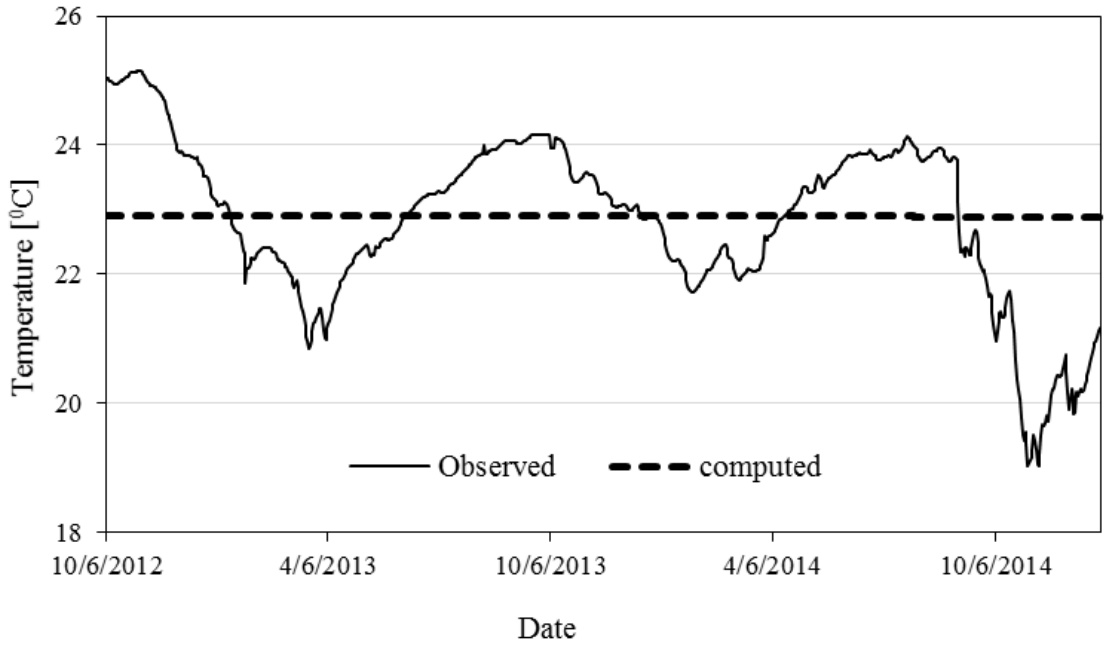

Figure 47: The observed and computed groundwater temperature of weather station piezometer (Solinst levelogger sensor)

6.3.1.2 Seawater intrusion

The seawater intrusion was examined at the Wetland and the coastal line under the effects of the wetland restoration (LU), climate change (CL), and sea level rise (SLR). Based on these factors, two scenarios were formulated as follow:

a. The first scenario assessed the combined effects of LU and CL. Hereafter, it is called CLLU.
b. The second scenario, examined the effects of SRL by increasing the current values by 0.4 m (0.4SRL) for mid 21st century and by 1.1 m (1.1SRL) for the late 21st century.

The results of salt intrusion within the Wetland, calculated for three dimensional case, indicated that the daily change of total dissolved salt (TDS) mass would be increased by a factor of 20 when the sea level is risen by 1.1 m compared with 0.4 m. However, while it is expected to be increased by 229 times when the sea level is risen by 1.1 m as compared to the CLLU scenario, the relative change would be less than 1% compared to the baseline (Figure 48). The monthly change in TDS mass per meter along the shoreline indicated that the values would be increased by about 1.4 and 19 times more than under 0.4SLR and CLLU scenarios, respectively. However, the change relative to the baseline still less than 1% (Figure 49). Similar results were found for the daily change in TDS under 50% probability of exceedance (Figure 50). The findings indicated that the sea level rise and climate-wetland restoration changes would not significantly impact seawater intrusion in the Heeia coastal zone. This could be expected due to the hydrogeological setting of Heeia coastal aquifer, including the steep slope of groundwater levels and the high land elevation at the fresh groundwater-seawater interface (Barlow, 2003, Chang, *et al.*, 2011).

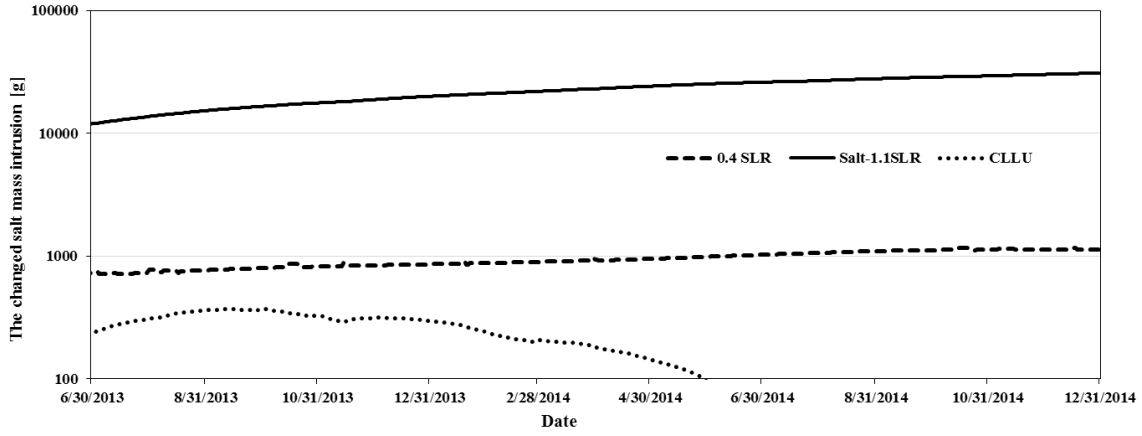

Figure 48: The semi-log plot of the daily changed in salt mass intrusion relative to the baseline into the restored wetland under sea level rise, combine wetland restoration and climate change impacts scenario.

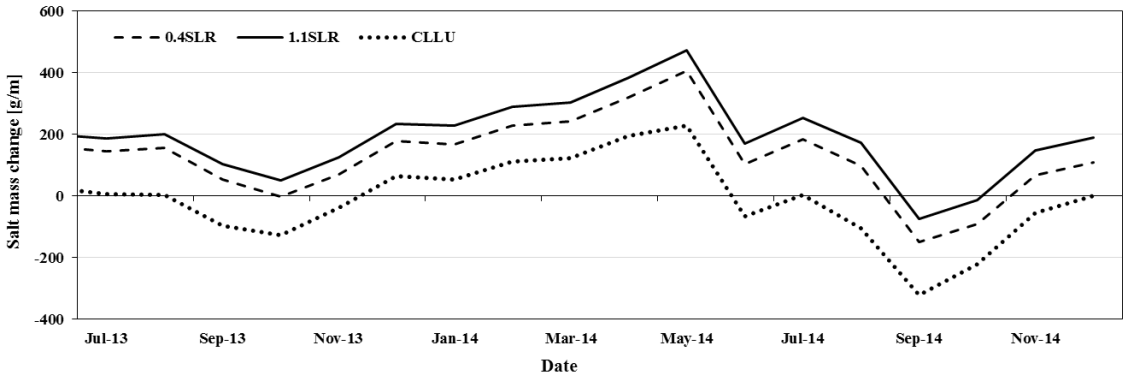

Figure 49: The monthly change in salt mass relative to the baseline in each meter of coastal line under various scenarios.

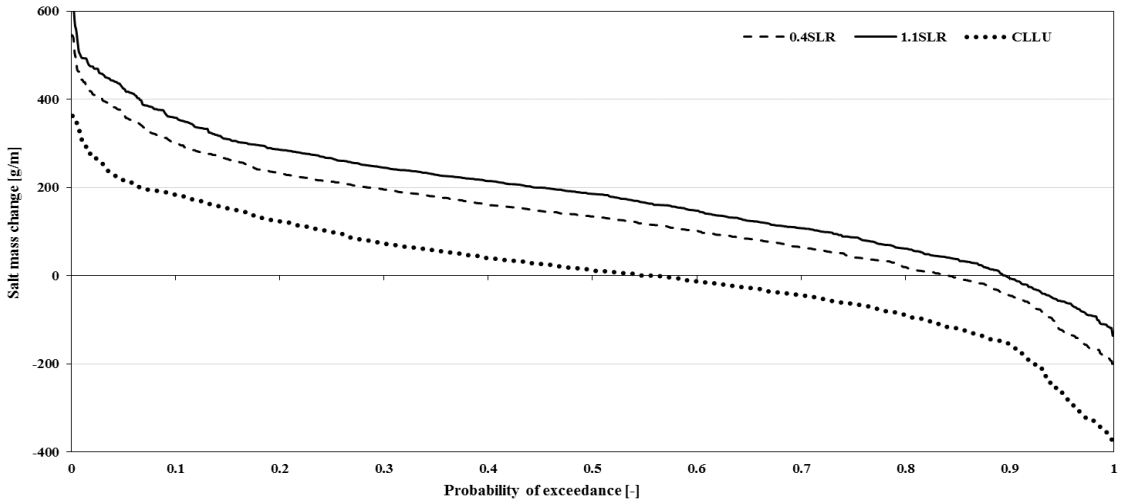

Figure 50: The daily relative change in salt mass duration curve per meter of coastal line under different scenarios of land use change, climate change, and sea level rise.

6.3.1.3 Dissolved silicate fluxes

Estimating DSi is very challenging due to the fact that the nutrient fluxes magnitude can vary spatially and temporally, which in turn depends on the groundwater flow as the main source of DSi. In Hawaii, the main sources of DSi are the weathering products of basaltic rock and volcanic ashes. The SEAWAT models were constructed to estimate DSi fluxes under different scenarios that consist of the land cover change, climate change, and SLR (Figure 51). The model calibration could be judged as satisfactory as reflected by high coefficient of determination value (0.99). Also, the observed and computed DSi showed good agreement (Figure 52). The results illustrated that the average DSi flux was about 48 mole per day and increased by 15% during the wet season but decreased by 16% during the dry season due to the temporal variation of FSGD (Figure 53). An important note is that the climate change has more negative effect on reducing the DSi fluxes than SLR, resulting in a more decrease in FSGD by 5% compare to the 1.1 meter sea level rise (Figure 54). The daily decreases in DSi fluxes across the coastal line relative to the baseline (grassland) were 0.3%, 2.6%, 8.5, and 16.3 % as a result of SLR by 0.4 m and 1.1 m, climate change (CL), and their combined effect of the latter two with taro land cover change (CLLU1.1SLR), respectively (Figure 54 and Table 22). On the other hand, the conversion of california grassland into taro showed an increase in the DSi magnitude of 1.7%, which is due to decrease in the uptake of DSi by taro land cover.

The decrease in DSi fluxes under SLR and climate change had a positive effect on the accumulative storage of DSi within the coastal wetland (Figure 55). The reduction in DSi storage within delineated wetland due to climate change impact would be 4% less than the impact of sea level rise (1.1m). This is partly because of decrease in recharge and specified fluxes by 15% according to climate projection at the end of 21 century and the effect of land cover change (Knee and Paytan, 2011).

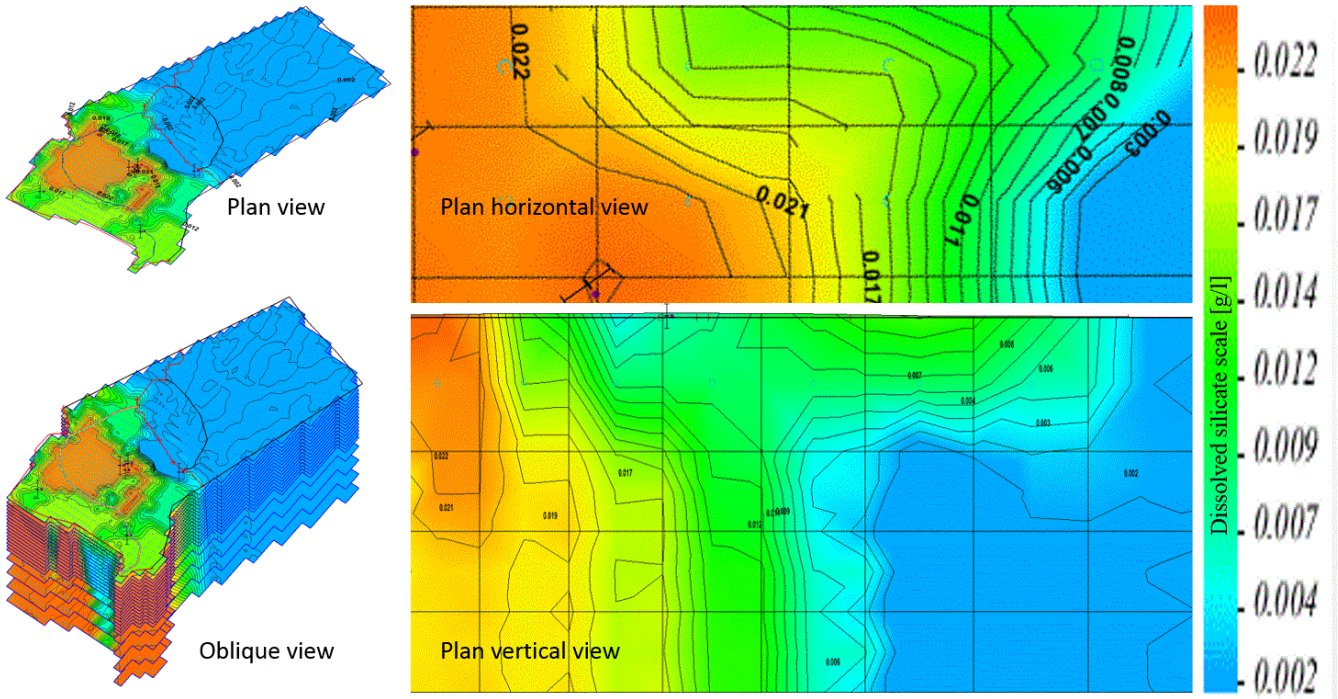

Figure 51: The dissolved silicate simulation of the Heeia coastal zone by SEAWAT model.

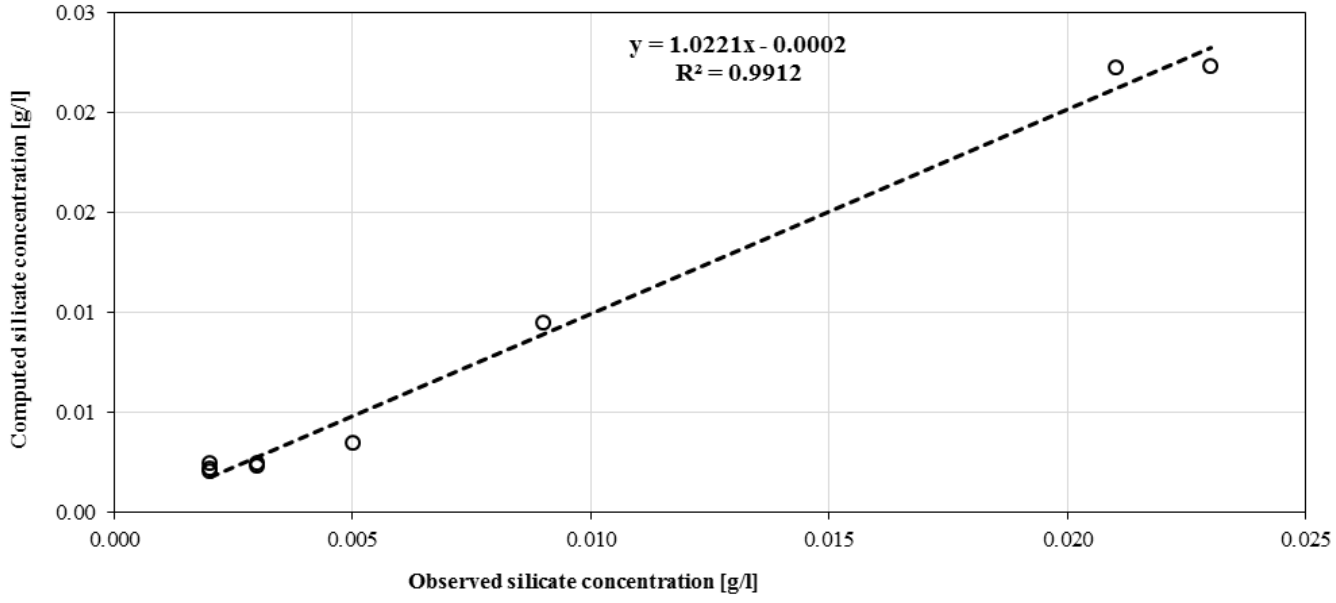

Figure 52: Regression plot for dissolved silicate concentration simulation.

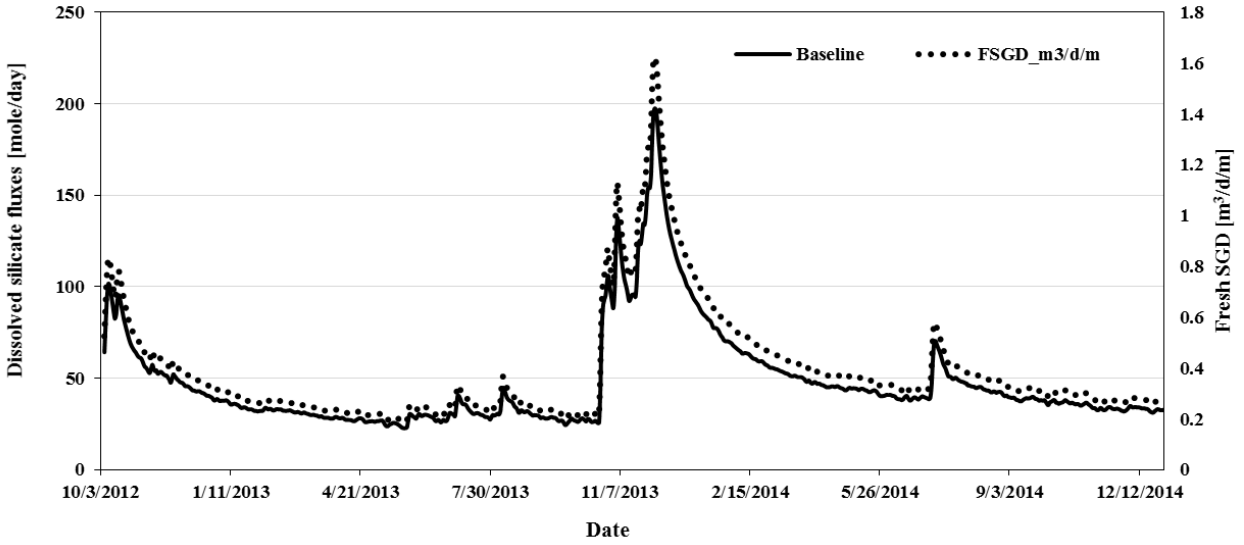

Figure 53: The daily estimated dissolved silicate fluxes across the Heeia coastal shore line.

Table 22: The statistical criteria of the daily dissolved silicate fluxes [mole/day] under different scenarios of land cover change, climate change, sea level rise, and combined effect.

Scenario	maximum	minimum	average	St.dev	% change
California grass (baseline)	194.2	22.3	47.6	27.7	……
taro land cover (LU)	197.4	22.7	48.5	28.2	1.7
Sealevel rise (0.4SLR)	193.7	22.3	47.6	27.7	-0.3
Sea level rise (1.1SLR)	189.1	21.8	46.5	27.1	-2.6
Climate change (CL)	177.7	20.4	43.6	25.4	-8.5
Combined effect CLLU1.1SLR	158.3	18.1	38.8	22.6	-16.3

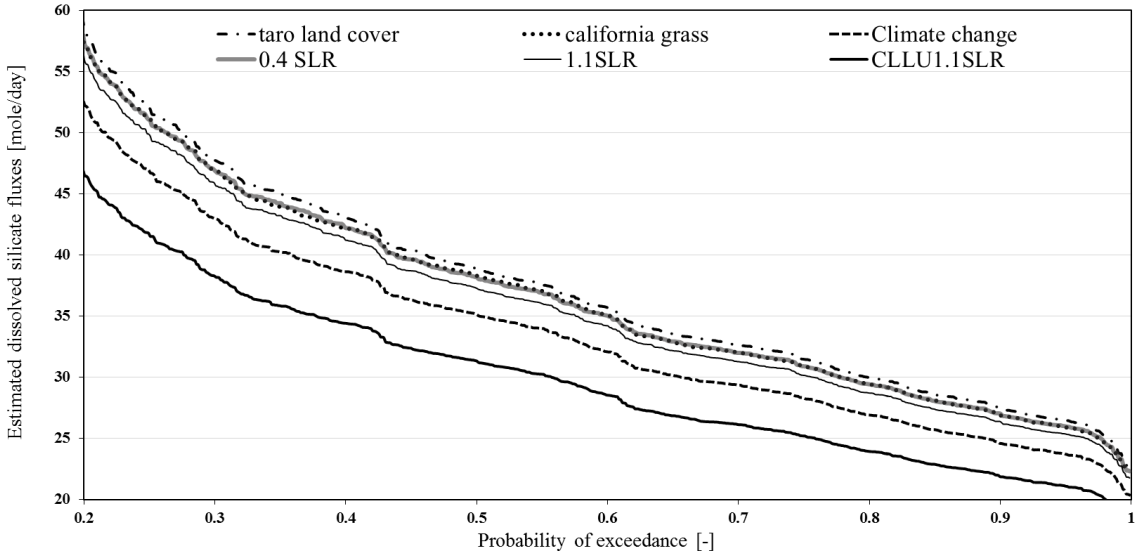

Figure 54: The daily dissolved silicate fluxes duration curve for different scenarios of land use change, climate change, and sea level rise.

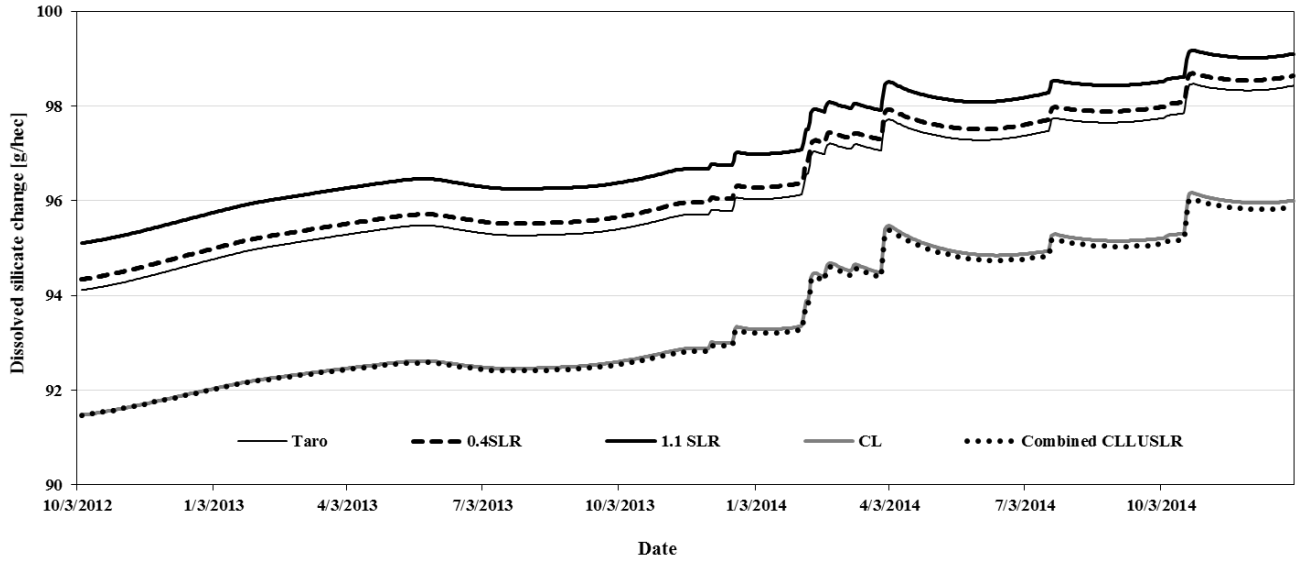

Figure 55: The daily changed dissolved silicate relative to the baseline (grassland) within taro patches under various scenarios.

6.3.1.4 Heat transport

The results indicated that the groundwater temperature was influenced by land cover type (Figure 56). The measured average groundwater temperature under taro cultivation was 1 ^{o}C more than under california grass. The SEAWAT simulations indicated that there was a thermal (hydraulic) gradient at the land-ocean interface both horizontally and vertically (Figure 58), which is likely due to the incoming coldest groundwater flow from the mountain zones (Mink, 1964, Peterson, *et al.*, 2009). The continuous temperature records, salinity, density, and piezometric groundwater head within the Heeia coastal zone indicated that there was a significant relationship among these variables (Figure 60, Figure 61, and Figure 61). In this study, two criteria were used to evaluate the effect of cold groundwater on the ecosystems of the Heeia coastal zone, salinity distribution and heat energy fluxes. The results indicated that the cold groundwater reduced the salinity by 3.5% within a transitional zone of 30 meters width and 380 meters vertically depth (Figure 61 and Figure 62). For the criteria of heat fluxes, the evaluation focused on the heat exchanger at the southern west boundary of wetland (inflow groundwater discharge) and the northern east boundary (outflow of FSGD). The results illustrated that the heat energy reduction at inflow groundwater (kilojoule per cubic meter of groundwater flow) were 0.81, 1.12 under california grassland and Taro cultivation respectively. The average heat energy reduction at outflow groundwater (coastal shoreline) was 4.69, 3.13 under california grassland and taro cultivation respectively of outflow (Figure 63 and Figure 64). The heat energy reduction was a function of groundwater temperature

variation and land cover type. In addition, the average reduction in wet season was more than 15% compared to the dry season due to increase groundwater fluxes, which in turn increased heat energy reduction (Figure 63).

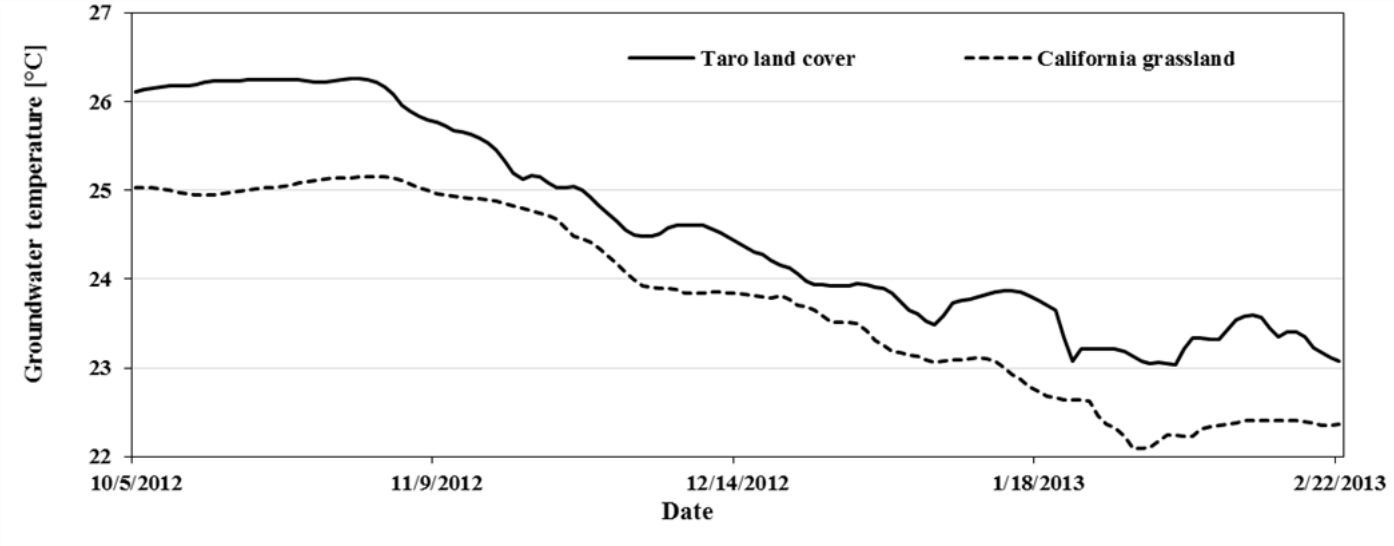

Figure 56: The daily observed groundwater temperature under different land cover.

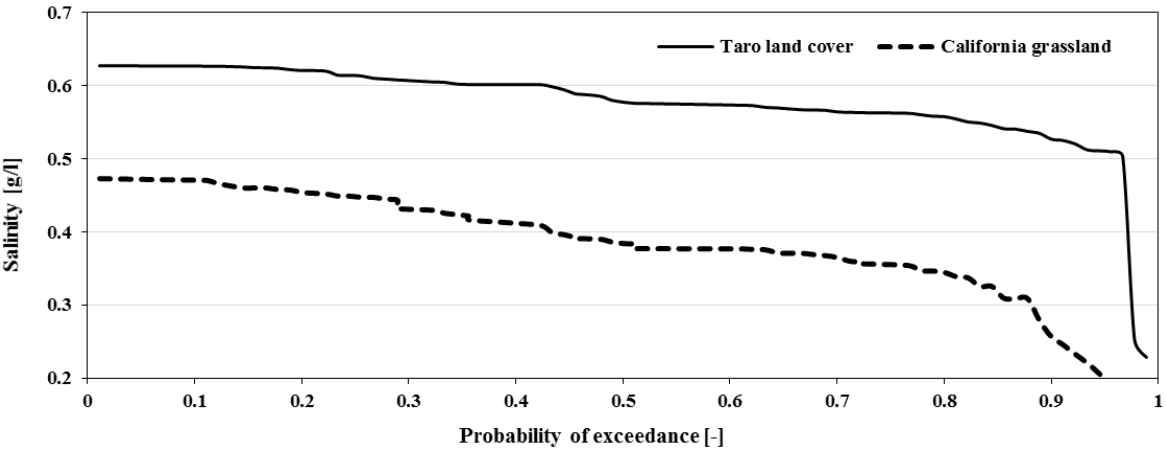

Figure 57: The daily salinity duration curve under different land cover.

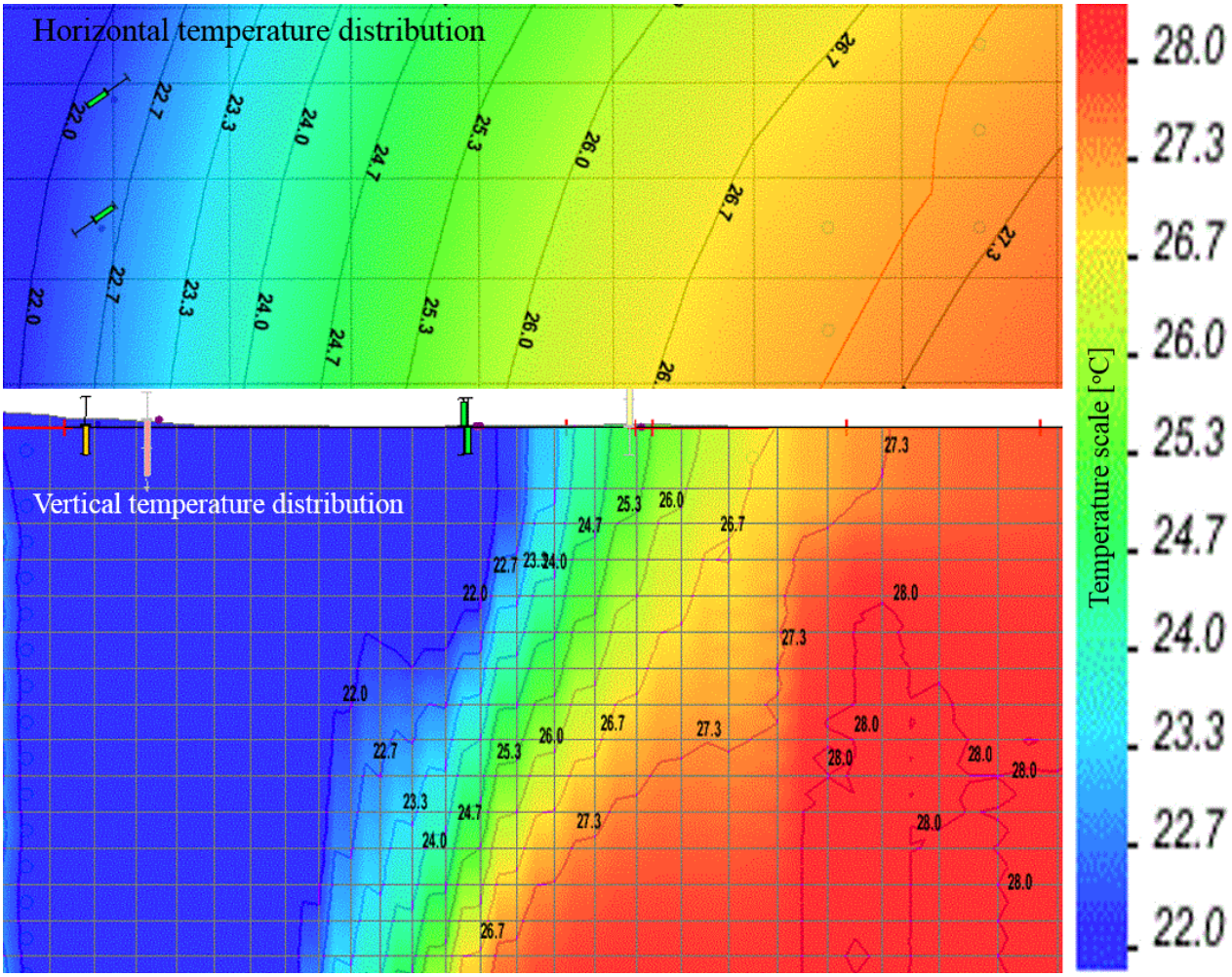

Figure 58: The temperature of groundwater and sea water distribution within the Heeia coastal zone.

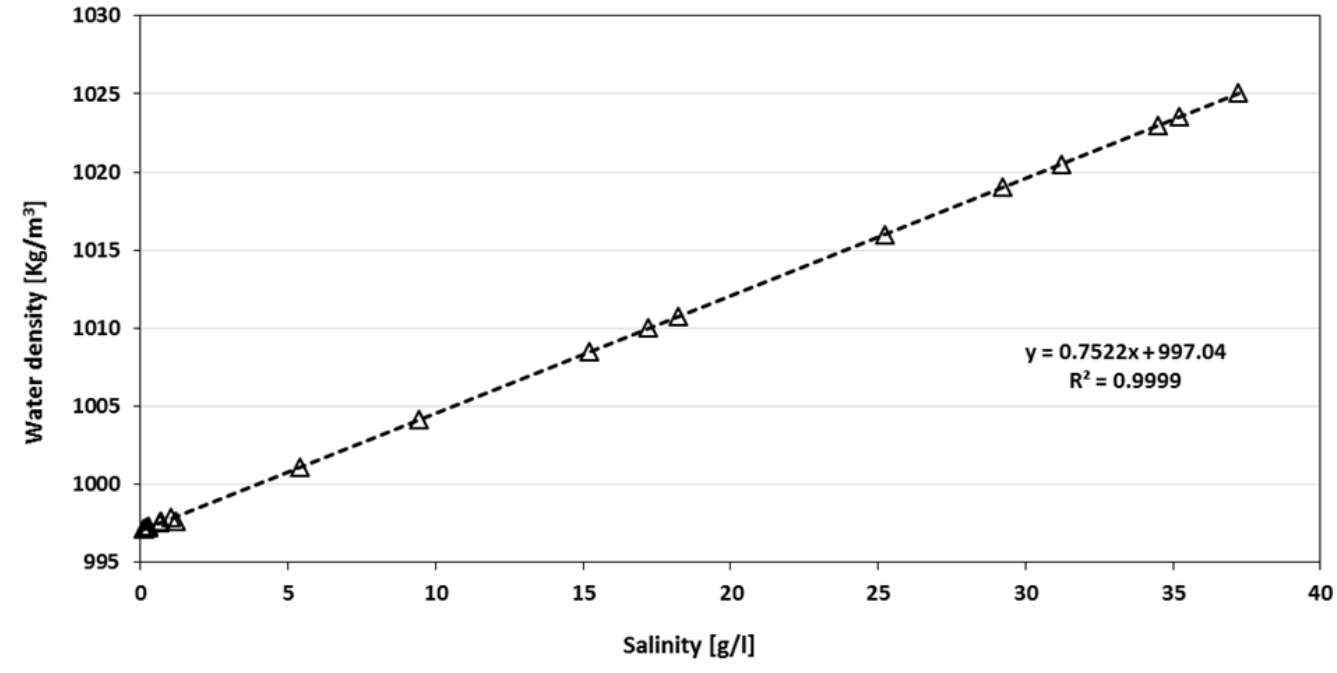

Figure 59: The daily regression plot of the variable density of groundwater and seawater versus salinity.

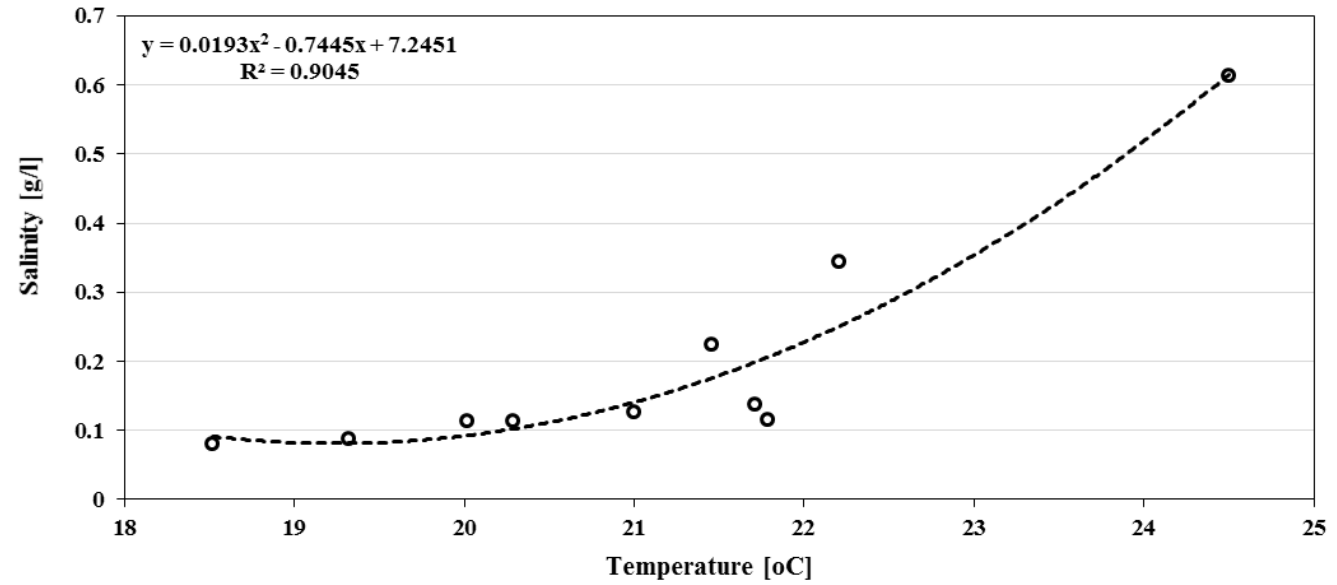

Figure 60: The daily regression plot of the groundwater temperature and salinity within the Heeia aquifer.

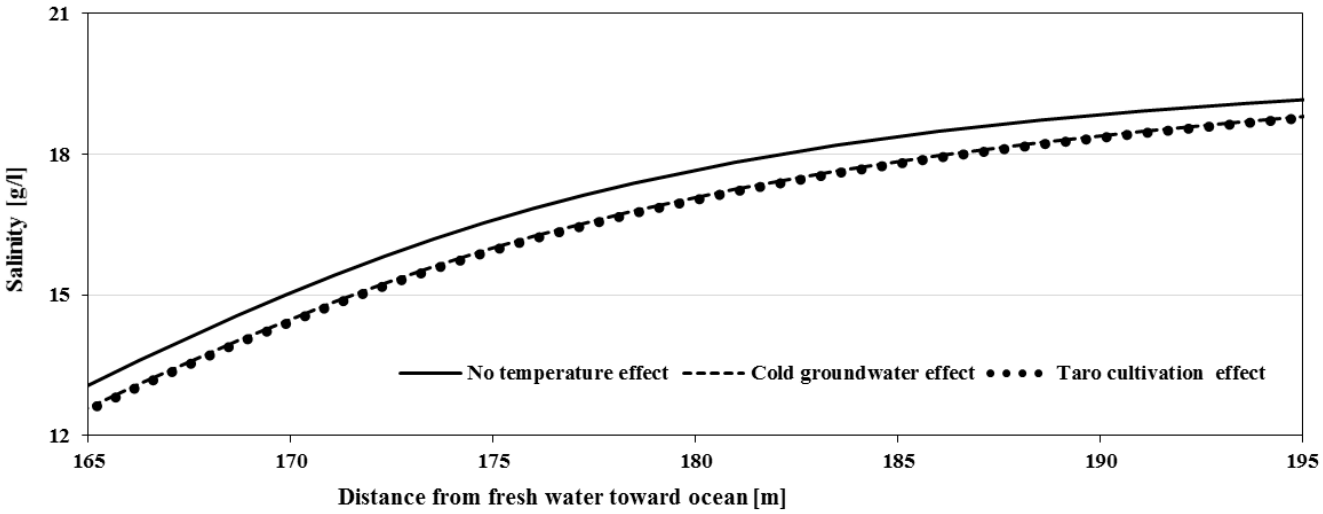

Figure 61: The horizontal effect of cold groundwater on the salinity distribution within transitional zone of fresh water–seawater interface.

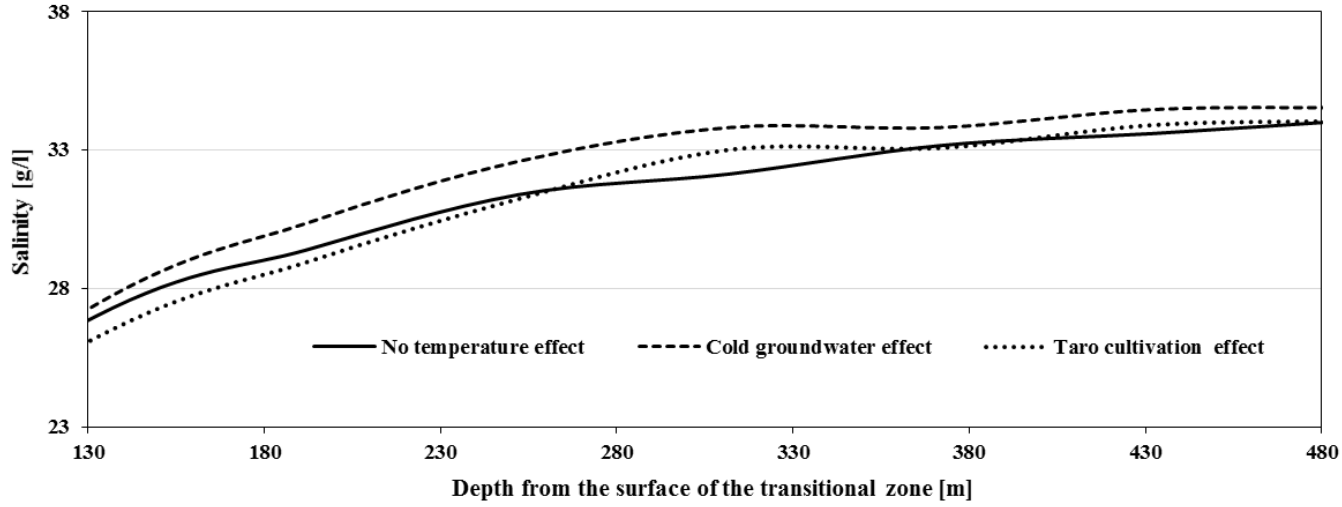

Figure 62: The vertical effect of cold groundwater on the salinity distribution within transitional zone of fresh water–seawater interface.

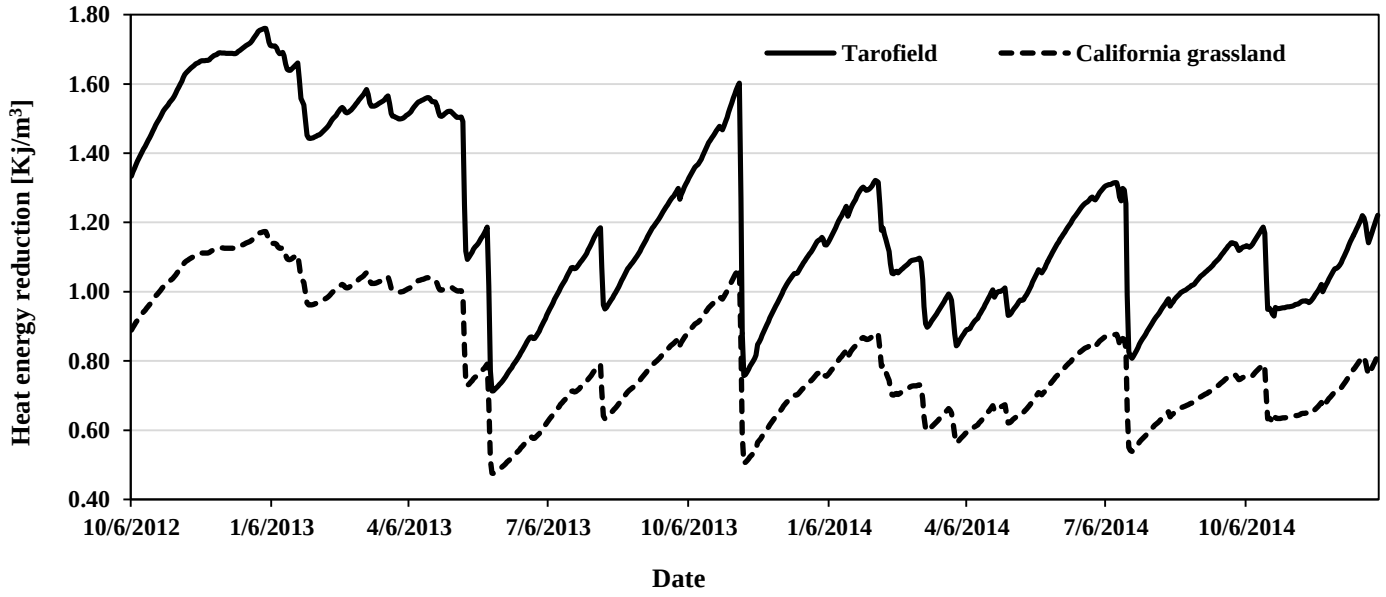

Figure 63: The daily estimated heat energy reduction of groundwater within the Heeia Coastal Wetland by cold groundwater flowing from upland under different land cover.

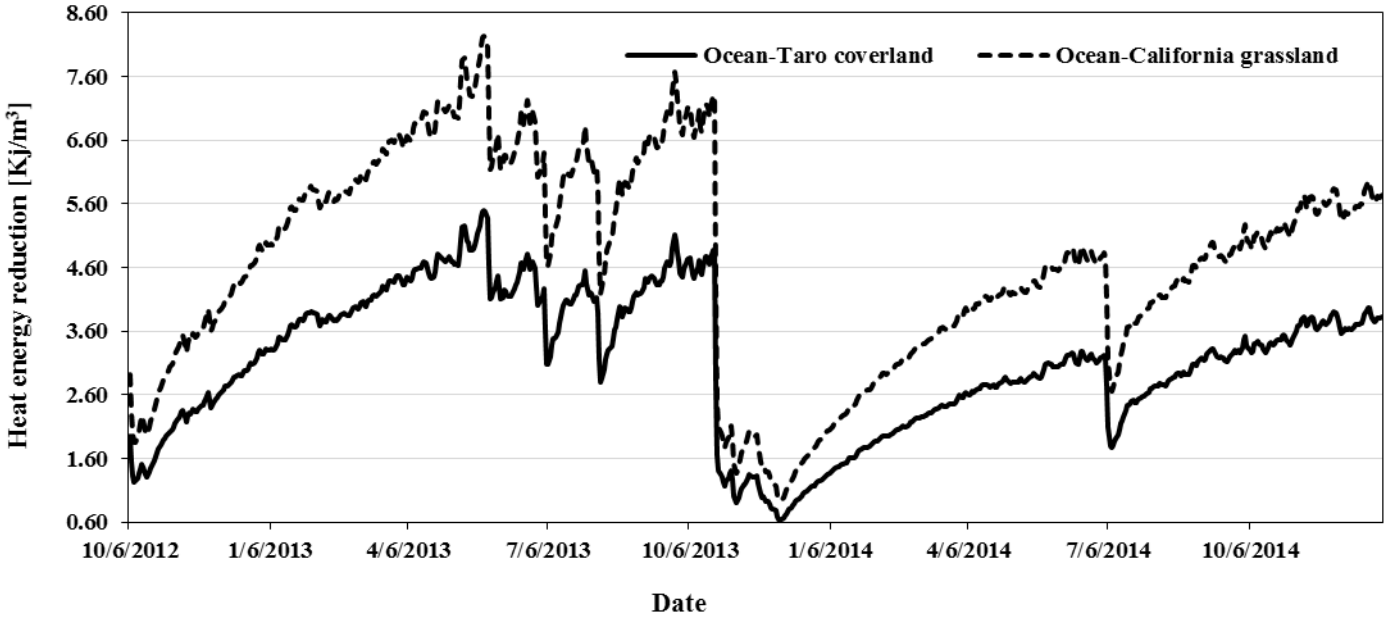

Figure 64: The daily estimated heat energy reduction of coastal shoreline sea water by FSGD under different land cover of the Heeia Coastal Wetland.

6.4 Conclusion

The SEAWAT model was used to simulate sea water intrusion, DSi fluxes, and heat transport within the Heeia coastal zone. The constructed model considered, reasonably estimated the transient simulation of seawater intrusion, DSi fluxes, and heat transport. The daily and monthly species concentrations were estimated to evaluate the species storing, sorption, and fluxes within the wetland and across the coastal shoreline. Three scenarios of SLR, climate change, and wetland restoration impacts were tested to assess their effect on salinity and DSi. The findings showed that the increase in salinity was not more than 1% under different scenarios relative to the baseline. However, the Heeia coastal zone may be threatened by seawater intrusion by seepage, in case of flooding and Tsunami occurrence. Basically, the potentially, a more significant seawater intrusion phenomenon usually may occur in the coastal regions with excessive or intermittent groundwater pumping rates. Specifically for the Heeia coastal zone has limited pumping wells and a high slope of fresh groundwater floating above saline water. This could be considered as a natural barrier to seawater encroachment. On the other hand, the findings depicted that the DSi fluxes were about 48 mole per day, which increased by 15% during the wet season but decreased by16% during the dry season. As expected, the DSi fluxes were a function of FSGD. Climate change more negatively impacted on DSi fluxes compared to SLR. Consequently, predicted DSi in FSGD will decrease by more than 5% due to SLR by1.1 m. Wetland restoration did not show a significant effect on DSi fluxes. The decrease in DSi fluxes under SLR and climate change might thus have a positive effect on the accumulative storing of DSi within coastal wetland.

Considering heat transport modeling; temperature effect simulations indicated that the cold groundwater reduced the salinity of the transitional zone by 3.5% within an area of 30 meters width horizontally and 380 meters vertically depth. The respective average heat energy reduction within wetland under california grassland and taro cultivation would be 0.81 and 1.12 Kj/ m^3 for inflow groundwater, and 4.69 and 3.13 Kj/ m^3 for outflow FSGD, respectively. The heat energy reduction is a function of groundwater temperature variation. In addition, the average reduction in wet season would be more than about 15% when compared to the dry season, which is probably due to increased groundwater fluxes that in turn trigger heat energy reduction.

Overall, the integrated hydrological modeling approach provides comprehensive information about seawater intrusion, DSi fluxes, cold groundwater effects, and their behaviors under various conditions within the Heeia coastal zone.

Chapter7 Conclusions, recommendation, and outcomes

7.1 Conclusions

The Heeia Coastal Wetland restoration is significantly influenced by the hydrological processes of the whole Watershed. Therefore, assessing the Watershed scale hydrological processes and understanding its influences on coastal wetland is useful information to prioritize the actions of the coastal wetland restoration. In addition, the water resources management of coastal wetland is considered to be the basic factor to optimize the sustainability of the coastal ecosystems. Such approach needs tools that can help in assessing the coastal water resources. Integrated hydrological models were the tools that used in this study to assess the water resources management within the Heeia coastal zone.

Assessing water resources basically needs good quality data at several locations and collect at large scale (e.g. Watershed). While topography, land use, and soil type data are easily available, capturing climate spatial variability is challenging for the Heeia Watershed due to scarce of climatic data within Watershed. This would have sequences on hydrologic processes modeling. For example, relevant information on runoff generation process in the mountains or upstream part of the Watershed might not be well derived if the field data collection is conducted at the downstream part. Additionally, field data may not provide sufficient information on Watershed scale hydrologic processes such as water budget components (rainfall, overland flow, subsurface flow, recharge, evapotranspiration, etc.), in order to make some conclusions through rescaling or aggregating techniques.

Since the Watershed processes are largely dependent on geo-spatial data and local climate effects, generalizing the hydrologic processes based on limited data information may lead to large uncertainty. Hence, spatially distributed data and hydrologic processes estimation are required at least to capture the important hydrologic phenomena that take place at Watershed scale. However, collecting field-nested data on water hydrologic processes is very cumbersome and economically not feasible. Therefore, we need to use other techniques that can enable us to obtain some information on variable hydrological processes at Watershed scale.

Thanks to advance in technologies, spatially distributed geo-spatial data are getting more available. In such case, spatially distributed hydrologic models can be used as a useful tool to express Watershed

performance and to understand the different Watershed hydrologic processes. By utilizing distributed hydrologic models, both spatial and temporal variability can be summarized.

This study applied integrated hydrological modeling approach in order to integrally manage the water resources of the Heeia Coastal Wetland in Oahu, Hawaii. The integrated models consists of SWAT, MODFLOW, and SEAWAT are the main components of integrated hydrological modeling approach in this study.

The surface water of the study area comprises just under 50% of the total water resources. The Heeia stream and its tributaries are considered the main surface water supply for the traditional practice of taro cultivation, the ponding water in coastal zone, and receiving waters (estuary and fresh water nearshore). In addition, it is active transporter for nutrients (DSi), cold water, and freshwater for coastal wetland and fishpond. It is a perennial stream in the Heeia Watershed and very rare days to become an imminent dry under severe climate and land cover changes scenarios. The Heeia stream originates in mountainous region and terminates at the northern west corner of fishpond. Therefore, it is a flashy stream due to severe steep flow and limited channel storage, which in turn causes flooding and excessive erosion during intensive rainfall events.

The groundwater is another important fresh water resources in the Heeia Watershed. It encompasses about 50% of the total water resources, but it is likely to increase during dry season due to the unique hydrogeological setting of the Heeia aquifer. Groundwater storage and baseflow are a function of recharge rate, which in turn depends on the rainfall amount and intensity, land topography, soil type, and land use. Groundwater is the main source of the protected fresh water, dissolved silicate fluxes, and cold groundwater in the Heeia coastal wetland, fishpond, and nearshore regions. The fresh water discharge across the coastal shoreline via FSGD pathway is about two times more than those discharge in the Heeia stream estuary. The impounded groundwater within dikes zone in the windward side of Oahu Island create it up to be perennial flowing and more protected against contamination sources, which supports the coastal region by ample fresh water for farming and aquaculture.

The SWAT model assessed the impacts of proposed wetland restoration on the water balance components. In spite of data scarcity, majority of the climatic data were derived from the nearby Watersheds and rescaling techniques used in order to capture the spatial variability of climate data especially rainfall. The SWAT model reasonably represented the temporal variability of observed daily

streamflow hydrograph. The simulated streamflow for upstream and downstream stations showed an acceptable performance and satisfactorily statistical evaluation values. Under current conditions, the baseline simulation of the water budget components were about 6%, 15%, 34%, and 45% of the annual rainfall (2043 mm), runoff, lateral flow, recharge, and evapotranspiration, respectively. The annual stream flow was about 44% of rainfall, which composed of about 13% surface runoff and 87% baseflow, consequently. The streamflow was highly influenced by groundwater discharge within the Heeia Watershed. The contribution of baseflow was very strong during dry season (May – October) and weak through wet season (November – April) as it was evidenced with 62% and 43% respectively. In contrast, the streamflow was strongly influenced with lateral flow and surface runoff during wet season and weakly during dry season. In addition, the annual rainfall upstream of the coastal Wetland about two times of the downstream, while the annual recharge upstream of the coastal Wetland about six times of the downstream.

The coastal wetland restoration would be expected to be impacted by the WBCs. Compared to baseline, the ET would be expected to increase that may result in decrease the other water balance components and increased the ponding water area. Conversion of existing wetland (california grass) to taro cultivation would cause an overall decrease in total stream flow due to decrease baseflow. The impact of applied irrigation diversions after restoration of taro cultivation and pond creation relative to the baseline (no-irrigation), was about 23, 109, 437, and 3886 mm/y, when water diversion was set to 50%, 75%, and 90% of the minimum streamflow. However, in general, the change in WBCs at Watershed scale was insignificant, which could be due to the small percent change in california grassland area compared to the Watershed's area. In contrast, the WBCs at wetland scale was significantly impacted by this land cover change. For example, recharge is likely to decrease while ET, surface runoff, and lateral flow are expected to increase.

The combined effects of wetland restoration and climate change may have profound impact on the WBCs of Heeia Wetland. The spatial and temporal rainfall variation was the determinant factor for the negative impact on WBCs. The recharge and baseflow were the highly sensitive components to the combined effects of the land cover and climate changes especially during dry season. Overall, the WBCs were more impacted in the late of 2080s than the 2050s period.

For FSGD assessment under wetland restoration, climate change, and sea level rise scenarios, the MODFLOW model was developed for the Heeia Watershed for both the transient and steady state conditions. Results indicated that the FSGD values were significantly influenced by the combined effects of anthropogenic activity, recharge rate, and climate change effects especially by the end of twenty first century. The relative average decline in FSGD flux during the post development would be about 53% due to the considerable decrease in recharge by 33% and increase in groundwater withdrawals, compared to pre-development condition. In addition, the average FSGD fluxes would be expected to decrease by 0.3 %, 2 %, and 10 % due to land cover change, climate change, and the combined effect of the land cover, climate change, and SLR by 1.1 m, respectively. The average decline in FSGD fluxes during only SLR, were 0.5%, 2%, and 5% as a result of 0.12 m and 0.4 m increase in sea level for the midcentury and 1.1 m for the end century. The FSGD had exponential relationship with groundwater head for the coastal unconfined aquifer. The FSGD comprised of 18%, 11%, and 3% of the baseflow, recharge, and rainfall, respectively.

Finally the SEAWAT model was used for simulating the density dependent groundwater flow, DSi fluxes, and heat transport with refine grid approach within the Heeia coastal zone. Three scenarios: sea level rise, climate change, and land cover change impacts were implemented to assess their effect on the salinity and DSi fluxes. The SEWAT model well represented the observed groundwater flow. Under various scenarios, the increase in salinity was not more than 1% relative to the baseline. Under normal conditions, the seawater intrusion phenomenon usually occurs in the coastal regions with excessive groundwater pumping rate, which is absent under the current Heeia Coastal Wetland conditions. The DSi fluxes were about 48 mole per day that could be increased by 15% during the wet season, but decreased by16% during the dry season. The climate change has negatively impacted the DSi fluxes compared to SLR. The decrease in DSi fluxes under SLR and climate change had a positive effect on the accumulative storage of the DSi within the coastal wetland. On the other hand, the cold groundwater reduced the salinity of transitional zone by 3.5% within 30 meter width area horizontally and 380 meter vertically. Lastly the average heat energy reduction within wetland under california grassland and taro cultivation would be 0.81, 1.12 (Kj/m^3) for inflow groundwater and 4.69, 3.13 (Kj/m^3) for outflow FSGD, respectively. The cold groundwater discharge in shoreline was significantly mitigated the seawater temperature due to the high thermal gradient between FSGD and seawater.

Despite data scarcity, the study has provided a comprehensive assessment of the water resources that can help in the management of the Heeia Coastal Wetland under various land cover and climate conditions.

7.2 Outcomes

1. Incorporating taro crop database in the SWAT model and management is considered as a new contribution for SWAT model applicability in tropical regions and pacific Islands, where taro crop gets special attention due to its uses as important staple food and spiritual plant in tropical community and Hawaiian cultural heritage.
2. Strengthen the coastal wetland conservation and protection against the twin impacts of climate change and human activities.
3. The study provides specific information about the coastal wetland hydrology for various scenarios that can help the decisions of makers in both environmental health and economic fields.
4. The integrated hydrological modeling approach of the Heeia Coastal Wetland could serve as a tool for other tropical wetlands with similar conditions.
5. Information about water resources management strategy could be adapted for future climate change, which is invaluable not only for the Heeia community but for other coastal communities of Hawaii.
6. Some aspects of the small-scale restoration proposed here may be applied to larger scaled Watersheds to understand how the linked processes driven by hydrology respond to climate and land cover changes.
7. The study will also provide direct information about how conversion of an invasive species (e.g., california grass) and replacement with taro effects on temperature, dissolved silicate uptake, and WBCs within the Heeia Coastal Wetland.
8. This project assist in building capacity within Kako'o Oiwi Organization so that they can better manage land use, water flow, and sustainable food production, positively impacting downstream coastal ecosystems.

9. Defined exponential relationship between FSGD and groundwater head, could be used as a simplified approach to continuously estimate FSGD from groundwater head within coastal unconfined aquifer.
10. This study can be used as a baseline for the future studies regarding water quality, soil erosion, nutrient fluxes, and the effect of california grass change on the heavy metal uptake versus taro cultivation. Such studies are relevant to the phytoremediation approach, which plays a vital role in the coastal environmental health.

7.3 Recommendations

Based on the results obtained during this study, the following key research recommendations would be drawn to enhance the future studies of the Heeia coastal region in Hawaii:

1. Due to the lack of long-term historical climatic data, this study utilized most of the data from outside of the Watershed, but these were not able to capture the local climate variability. Therefore, this study recommends to install three weather stations within the Heeia Watershed that cover the climatic parameters variation. I propose one of the climate weather station at the mountain zone, second at the old USGS flow station (Mauka), and the third one in the coastal wetland.
2. Another issues during this study, the lack of flow gauging station at the downstream of the Heeia Watershed. In order to capture the upstream and downstream streamflow spatial variability and better represent the Watershed characteristics with model parameters, constructing two more flow stations in which one of them should be located at the upland of the Heeia Wetland and the second at the estuary of the Heeia Stream would be useful for future research. Additional records such as stream flow temperature, sediment, salinity, and nutrients would be helpful for future studies.
3. Dig at least three monitoring wells along the perpendicular line on the coastal shoreline to monitor the groundwater level, temperature, salinity, dissolved oxygen and nutrient fluxes.
4. This study recommends to construct retention pond at the upstream of the Heeia Wetland to prevent flooding and conserve fresh water.

5. Start taro cultivation at the southern east of wetland in which fresh cold water is more available than other parts to avoid water scarcity during dry season. According to the hydrological research analysis, there were very rare dry days of the Heeia stream flow for various scenarios. To avoid the risk of irrigation diversions during taro cultivation, the recommended minimum flow in the main stream is about 0.75 m^3/ s, which in turn maintain the stream flowing to the water pond (habitats for aquatic species) and water ponding within taro patches.
6. Sustain stream flow and ponding water within taro patches are good management strategy for wetland and coastal restoration.
7. The ongoing coastal wetland restoration should consider the effect of projected climate change in Hawaii and sea level risen by the end of 21 century in to achieve sustain the water resources within the Heeia Watershed.
8. Water resources assessment process is periodically needed to sustain the functionalities of the ecosystems of the Heeia Watershed and maintain the environmental health.

References

Abbaspour KC, Yang J, Maximov I, Siber R, Bogner K, Mieleitner J, Zobrist J, Srinivasan R (2007) Modelling hydrology and water quality in the pre-alpine/alpine Thur watershed using SWAT. Journal of hydrology 333: 413-430

Alden R (1983) Water yield improvement potential by vegetation management on western rangelands'. Water Resources Bulletin 19

Allen J, Newman ME, Riford M, Archer GH (1995) Blood and plant residues on Hawaiian stone tools from two archaeological sites in Upland Kāne'ohe, Ko'olau Poko district, O'ahu Island. Asian Perspectives: 283-302

Allen R, Pruitt W, Businger J, Fritschen L, Jensen M, Quinn F (1996) Hydrology handbook. ASCE manuals and reports on engineering practice, 2nd edn ASCE, Reston: 125-252

Allen W (2000) Restoring Hawaii's Dry Forests Research on Kona slope shows promise for native ecosystem recovery. Bioscience 50: 1037-1041

Andersen MS, Baron L, Gudbjerg J, Gregersen J, Chapellier D, Jakobsen R, Postma D (2007) Discharge of nitrate-containing groundwater into a coastal marine environment. Journal of Hydrology 336: 98-114

ARIS AZ (2010) A numerical modelling of seawater intrusion into an oceanic island aquifer, Sipadan Island, Malaysia. Sains Malaysiana 39: 525-532

Armstrong RW, Bier JA (1973) Atlas of Hawaii

Arnold J, Kiniry J, Srinivasan R, Williams J, Haney E, Neitsch S (2012) Soil and Water Assessment Tool input/output file documentation: Version 2012. US Department of Agriculture–Agricultural Research Service, Grassland, Soil and Water Research Laboratory, Temple, TX and Blackland Research and Extension Center, Texas AgriLife Research, Temple, TX Texas Water Resources Institute Technical Report

Arnold J, Moriasi D, Gassman P, Abbaspour K, White M, Srinivasan R, Santhi C, Harmel R, Van Griensven A, Van Liew M (2012) SWAT: Model use, calibration, and validation. Transactions of the ASABE 55: 1491-1508

Arnold JG, Srinivasan R, Muttiah RS, Williams JR (1998) Large area hydrologic modeling and assessment part I: Model development1 Wiley Online Library.

ASCE (1996) Hydrology handbook. ASCE Publications, Reston, VAAtaie-Ashitani B, Volker RE, Lockington DA (2001) Tidal effects on groundwater dynamics in unconfined aquifers Hydrol Processes 15: 655669

Aumen N, Berry L, Best R, Edwards A, Havens K, Obeysekera J, Rudnick D, Scerbo M (2013) Predicting Ecological Changes in the Florida Everglades Under a Future Climate Scenario, 33 pp. US Geological Survey, Florida Sea Grant, Florida Atlantic University[Available online at http://www ces fau edu/climate_ change/ecology-february-2013/PECFEFCS_Report pdf]

Bankoff G (2006) Winds of colonisation: the meteorological contours of Spain's Imperium in the Pacific 1521-1898. Environment and History: 65-88

Bantilan-Smith M, Bruland GL, MacKenzie RA, Henry AR, Ryder CR (2009) A comparison of the vegetation and soils of natural, restored, and created coastal lowland wetlands in Hawai ‘i. Wetlands 29: 1023-1035

Barlow PM (2003) Ground Water in Fresh Water-salt Water Environments of the Atlantic Geological Survey (USGS)

Barnett B, Townley L, Post V, Evans R, Hunt R, Peeters L, Richardsdon S, Wenner A, Knapton A, Boronkay A (2012) Australian groundwater modeling Guidelines. Sinclair Knight Merz and National Centre for Groundwater Research and Training. Waterlines Report Series

Barnett J (2001) Adapting to climate change in Pacific Island countries: the problem of uncertainty. World Development 29: 977-993

Bassiouni M, Oki DS (2013) Trends and shifts in streamflow in Hawai ‘i, 1913–2008. Hydrological Processes 27: 1484-1500

Benning TL, LaPointe D, Atkinson CT, Vitousek PM (2002) Interactions of climate change with biological invasions and land use in the Hawaiian Islands: modeling the fate of endemic birds using a geographic information system. Proceedings of the National Academy of Sciences 99: 14246-14249

Bishop JM, Glenn CR, Amato DW, Dulai H (2015) Effect of land use and groundwater flow path on submarine groundwater discharge nutrient flux. Journal of Hydrology: Regional Studies

Black B, Dawoud M, Herrmann R, Largeau D, Maliva R, Will B (2008) Managing a precious resource. Oilfield Review 20: 18-33

Blecker SW, McCulley RL, Chadwick OA, Kelly EF (2006) Biologic cycling of silica across a grassland bioclimosequence. Global Biogeochemical Cycles 20

Blecker SW, McCulley RL, Chadwick OA, Kelly EF (2006) Biologic cycling of silica across a grassland bioclimosequence. Global Biogeochemical Cycles 20: GB3023 DOI 10.1029/2006GB002690

Board of Water Supply (2012) KOOLAU POKO WATERSHED MANAGEMENT PLAN OAHU WATER MANAGEMENT PLAN Waimanalo Public Library, City and County of Honolulu, pp. 55.

Brasher AM (2003) Impacts of human disturbances on biotic communities in Hawaiian streams. BioScience 53: 1052-1060

Bruijnzeel L (1988) Estimates of evaporation in plantations of Agathis dammara Warb. in south-central Java, Indonesia. Journal of Tropical Forest Science: 145-161

Bruijnzeel LA (2002b) Hydrological impacts of converting tropical montane cloud forest to pasture, with initial reference to northern Costa Rica.Project Memorandum Form, Project No R7991 within the Forestry Research Programme of the

management 13: 85

Bullock A, Acreman M (2003) The role of wetlands in the hydrological cycle. Hydrology and Earth System Sciences Discussions 7: 358-389

Burnett WC, Aggarwal PK, Aureli A, Bokuniewicz H, Cable JE, Charette MA, Kontar E, Krupa S, Kulkarni KM, Loveless A (2006) Quantifying submarine groundwater discharge in the coastal zone via multiple methods. Science of the Total Environment 367: 498-543

Carlquist S (1980) Hawaii: a natural history. Geology, climate, native flora and fauna above the shoreline Honolulu: SB Printers, Inc. for Pacific Tropical Botanical Garden (xii), 468p.-illus., col. illus., maps.. En Icones, Maps. Geog

Chang SW, Clement TP, Simpson MJ, Lee K-K (2011) Does sea-level rise have an impact on saltwater intrusion? Advances in water resources 34: 1283-1291

Chen Y, Jessel B, Fu B, Yu X, Pittock J (2013) Ecosystem services and management strategy in China Springer Science & Business Media

Church TM (1996) An underground route for the water cycle. Nature 380: 579-580

Conference W (2015) The Second Conference on Water Resource Sustainability Issues on Tropical Islands, Honolulu, Hawaii.

Cortes G, Ragettli S, Pellicciotti F, McPhee J (2011) Hydrological models and data scarcity: on the quest for a model structure appropriate for modeling water availability under the present and future climateAGU Fall Meeting Abstracts, pp. 01.

Cronshey R (1986) Urban hydrology for small watersheds US Dept. of Agriculture, Soil Conservation Service, Engineering Division.

Dale VH (1997) The relationship between land-use change and climate change. Ecological applications 7: 753-769

De Wiest RJ (1998) Ghyben-Herzberg theoryGhyben–herzberg theoryEncyclopedia of Hydrology and Lakes:340-341.

Derry LA, Kurtz AC, Ziegler K, Chadwick OA (2005) Biological control of terrestrial silica cycling and export fluxes to watersheds. Nature 433: 728-731

Devaney DM (1976) Kaneohe: A History of Change, 1778-1950 ICON Group International

Diaz HF, Giambelluca TW, Eischeid JK (2011) Changes in the vertical profiles of mean temperature and humidity in the Hawaiian Islands. Global and Planetary Change 77: 21-25 DOI http://dx.doi.org/10.1016/j.gloplacha.2011.02.007

Diersch H-J, Kolditz O (2002) Variable-density flow and transport in porous media: approaches and challenges. Advances in Water Resources 25: 899-944

Doherty J, Hunt RJ (2009) Two statistics for evaluating parameter identifiability and error reduction. Journal of Hydrology 366: 119-127

Duarte TK, Pongkijvorasin S, Roumasset J, Amato D, Burnett K (2010) Optimal management of a Hawaiian Coastal aquifer with nearshore marine ecological interactions. Water Resources Research 46

Dulai H, Kleven A, Ruttenberg K, Briggs R, Thomas F (2016) Evaluation of Submarine Groundwater Discharge as a Coastal Nutrient Source and Its Role in Coastal Groundwater Quality and QuantityEmerging Issues in Groundwater Resources:187-221.

EMI TT (2010) Hawai`i Watershed Guidance. In: Planning THiOo, Management CZ (eds), Honolulu, HI 96813.

Erwin KL (2009) Wetlands and global climate change: the role of wetland restoration in a changing world. Wetlands Ecology and management 17: 71-84

Eversole D, Andrews A, Anthony S, Chu P-S, Fletcher C, Gonser M, Hamilton K, Hwang D, Keener V, Lemmo SJ, Lewis N, Oki D, Owens T, Pap R, Porro R, Romine B, Souki J, Thiel JK, Tribble G (2014) CLIMATE CHANGE IMPACTS IN HAWAI'I, University of Hawai'i at Mānoa Sea Grant College Program.

Fang X, Ren L, Li Q, Zhu Q, Shi P, Zhu Y (2013) Hydrologic response to land use and land cover changes within the context of catchment-scale spatial information. Journal of Hydrologic Engineering 18: 1539-1548

Fares A (2008) Water Management Software to Estimate Crop Irrigation Requirements for Consumptive Use Permitting In Hawaii State of Hawaii, May.

Feng X, Zhang G, Xu YJ (2013) Simulation of hydrological processes in the Zhalong wetland within a river basin, Northeast China. Hydrology and Earth System Sciences 17: 2797

Frings PJ, Clymans W, Fontorbe G, Christina L, Conley DJ (2016) The continental Si cycle and its impact on the ocean Si isotope budget. Chemical Geology 425: 12-36

Gardner RC, Davidson NC (2011) The Ramsar ConventionWetlands:189-203.

Gassman PW, Reyes MR, Green CH, Arnold JG (2007) The soil and water assessment tool: historical development, applications, and future research directions

Giambelluca T, Chen Q, Frazier A, JP P, Chen Y-L, Chu P-S, Eischeid J, Delparte D (2011) The Rainfall Atlas of Hawai'i

Giambelluca T, Shuai X, Barnes M, Alliss R, Longman R, Miura T, Chen Q, Frazier A, Mudd R, Cuo L (2014) Evapotranspiration of Hawai 'i. Final report submitted to the US Army Corps of Engineers—Honolulu District, and the Commission on Water Resource Management, State of Hawai 'i

Gingerich SB, Oki DS (2000) Ground water in Hawaii US Department of the Interior, US Geological Survey

Gingerich SB, Yeung CW, Ibarra T-JN, Engott JA (2007) Water use in wetland kalo cultivation in Hawaii U. S. Geological Survey.

Glavan M, Pintar M (2012) Strengths, weaknesses, opportunities and threats of catchment modelling with Soil and Water Assessment Tool (SWAT) model. Water Resources Management and Modeling InTech, Rijeka, Croatia: 310

Grant N, Saito L, Weltz M, Walker M, Daly C, Stewart K, Morris C (2013) Instrumenting wildlife water developments to collect hydrometeorological data in remote western US catchments. Journal of Atmospheric and Oceanic Technology 30: 1161-1170

Green C, Tomer M, Di Luzio M, Arnold J (2006) Hydrologic evaluation of the soil and water assessment tool for a large tile-drained watershed in Iowa. Transactions of the ASAE 49: 413-422

Group MRIEW (2015) Elevation-dependent warming in mountain regions of the world. Nature Climate Change 5: 424-430

Guardiola-Claramonte MT (2009) Effects of land use/land cover change on the hydrological partitioning

Guha S (2010) Variable-density flow models of saltwater intrusion in coastal landforms in response to climate change induced sea level rise and a chapter on time-frequency analysis of ground penetrating radar signals. University of South Florida

Guntzer F, Keller C, Meunier J-D (2012) Benefits of plant silicon for crops: a review. Agronomy for Sustainable Development 32: 201-213

Hanna S, Haukenes A, Foy R, Buck C (2008) Temperature effects on metabolic rate, swimming performance and condition of Pacific cod Gadus macrocephalus Tilesius. Journal of Fish Biology 72: 1068-1078

Hastert Ha, Planners F (2007) Heeia Fishpond Aquaculture Support Facilities, City and County of Honolulu, pp. 219.

Henry AR (2006) Strategic plan for wetland conservation in Hawai'i PACIFIC COAST JOINT VENTURE HAWAI`I.

Hornbeck J, Pierce R, Federer C (l970) Streamflow Changes after Forest Clearing in New England. Water Resources Research 6: ll24-ll32

Hughes JD, Sifuentes DF, White JT (2016) Potential effects of alterations to the hydrologic system on the distribution of salinity in the Biscayne aquifer in Broward County, Florida US Geological Survey.

Hugman R, Stigter T, Monteiro J, Costa L, Nunes L (2015) Modeling the spatial and temporal distribution of coastal groundwater discharge for different water use scenarios under epistemic uncertainty: case study in South Portugal. Environmental Earth Sciences 73: 2657-2669

Hunter CL, Evans CW (1995) Coral reefs in Kaneohe Bay, Hawaii: two centuries of western influence and two decades of data. Bulletin of Marine Science 57: 501-515

Izuka SK, Hill BR, Shade PJ, Tribble GW (1993) Geohydrology and possible transport routes of polychlorinated biphenyls in Haiku Valley, Oahu, Hawaii US Department of the Interior, US Geological Survey

Jha M, Pan Z, Takle ES, Gu R (2004) Impacts of climate change on streamflow in the Upper Mississippi River Basin: A regional climate model perspective. Journal of Geophysical Research: Atmospheres 109

Jokiel PL (1991) Jokiel's illustrated scientific guide to Kaneohe Bay, Oahu Hawaiian Coral Reef Assessment and Monitoring Program, Hawaii Institute of Marine Biology, Kaneohe, Hawaii.

Jokiel PL, Rodgers KS, Brown EK (2004) Assessment, Mapping and Monitoring of Selected "Most Impaired" Coral Reef Areas in the State of Hawai'i. Hawai‘i Institute of Marine Biology.

Kakoo Oiwi (2010) Heeia Wetland Restoration Strategic Plan 2010 - 2015, pp. 16.

Kakoo Oiwi (2011) Heeia Wetlands Restoration.

KBAC (2007) Ko'olaupoko Watershed Restoration Action Strategy Kailua Bay Advisory Council (KBAC) Hawaii's Department of Health, Hawaii state.

Kealoha P (2009) Final Environmental Assessment WINDWARD COMMUNITY COLLEGE LIBRARY AND

Keener V (2013) Climate change and pacific islands: indicators and impacts: report for the 2012 pacific islands regional climate assessment Island press

Kelly JL, Glenn CR, Lucey PG (2013) High-resolution aerial infrared mapping of groundwater discharge to the coastal ocean. Limnol Oceanogr: Methods 11: 262-277

Khan M, Mahmood K, Skogerboe G (1997) Current meter discharge measurements for steady and unsteady flow conditions in irrigation channels International Water Management Institute.

King KW, Arnold J, Bingner R (1999) Comparison of Green-Ampt and curve number methods on Goodwin Creek watershed using SWAT. Transactions of the ASAE 42: 919

Kiros G, Shetty A, Nandagiri L (2015) Performance Evaluation of SWAT Model for Land Use and Land Cover Changes in Semi-Arid Climatic Conditions: A Review. Hydrology: Current Research 2015

Kløve B, Ala-Aho P, Bertrand G, Gurdak JJ, Kupfersberger H, Kværner J, Muotka T, Mykrä H, Preda E, Rossi P (2014) Climate change impacts on groundwater and dependent ecosystems. Journal of Hydrology 518: 250-266

Knee K, Paytan A (2011) 4.08 Submarine groundwater discharge: A source of nutrients, metals, and pollutants to the coastal ocean. Treatise Estuar Coast Sci 4: 205-234

Knee KL, Crook ED, Hench JL, Leichter JJ, Paytan A (2016) Assessment of Submarine Groundwater Discharge (SGD) as a Source of Dissolved Radium and Nutrients to Moorea (French Polynesia) Coastal Waters. Estuaries and Coasts: 1-18

Kuniansky EL, Gómez-Gómez F, Torres-González S (2004) Effects of Aquifer Development and Changes in Irrigation Practices on Ground-water Availability in the Santa Isabel Area, Puerto Rico US Geological Survey

Kunkel KE (2013) Regional climate trends and scenarios for the US national climate assessment US Department of Commerce, National Oceanic and Atmospheric Administration, National Environmental Satellite, Data, and Information Service

Kusler JA (1990) Wetland creation and restoration: the status of the science Island Press

Langevin CD (2009) SEAWAT: A computer program for simulation of variable-density groundwater flow and multi-species solute and heat transport US Geological Survey.

Langevin CD, Thorne Jr DT, Dausman AM, Sukop MC, Guo W (2008) SEAWAT Version 4: a computer program for simulation of multi-species solute and heat transport Geological Survey (US).

Lau L-KS, Mink JF (2006) Hydrology of the Hawaiian Islands University of Hawaii Press

Lee E, Hyun Y, Lee K-K (2013) Sea level periodic change and its impact on submarine groundwater discharge rate in coastal aquifer. Estuarine, Coastal and Shelf Science 121: 51-60

Legates DR, McCabe GJ (1999) Evaluating the use of "goodness-of-fit" measures in hydrologic and hydroclimatic model validation. Water resources research 35: 233-241

Leta OT, El-Kadi AI, Dulai H, Ghazal KA (2016) Assessment of climate change impacts on water balance components of Heeia watershed in Hawaii. Journal of Hydrology: Regional Studies 8: 182-197 DOI http://dx.doi.org/10.1016/j.ejrh.2016.09.006

Libes S (2011) Introduction to marine biogeochemistry Academic Press

Lin Y-P, Hong N-M, Wu P-J, Wu C-F, Verburg PH (2007) Impacts of land use change scenarios on hydrology and land use patterns in the Wu-Tu watershed in Northern Taiwan. Landscape and Urban Planning 80: 111-126

Longman RJ, Giambelluca TW, Alliss RJ, Barnes ML (2014) Temporal solar radiation change at high elevations in Hawai 'i. Journal of Geophysical Research: Atmospheres 119: 6022-6033

Loveland T, Mahmood R, Patel-Weynand T, Karstensen K, Beckendorf K, Bliss N, Carleton A (2012) National climate assessment technical report on the impacts of climate and land use and land cover change. US Geological Survey Open-File Report 1155: 87

Luoma S, Okkonen J (2014) Impacts of future climate change and Baltic sea level rise on groundwater recharge, groundwater levels, and surface leakage in the Hanko aquifer in southern Finland. Water 6: 3671-3700

Macdonald GA, Abbott AT, Peterson FL (1983) Volcanoes in the sea: the geology of Hawaii University of Hawaii Press

Mat N, Hamzah Z, Maskin M, Wood AK (2006) MINERAL UPTAKE BY TARO (COLOCASIA ESCULENTA) IN SWAMP AGROECOSYSTEM FOLLOWING GRAMOXONE®(PARAQUAT) HERBICIDE SPRAYING

McCoy C, Corbett D (2009) Review of submarine groundwater discharge (SGD) in coastal zones of the Southeast and Gulf Coast regions of the United States with management implications. Journal of environmental management 90: 644-651

McDonald MG, Harbaugh AW (1988) A modular three-dimensional finite-difference ground-water flow model

McGowan MP (2004) Submarine groundwater discharge: freshwater and nutrient input into Hawaii's coastal zone. UNIVERSITY OF HAWAI'I

Menberg K, Blum P, Kurylyk B, Bayer P (2014) Observed groundwater temperature response to recent climate change. Hydrology and Earth System Sciences 18: 4453-4466

Meteorology A, CSIRO (2011) Climate Change in the Pacific: Scientific Assessment and New Research.

Mink J (1964) Groundwater temperatures in a tropical island environment. Journal of Geophysical Research 69: 5225-5230

Mink J, Lau S (1993) Aquifer Identification and Classification for the Island of Lana'i: Groundwater Protection Strategy for Hawai'i (April 1993): Water Resources Research Center, University of Hawai'i at Manoa Technical Report.

Mitsch WJ, Gosselink JG (2007) Wetlands, 4th edition edn, John Wiley & Sons, Inc., New York, NY, USA

Miyasaka SC, Ogoshi RM, Tsuji GY, Kodani LS (2003) Site and Planting Date Effects on Taro Growth. Agronomy journal 95: 545-557

Moore W, John H, Steve A (2009) Submarine Groundwater Discharge Encyclopedia of Ocean Sciences. Academic, Oxford: 4530-4537

Moriasi DN, Arnold JG, Van Liew MW, Bingner RL, Harmel RD, Veith TL (2007) Model evaluation guidelines for systematic quantification of accuracy in watershed simulations. Transactions of the ASABE 50: 885-900

Mulligan AE, Charette MA (2009) Groundwater flow to the coastal ocean. Elements of Physical Oceanography: A derivative of the Encyclopedia of Ocean Sciences: 465

Nash JE, Sutcliffe JV (1970) River flow forecasting through conceptual models part I—A discussion of principles. Journal of hydrology 10: 282-290

Ncube M (2008) The impact of land cover and land use on the hydrologic response in the Olifants.

Ndomba P, Mtalo F, Killingtveit A (2008) SWAT model application in a data scarce tropical complex catchment in Tanzania. Physics and Chemistry of the Earth, Parts A/B/C 33: 626-632

Neitsch SL, Arnold JG, Kiniry JR, Williams JR (2011) Soil and water assessment tool theoretical documentation version 2009 Texas Water Resources Institute.

Nichols WD, Shade PJ, Hunt CD (1997) Summary of the Oahu, Hawaii, regional aquifer-system analysis USGPO

NOAA (2016) He‘eia National Estuarine Research Reserve, NOAA Office for Coastal Management.

Nyeko M (2015) Hydrologic modelling of data scarce basin with SWAT Model: Capabilities and Limitations. Water Resources Management 29: 81-94

Oki DS (1997) Geohydrology and numerical simulation of the ground-water flow system of Molokai, Hawaii Geological Survey (US).

Onwueme I (1999) Taro cultivation in Asia and the Pacific. Rap Publication 16: 1-9

Osorio J, Jeong J, Bieger K, Arnold J (2014) Influence of potential evapotranspiration on the water balance of sugarcane fields in Maui, Hawaii. Journal of Water Resource and Protection 6: 852

Pachauri RK, Allen MR, Barros V, Broome J, Cramer W, Christ R, Church J, Clarke L, Dahe Q, Dasgupta P (2014) Climate change 2014: synthesis Report. Contribution of working groups I, II and III to the fifth assessment report of the intergovernmental panel on climate change IPCC

Pandey BK, Gosain A, Paul G, Khare D (2016) Climate change impact assessment on hydrology of a small watershed using semi-distributed model. Applied Water Science: 1-13

Paul S, Küsel K, Alewell C (2006) Reduction processes in forest wetlands: tracking down heterogeneity of source/sink functions with a combination of methods. Soil Biology and Biochemistry 38: 1028-1039

Penn DC (1997) Water and Energy Flows in Hawaii Taro Pondfields. University of Hawaii at Manoa

Pervez MS, Henebry GM (2015) Assessing the impacts of climate and land use and land cover change on the freshwater availability in the Brahmaputra River basin. Journal of Hydrology: Regional Studies 3: 285-311

Peterson RN, Burnett WC, Glenn CR, Johnson AG (2009) Quantification of point-source groundwater discharges to the ocean from the shoreline of the Big Island, Hawaii. Limnol Oceanogr 54: 890-904

Pratiwi SH, Soelistyono R, Maghfoer MD (2014) The Growth and Yield of Taro (Colocasia

esculenta (L.) Schott) var. Antiquorum in Diverse

Sizes of Tuber and Numbers of Leaf. International Journal of Science and Research 3 4

Pritchard D (2010) Wise use of Wetlands: Concepts and Approaches for the wise use of Wetlands Volume I Switzerland: Ramsar Secretariat.

Pulwarty RS, Nurse LA, Trotz UO (2010) Caribbean Islands in a changing climate. Environment 52: 16-27

Ranjan SP, Kazama S, Sawamoto M (2006) Effects of climate and land use changes on groundwater resources in coastal aquifers. Journal of Environmental Management 80: 25-35

Rashford BS, Adams RM, Wu J, Voldseth RA, Guntenspergen GR, Werner B, Johnson WC (2016) Impacts of climate change on land-use and wetland productivity in the Prairie Pothole Region of North America. Regional Environmental Change 16: 515-526

Rasmussen P, Sonnenborg T, Goncear G, Hinsby K (2013) Assessing impacts of climate change, sea level rise, and drainage canals on saltwater intrusion to coastal aquifer. Hydrology and Earth System Sciences 17: 421-443

Robinson JL, Carmichael JK, Halford KJ, Ladd DE (1997) Hydrogeologic framework and simulation of ground-water flow and travel time in the shallow aquifer system in the area of Naval Support Activity Memphis, Millington, Tennessee. US Geological Survey Water-Resources Investigations Report: 97-4228

Root TL, Price JT, Hall KR, Schneider SH, Rosenzweig C, Pounds JA (2003) Fingerprints of global warming on wild animals and plants. Nature 421: 57-60

Rotzoll K, Fletcher CH (2013) Assessment of groundwater inundation as a consequence of sea-level rise. Nature Climate Change 3: 477-481

Rotzoll K, Oki DS, El-Kadi AI (2010) Changes of freshwater-lens thickness in basaltic island aquifers overlain by thick coastal sediments. Hydrogeology journal 18: 1425-1436

Safeeq M, Fares A (2012) Hydrologic response of a Hawaiian watershed to future climate change scenarios. Hydrological Processes 26: 2745-2764

Safeeq M, Grant G, Lewis S, Nolin A, Hempel L, Cooper M, Tague C (2014) Integrated snow and hydrology modeling for climate change impact assessment in Oregon CascadesAGU Fall Meeting Abstracts, pp. 1093.

Sahoo G, Ray C, De Carlo E (2006) Calibration and validation of a physically distributed hydrological model, MIKE SHE, to predict streamflow at high frequency in a flashy mountainous Hawaii stream. Journal of Hydrology 327: 94-109

Schopka HH, Derry LA (2012) Chemical weathering fluxes from volcanic islands and the importance of groundwater: The Hawaiian example. Earth and Planetary Science Letters 339: 67-78

Shade PJ, Nichols WD (1996) Water budget and the effects of land-use changes on ground-water recharge, Oahu, Hawaii US Government Printing Office Sherrod DR, Sinton JM, Watkins SE, Brunt KM (2007) Geologic map of the State of Hawaii Geological Survey (US).

Shih S, Snyder G (1984) Leaf area index and dry biomass of taro. Agronomy journal 76: 750-753

Simmons CT (2005) Variable density groundwater flow: From current challenges to future possibilities. Hydrogeology Journal 13: 116-119

Singh J, Knapp HV, Arnold J, Demissie M (2005) Hydrological modeling of the iroquois river watershed using HSPF and SWAT1 Wiley Online Library.

Sorooshian S, Duan Q, Gupta VK (1993) Calibration of rainfall-runoff models: application of global optimization to the Sacramento soil moisture accounting model. Water resources research 29: 1185-1194

Stearns HT, Vaksvik KN (1935) Geology and ground-water resources of the island of Oahu, Hawaii. Hawaii Div Hydrography, Bull 1: 536

Street JH, Knee KL, Grossman EE, Paytan A (2008) Submarine groundwater discharge and nutrient addition to the coastal zone and coral reefs of leeward Hawai'i. Marine Chemistry 109: 355-376

Sun L, Jin X, Yang W, Xu M, Zhong Y, Zhu L, Zhuang Y (2007) Effects of silicate on the community structure of phytoplankton in enclosures. Huan jing ke xue= Huanjing kexue/[bian ji, Zhongguo ke xue yuan huan jing ke xue wei yuan hui" Huan jing ke xue" bian ji wei yuan hui] 28: 2174-2179

Swarzenski P, Dulai H, Kroeger K, Smith C, Dimova N, Storlazzi C, Prouty N, Gingerich S, Glenn C (2016) Observations of nearshore groundwater discharge: Kahekili Beach Park submarine springs, Maui, Hawaii. Journal of Hydrology: Regional Studies

Swarzenski P, Dulaiova H, Dailer M, Glenn C, Smith C, Storlazzi C (2013) A geochemical and geophysical assessment of coastal groundwater discharge at select sites in Maui and O'ahu, Hawai'iGroundwater in the Coastal Zones of Asia-Pacific:27-46.

Takasaki KJ, Hirashima GT, Lubke ER (1969) Water resources of windward Oahu, Hawaii Taniguchi PT (1982) Haiku Well at Haiku Valley, Koolaupoko, Oahu. In: supply Bow (ed) Board of water supply City and County of Honolulu, pp. 220.

Timm O, Diaz HF (2009) Synoptic-Statistical Approach to Regional Downscaling of IPCC Twenty-First-Century Climate Projections: Seasonal Rainfall over the Hawaiian Islands*. Journal of Climate 22: 4261-4280

Timm OE, Giambelluca TW, Diaz HF (2015) Statistical downscaling of rainfall changes in Hawai 'i based on the CMIP5 global model projections. Journal of Geophysical Research: Atmospheres 120: 92-112

Uchida J, Levin P, Miyasaka S, Teves G, Hollyer J, Nelson S, Ooka J (2008) Taro, mauka to makai: a taro production and business guide for Hawaiian growers. CTAHR, University of Hawaii at Manoa, HI

UNESCO (2004) Management Implications, Measurements and Effects Scientific Committee on Oceanic Research (SCOR)/Land-Ocean Interactions in the Coastal Zone (LOICZ), UNESCO: Paris, France.

Vaksvik KN (1935) Geology and ground-water resources of the island of Oahu, Hawaii. Hawaii Div Hydrography, Bull 1: 479

Van Liew M, Arnold J, Garbrecht J (2003) Hydrologic simulation on agricultural watersheds: Choosing between two models. Transactions of the ASAE 46: 1539

Van Liew MW, Arnold J, Bosch D (2005) Problems and potential of autocalibrating a hydrologic model. Transactions of the ASAE 48: 1025-1040

Visher FN, Mink JF (1964) Ground-water resources in southern Oahu, Hawaii US Government Printing Office

VTN Pacific (1983) Iolekaa Well at Haiku Valley, Koolaupoko, Oahu, City and County of Honolulu, pp. 106.

Whittier RB, Rotzoll K, Dhal S, El-Kadi AI, Ray C, Chang D (2010) Groundwater source assessment program for the state of Hawaii, USA: methodology and example application. Hydrogeology journal 18: 711-723

Whittier RB, Rotzoll K, Dhal S, El-Kadi AI, Ray C, Chen G, Chang D (2006) HAWAII SOURCE WATER ASSESSMENT PROGRAM REPORT.

Wilder RJ, Tegner MJ, Dayton PK (1999) Saving marine biodiversity. Issues in Science and Technology 15: 57-64

Willems P (2004) WETSPRO: Water Engineering Time Series PROcessing tool. KU Leuven Hydraulics Laboratory, Leuven Belgium

Williams JR (1969) Flood routing with variable travel time or variable storage coefficients. Transactions of the ASAE 12: 100-0103

Wilson OC (2004) Kane'ohe-Kahalu'u stream restoration & maintenance, a community guidbook.

Wilson OC (2008) Water Resource Protection PlanHawaii Water Plan.

Xie S-P, Okumura Y, Miyama T, Timmermann A (2008) Influences of Atlantic Climate Change on the Tropical Pacific via the Central American Isthmus*. Journal of Climate 21: 3914-3928

Xie X, Cui Y (2011) Development and test of SWAT for modeling hydrological processes in irrigation districts with paddy rice. Journal of Hydrology 396: 61-71

Yost R, El-Kadi A, Yanagida J, Bruland G, Mills-Packo P, Unser C, Mamiit R, Barber K, Wedding L, Walsh C (2009) Demonstrating Watershed Participatory Assessment and Action, Kaiaka Bay Watershed, Oahu, Hawaii. une 30: 200

Zhang L, Walker GR, Fleming M (2002) Surface water balance for recharge estimation Csiro Publishing

Zheng C (2006) MT3DMS v5. 2 supplemental user's guide. Department of Geological Sciences, University of Alabama, Tuscaloosa, AL